UNIVERSITY OF SOUTHAMPTON

FACULTY OF PHYSICAL SCIENCES AND ENGINEERING

Electronics and Computer Science

Repetitive Process Based Higher-order Iterative Learning Control Law Design

by

Xuan Wang

Thesis for the degree of Doctor of Philosophy

August 2017

UNIVERSITY OF SOUTHAMPTON

ABSTRACT

FACULTY OF PHYSICAL SCIENCES AND ENGINEERING
Electronics and Computer Science

Doctor of Philosophy

REPETITIVE PROCESS BASED HIGHER-ORDER ITERATIVE LEARNING CONTROL LAW DESIGN

by Xuan Wang

Iterative learning control has been developed for processes or systems that complete the same finite duration task over and over again. The mode of operation is that after each execution is complete the system resets to the starting location, the next execution is completed and so on. Each execution is known as a trial and its duration is termed the trial length. Once each trial is complete the information generated is available for use in computing the control input for next trial.

This thesis uses the repetitive process setting to develop new results on the design of higher-order ILC control laws. The basic idea of higher-order ILC is to use information from a finite number of previous trials, as opposed to just the previous trial, to update the control input to be applied on next trial, with the basic objective of improving the error convergence performance. The first set of new results in this thesis develops theory that shows how this improvement can be achieved together with a measure of the improvement available over a non-higher order law.

The repetitive process setting for analysis is known to require attenuation of the frequency content of the previous trial error from trial-to-trial over the complete spectrum. However, in many cases performance specifications will only be required over finite frequency ranges. Hence the possibility that the performance specifications could be too stringent. The second set of new results in this thesis develop design algorithms that allow different frequency specifications over finite frequency ranges.

As in other areas, model uncertainties arise in applications. This motivates the development of a robust control theory and associated design algorithms. These constitute the third set of new results. Unlike alternatives, the repetitive process setting avoids the appearance of product terms between matrices of the nominal system dynamics state-space model and those used to describe the uncertainty set. Finally, detailed simulation results support the new designs, based on one axis of a gantry robot executing a pick and place operation to which iterative learning control is especially suited.

Contents

List of Figures

Acknowledgements

Thanks to my supervisors Professor Eric Rogers and Dr Bing Chu to give me help in the research. Then thanks to Dr. Błażej Cichy and Professor Kaizhou Liu who give me support in my research.

Chapter 1

Introduction

Iterative learning control (ILC) is concerned with reference tracking control problems. In applications, many industrial robots do tasks in a repetitive mode over a finite duration and the basic control objective in such cases is to design control laws that force the output to track the reference trajectory. A typical example is the 'pick and place' operation, i.e., moving an object from one location to another, where time duration required can only be finite. In the literature, each execution is known as a trial, or a pass, and the finite of each trial is termed the trial length.

Once each trial is complete in the pick and place operation, the robot returns to the starting location and the next trial can begin, either immediately after the resetting is complete or after a further period of time has elapsed. Moreover, once a trial is complete then all information generated over the trial length is available, at the cost of storage. In ILC, the novel feature is the use of this information in the construction of the next trial input. If a reference trajectory is given, then the error on any trial is the difference between this trajectory and the output on this same trial and hence a formulation of a control design problem in terms of the error sequence.

Let $y_k(p)$, $0 \leq p \leq \alpha - 1$, $k \geq 0$ denote the scalar or vector-valued variable on trial k and sample instant p, where α denotes the number of samples along the trial length for discrete dynamics, i.e., α times the sampling period gives the trial length. Also let $y_d(p)$, $0 \leq p \leq \alpha - 1$ denote the reference vector or trajectory, respectively, which is assumed to be the same for all trials. Then the error on trial k is $e_k(p) = y_d(p) - y_k(p), 0 \leq p \leq \alpha - 1$. Hence the ILC design problem can be formulated as ensuring that the error sequence $\{e_k\}$ converges to zero with increasing trials. Moreover, it is also required to ensure that the dynamics produced along the trial are also 'acceptable'.

Given the repeated trials, an obvious form of ILC law is to construct the input for the next trial as the sum of that used on the previous trial plus a correction term. Also, since all previous trial data is available, the basic question is: how best to use this data?

a core part of the answer is this question is the use of information that would be non-causal in the standard systems sense. In particular, at sample instant $p+\lambda$ can be used provided it is generated on the previous trial. This is a feature unique to ILC.

The first research on Iterative Learning Control (ILC) developed a derivative, or D-type, law for speed control of a voltage-controlled dc-servomotor. Since this first work ILC has been an established area of research and one starting point for the literature is the survey papers [1, 12]. A large volume of the currently available literature assumes a discrete model of the dynamics is available, by sampling if required and hence direct digital design.

Given the finite trial length, one approach to ILC design for discrete systems is to represent the dynamics by an equivalent standard systems model, where, e.g., the trial output is represented by a column vector formed from the values at the sample instants along the trial. This is often termed lifted ILC design and given the reference trajectory, the trial-to-trial error dynamics can be written as a discrete difference equation in the trial number. The basic task then is to design the ILC law such that trial-to-trial error convergence occurs. In this design setting it is assumed that the system is stable but if not a preliminary feedback control must be applied to ensure stability and acceptable transient dynamics along the trials and ILC designed for the resulting controlled dynamics.

Lifted ILC design is a two-stage procedure and an alternative is to exploit 2D systems theory where in this setting one indeterminate is the trial number and the other the along the trial variable. Repetitive processes are a distinct class of 2D systems where information propagation in one direction only occurs over a finite duration this is an inherent property of the dynamics and not an assumption introduced for analysis purposes. A detailed treatment of repetitive processes, including industrial examples can be found in [74].

As the trial length is finite, repetitive processes are a closer match to ILC and designs using this setting have seen experimental verification on a gantry robot that replicates the pick and place operation, see, e.g. [38, 67]. In the repetitive process setting, it is possible to do control law design for error convergence and transient dynamics along the trials in one step. Moreover, unlike the lifted approach, this setting extends naturally to differential dynamics, i.e., to cases where design by emulation is the preferred or only setting for design.

The 2D systems structure of repetitive processes arises from the fact that they make a series of sweeps through a set of dynamics defined over a finite duration. Once a sweep is complete, the process resets to the starting location and the next sweep can begin. Also the output produced on the previous sweep acts as a forcing function on the dynamics produced on the next sweep. The result can be oscillations that increase in amplitude from sweep-to-sweep that cannot be removed by standard control actions.

A rigorous stability theory for these processes has been developed and imposes a bounded input bounded output property on the dynamics, either over the finite and fixed finite trial length or uniformly, where this last property can be analysed by considering $\alpha \to \infty$. The latter property is stronger but, for linear time invariant dynamics, imposes frequency attenuation over the complete frequency spectrum. This can be a very strict requirement with consequent implications of designing a control law.

The possibility to specify different performance specifications over finite frequency ranges has considerable practical significance since common performance issues occur over different frequency ranges. For example, the low frequency range influence the error convergence performance. Moreover, in many cases of ILC, the reference trajectory often has dominant frequency content only over a finite frequency ranges.

In this thesis, a major contribution is to develop repetitive process based ILC law design algorithms, with a particular emphasis on higher-order laws [10] that are still an underdeveloped area. It will be shown that such a law can improve the speed of trial-to-trial error convergence coupled with acceptable along the trial dynamics. Moveover, a bound on the convergence speed is established, where no such bound is known in the literature.

A second major contribution relates to avoiding the need to design over the complete frequency spectrum. In particular, the Kalman-Yakubovich-Popov (KYP) lemma [68] and its generalized version, denoted GKYP, are used develop results that allow the design of higher-order ILC laws with different frequency domain specifications imposed over finite frequency ranges. These results add to those currently available using this approach [67].

Robustness, as in other areas, is an important issue in ILC design. In standard linear systems theory one commonly used setting for robustness and control law design is to assume that the uncertainty present lies in a specified model class. Two commonly used classes are termed norm-bounded and polytopic, respectively and in the thesis the former is considered in the ILC setting and the previous results are extended to the robust case [23, 35].

This thesis consists of six further chapters, where Chapter 2 gives a literature review of ILC is given and also the necessary background on repetitive processes and their stability properties. Chapters 3 and 4 develop design algorithms for higher-order ILC. The results include Linear Matrix Inequality (LMI) based design for discrete and continuous-time systems, including the robust case. The major difference between the two chapters is that in Chapter 3 design is based KYP lemma and is over the complete frequency range. In Chapter 4 the analysis is based on the GKYP lemma over finite frequency ranges. In these two chapters, the control law includes state feedback and hence the assumption that all entries in the state vector can be measured or estimated. Chapter 5 develops output-feedback control laws for the cases considered. Chapter 6 gives the results of an in-depth evaluation of the new results of this thesis based on a model of one axis of a gantry robot identified from measured frequency response data. Finally, chapter 7 summarises the main new results in this thesis and discusses areas for possible future research.

Chapter 2

Literature Review

2.1 Overview of Iterative Learning Control

The development of iterative learning control (ILC) emerged from industrial applications where the system involved executes the same operation many times over a fixed finite time interval. When each operation is complete, resetting to the starting location takes place and the next operation can commence immediately, or after a stoppage time. A common example is a gantry robot undertaking a pick and place operation in synchronization with a moving conveyor or assembly line. The sequence of operations is: (a) the robot collects a payload from a fixed location, (b) transfers it over a finite duration, (c) places it on the moving conveyor, (d) returns to the original location for the next payload and then (e) repeats the previous four steps for as many payloads as is required or can be transferred before it is required to stop.

To operate in pick and place mode it is necessary to supply the robot with a trajectory to follow and the task for a control law is to ensure that the robot follows the prescribed trajectory exactly or, more realistically, to within a specified tolerance. In addition to controlling its own movement and that of the payload, the control law must prevent other effects, such as disturbances and signal noise, from degrading tracking and thereby forcing it outside of the tolerance bound. If the robot begins to operate outside permissible limits, the control task is to bring it back within specification as quickly as required or is physically possible. This task must be achieved without causing damage to, e.g., the sensing and actuating technologies used.

The widely recognized starting point for ILC is [6], which considered a simple first order linear servomechanism system for a voltage-controlled dc-servomotor. As in other areas, there is debate on the origins of ILC, for which the survey papers [1, 12] and, in particular, [1] give coverage and relevant references. In the opening paragraphs of [6] the analogy between ILC and human learning is drawn in the text: 'It is human to make mistakes, but it also human to learn from such experience. Is it possible to think of a way to implement such a learning ability in the automatic operation of dynamic systems?'.

The analysis in [6] developed, using the servomotor example as a particular example, a control law applicable to systems required to track a desired reference trajectory or vector of a fixed trial length α and specified a priori. On completion of each trial, the system states reset and during time taken to complete this task the measured output is used in the construction the next control output. The system dynamics were assumed to be trial-invariant and invertible. These distinguishing features led to the establishment of ILC as a major and ongoing area of control systems research and applications. Several of these assumptions, e.g., trial-invariant dynamics, have been relaxed in recent years but the concept of learning from experience gained over repeated trials of a task has been retained.

Since it was first introduced ILC has broadened in breadth and depth, including links with established fields such as robust, adaptive and optimal control. Application areas have also expanded beyond industrial robotics and process control. In the latter area, one starting point for the literature is the survey paper [85], which also considers the connections with repetitive control and run-to-run control.

The notation for a scalar or vector-valued variable when ILC is applied to discrete dynamics used in this thesis is $y_k(p)$, $p = 0, 1, \ldots, \alpha - 1$, where the nonnegative integer k is the trial number and $\alpha \in \mathbb{N}$ denotes the number of samples on each trial, with a constant sampling period. Suppose also that the dynamics of the system or process considered can be adequately modeled as linear and time-invariant. Then the state-space model of such a system in the ILC setting is

$$\begin{aligned} x_k(p+1) &= Ax_k(p) + Bu_k(p) \\ y_k(p) &= Cx_k(p), \;\; x_k(0) = x_0 \end{aligned} \tag{2.1}$$

where on trial k, $x_k(p) \in \mathbb{R}^n$ is the state vector, $y_k(p) \in \mathbb{R}^m$ is the output vector and $u_k(p) \in \mathbb{R}^l$ is the control input vector.

In this model it is assumed that the initial state vector does not change from trial-to-trial. The case when this assumption is not valid has also been considered in the literature. The dynamics are assumed to be disturbance-free but again this assumption can be relaxed. It also possible to write the dynamics in input-output form involving the convolution operator or take the one-sided z transform and hence analysis and design in the frequency domain is possible.

To apply the z transform it is necessary to assume $\alpha = \infty$ but in most cases the consequences of this requirement have no detrimental effects. For a more detailed analysis of cases where there are unwanted effects arising from this assumption, see the relevant references in [1, 12] and more recent work in [83].

Let $y_d(p) \in \mathbb{R}^m$ denote the supplied reference vector. Then the error on trial k is $e_k(p) = y_d(p) - y_k(p)$ and the core requirement in ILC is to construct a sequence of input functions $u_{k+1}(p)$, $k \geq 0$, such that the performance achieved is gradually improved with each successive trial and after a 'sufficient' number of these the current trial error is zero or within an acceptable tolerance. Mathematically this can be stated as a convergence condition on the input and error of the form

$$\lim_{k\to\infty} ||e_k|| = 0, \lim_{k\to\infty} ||u_k - u_\infty|| = 0 \tag{2.2}$$

where u_∞ is termed the learned control and $|| \cdot ||$ denotes an appropriate norm on the underlying function space.

As one possibility, let $|| \cdot ||_2$ denote the Euclidean norm of its argument then one choice is $||e|| = \max_{p\in[0,\alpha-1]} ||e(p)||_2$. The reason for including the requirement on the control vector is to ensure that strong emphasis on reducing the trial-to-trial error does not come at the expense of unacceptable control signal demands. In application, only a finite number of trials will ever be completed but mathematically letting $k \to \infty$ is required in analysis of, e.g., trial-to-trial error convergence.

Remark 2.1. When a specific norm is used in this thesis, this will be indicated by adding a subscript.

2.2 Some Basic ILC Algorithms

As in other areas, initial research considered simple structure ILC laws. Arimoto et al.[6] proposed the derivative type ($D - type$) ILC law for continuous-time system. This ILC law can also be used for discrete-time system. Consider the discrete time-invariant state-space model in ILC setting (2.1) over a fixed finite time interval $p \in [0, \alpha - 1]$. Define the reference trajectory as $y_d(p)$, then the error on trial k is $e_k(p) = y_d(p) - y_k(p)$ and initial state in each trial is zero. The D-type ILC law has the form

$$u_{k+1}(p) = u_k(p) + L(e_k(p+1) - e_k(p)) \tag{2.3}$$

where L is an $m \times m$ matrix function to be designed and $e_k(p+1) - e_k(p)$ is the difference of the error. It is shown in [6] that trial-to-trial convergence occurs if

$$\|I - CBL\| < 1 \tag{2.4}$$

holds.

Arimoto et al.[7] also proposed the proportional-type ($P-type$) ILC law. Consider again (2.1) this control law is of the form

$$u_{k+1}(p) = u_k(p) + Le_k(p) \tag{2.5}$$

The convergence condition for the P-type ILC law is again (2.4).

Many control laws are based on a PID structure, e.g. in addition to D-type and P-type ILC, PI-type ILC and PD-type ILC, and Kim et al.[46] gave the general form of PID-type ILC. Consider again (2.1), then this control law has the form

$$u_{k+1}(p) = u_k(p) + K_P e_k(p+1) + K_I \sum_{i=0}^{T} e_k(i) + K_D[e_k(p+1) - e_k(p)] \tag{2.6}$$

where K_P, K_I and K_D are the proportional, integral and derivative gains, respectively. If K_I and K_P are zero, this law becomes D-type ILC. The convergence condition of PID-type ILC is

$$\|I - CB(K_P + K_I + K_D)\| < 1 \tag{2.7}$$

Heinzinger et al.[37] proposed an ILC law with forgetting factor to improve the stability of ILC with uncertain initial conditions. The general form of D-type ILC with forgetting factor for the system model (2.1) is

$$u_{k+1}(p) = (1-\gamma)u_k(p) + \gamma u_0(p) + L(e_k(p+1) - e_k(p)) \tag{2.8}$$

where γ is the forgetting factor and $0 \leq \gamma < 1$, if $\gamma = 0$ this law becomes the D-type ILC algorithm. The convergence condition is

$$\|(1-\gamma)I - LCB\|_\infty < 1 \tag{2.9}$$

In [37] this algorithm was given for systems with state disturbance, output noise and errors in initial conditions.

Wang et al.[82, 83, 84, 90] proposed the phase-lead ILC law and analyzed it in the frequency domain. The control law for the system model (2.1) is

$$u_{k+1}(p) = u_k(p) + Le_k(p+\Delta) \tag{2.10}$$

where $\Delta > 0$ is the lead phase. In order to analyze the convergence in the frequency domain and derive the condition for error convergence, the learnable bandwidth was introduced. Bandwidth was introduced where learning only takes place over a finite frequency range. The presence of $\Delta > 0$, in the last control law represents the use of data that would be noncausal in the standard case. This is the unique feature of ILC.

2.3 Inverse Model-based ILC

Harte et al.[36] analyzed the monotonic convergence condition and robustness for uncertain systems. Suppose that the linear system under consideration has a model G that is invertible. Then an inverse ILC law has the form

$$u_{k+1} = u_k + \beta G^{-1} e_k \tag{2.11}$$

where β is the learning gain, which can be used to enhance performance. The convergence condition by [36] is

$$\|I - \beta G_e G^{-1}\|_\infty < 1 \tag{2.12}$$

As the above condition shows, the convergence of inverse model-based ILC depends on multiplicative uncertainty representation $G_e = UG$, where U is an uncertainty square matrix. Suppose $U + U^T$ is positive-definite matrix. Then [36] also gave the robust monotonic convergence condition and tested is in the frequency domain. The condition of the monotonic convergence depends on the relationship between learning gain β and U.

A gradient-based ILC law has the form

$$u_{k+1} = u_k + \beta G^T e_k \tag{2.13}$$

with convergence condition

$$\|I - \beta G G^T\|_\infty < 1 \tag{2.14}$$

2.4 Norm-optimal ILC (NOILC)

This form of ILC constructs the current trial input as the solution of an optimisation problem. The basics of this method are now given following in the main [4, 5].

Let the real Hilbert space $\mathbb{Y}$ be the space of output signals and the real Hilbert space $\mathbb{U}$ be the space of input signals. Define G as the system input/output operator from $\mathbb{U}$ to $\mathbb{Y}$. Then if the dynamics of the systems considered are the linear and represented in operator form

$$y = Gu + z_o \tag{2.15}$$

can be used where $u \in \mathbb{U}$ and $y \in \mathbb{Y}$, and z_o represents the effects of system initial conditions (always be assumed as z_o=0). Let the reference trajectory: $y_d \in \mathbb{Y}$ then $e_k = y_d - y_k$. Then the objective of NOILC is to find a corresponding input signal that minimize index J_k where

$$J_{k+1}(u_{k+1}) = \|e_{k+1}\|^2_{\mathbb{Y}} + \|u_{k+1} - u_k\|^2_{\mathbb{U}} \tag{2.16}$$

The first term in (2.16) reflects the error being small during every trial, and the second term make input u_{k+1} be not 'too' different from the previous input u_k [55, 57]. Therefore, the updating input on the $(k+1)$th trial is defined as

$$u_{k+1} = argmin_{u_k+1}\{J_{k+1}(u_k+1):\ e_{k+1} = r - y_{k+1},\ y_{k+1} = Gu_{k+1}\} \tag{2.17}$$

Minimization of the performance index gives the control law

$$u_{k+1} = u_k + G^* e_{k+1} \tag{2.18}$$

where G^* is the adjoint operator to the system G, and the final form of the control update is

$$u_{k+1}(p) = u_k(p) + [\{B^T K(p)B + R\}^{-1} B^T K(p) \times A\{x_{k+1}(p) - x_k(p)\}] + R^{-1}B^T \xi_{k+1}(p) \tag{2.19}$$

where $K(p)$ is the solution of the matrix Riccati equation on the interval $p \in [0,\ \alpha-1]$

$$K(p) = A^T K(p+1)A + C^T QC - A^T K(p+1)B(B^T K(p+1)B + R)^{-1} B^T K(p+1)A; \tag{2.20}$$

with terminal boundary condition $K(\alpha-1) = 0$ and $\xi_{k+1}(p)$ is the predict term

$$\xi_{k+1}(p) = (I + K(p)BR^{-1}B^T)^{-1}(A^T \xi_{k+1}(p+1) + C^T Q e_k(p)) \tag{2.21}$$

with terminal boundary condition

$$\xi_{k+1}(\alpha-1) = 0 \tag{2.22}$$

also Q, R and F are weights in the inner space $\mathbb{Y}$ and $\mathbb{U}$, respectively. In this control law, $\xi_{k+1}(p)$ is the feedforward term and $x_{k+1}(p) - x_k(p)$ is the feedback term.

Amann et al.[5] showed that the convergence rate for this control law satisfies

$$\|e_{k+1}\| \leq \frac{1}{1+\sigma^2}\|e_k\| \tag{2.23}$$

where σ is the smallest singular value of G, and $\frac{1}{1+\sigma^2}$ is the rate of convergence.

The advantages of this algorithm is the automatic choice of the step size in the control law, it also enforces the monotonic convergence. However, the computational cost of NOILC is larger than other basic algorithms and it is more complex. Despite this, NOILC has seen experimental verification and implementations. Examples include gantry robot [69], rehabilitation robotics [75], chain conveyor systems [2], roll to roll/micro-manufacturing system [79], and adaptive weights of the form [50].

Parameter-optimal ILC [54] uses only feedforward information and the system model G must be positive (all the eigenvalues of G are positive) and invertible. Again the error converges to zero as $k \to \infty$, and the control law in this case is

$$u_{k+1}(t) = u_k(t) + \beta_{k+1} e_k(t) \tag{2.24}$$

where β_{k+1} denotes the learning gain that varies from trial-to-trial and is chosen based on minimising the cost function

$$J(\beta_{k+1}) = \|e_{k+1}\|^2 + \varepsilon \beta_{k+1}^2 \tag{2.25}$$

for ε, the adaptive weights is used, which is defined as $\varepsilon = \varepsilon_1 + \varepsilon_2 \|e_k\|^2$. The condition $\partial J(\beta_{k+1})/\partial \beta_{k+1} = 0$ gives the optimal β_{k+1}.

$$\beta_{k+1} = \frac{\langle e_k, Ge_k \rangle}{\varepsilon_1 + \varepsilon_2 \|e_k\|^2 + \|Ge_k\|^2} \tag{2.26}$$

where $\langle \cdot \rangle$ denotes the inner product. Also the convergence of this law is

$$\|e_{k+1}\|^2 \leq \lambda \|e_k\|^2 \tag{2.27}$$

where $\lambda = 1 - \beta_{k+1}^2 (2\varepsilon_2 + \frac{\|Ge_k\|^2}{\|e_k\|^2})$. The aim of the term $\varepsilon \beta_{k+1}^2$ in performance index (2.25) is to enforce zero error. The convergence rate is dependent on β_{k+1}. However, when e_k reduces the gain β_{k+1} will also be reduced.

2.5 Newton-type ILC

For nonlinear dynamics one method is Newton-type ILC, which uses the Newton-Raphson method to obtain the automatic learning gain. Avrachenkov [8] proposed quasi-Newton based ILC for robotic manipulators.

Lin et al.[49, 50] developed Newton-type ILC for discrete nonlinear systems. Many ILC laws can give high performance for linear dynamics but not if the system dynamics are nonlinear. Newton-type ILC linearizes the nonlinear system to result in a time-varying linear system. Consider the nonlinear discrete-time system in ILC setting

$$\begin{cases} x_k(p+1) = f[x_k(p), u_k(p)] \\ y_k(p) = h[x_k(p)], \quad x_k(0) = x_{k0}, \ p \in [0, \alpha - 1] \end{cases} \tag{2.28}$$

where the relationship between input and output can be written as $y_k(p) = g(u_k(p))$. The control law is

$$u_{k+1} = u_k + g'(u_k)^{-1} e_k \tag{2.29}$$

Using this control law, it is difficult to calculate the inversion and derivative of the nonlinear system $g(u_k)$. The core of Newton ILC is to avoid the construction of this term. Assume $z_{k+1} = g'(u_k)^{-1} e_k$, the control law becomes $u_{k+1} = u_k + z_{k+1}$. The aim is to calculate z_{k+1}, from the definition, using

$$e_k = g'(u_k) z_{k+1} \tag{2.30}$$

where, the kth trial error e_k can be regarded as the designed signal and z_{k+1} is the input, and g' is the linearization of the nonlinear system. Therefore the objective is to find the input for the system $g'[u_k]$ which can track the error e_k. The linearization of the system $g'[u_k]$ is

$$\begin{cases} \tilde{x}_k(p+1) = A(p)\tilde{x}(p) + B(p)\tilde{u}(p) \\ \tilde{y}_k(p) = C(p)\tilde{x}(p) \end{cases} \tag{2.31}$$

where $A(p), B(p)$ *and* $C(p)$ are time-varying matrices and defined as

$$A(p) = (\frac{\partial f}{\partial x})_{u_k,x_k}, \quad B(p) = (\frac{\partial f}{\partial u})_{u_k,x_k}, \quad C(p) = (\frac{\partial h}{\partial x})_{u_k,x_k} \tag{2.32}$$

Any ILC design can be applied to this tracking operation and then the optimal input z_{k+1} is obtained. A major advantage of this ILC design is a fast convergence rate. The Newton-Kantrovich theorem shows that Newton-type ILC has semi-local quadratic convergence performance. Therefore, Newton-type ILC has a form of quadratic convergence.

Of course, there will be applications where Newton-type ILC cannot be applied, e.g., when the required partial derivatives do not exist. In such cases other fully nonlinear designs must be used such as feedback linearization. For background on this see, e.g.[89].

2.6 2D System Theory/Repetitive Process Based ILC Design

Iterative learning control can be viewed as a 2D system, i.e. information propagation in two independent directions where one of these is from trial to trial and the other is along the trial. Therefore, ILC analysis using 2D systems theory is possible. Repetitive processes [74, 76, 77] are a particular class of 2D systems with spatio-temporal dynamics where the temporal dynamics are defined over a finite duration. Moreover, this is an inherent property of the dynamics and not an assumption.

These process have their origins in the modeling and control of coal mining operations and they are a more natural fit to ILC. The repetitive process approach forms a major part of the analysis in this thesis and therefore the review of current results in this section is mainly related to ILC analysis and design in this setting.

Consider first 2D systems where Roesser [71] proposed a new model for linear image processing of the form

$$\begin{cases} x^h(i+1,j) = A_1 x^h(i,j) + A_2 x^v(i,j) + B_1 u(i,j) \\ x^v(i,j+1) = A_3 x^h(i,j) + A_4 x^v(i,j) + B_2 u(i,j) \\ y(i,j) = C_1 x^h(i,j) + C_2 x^v(i,j) + Du(i,j) \end{cases} \tag{2.33}$$

for $i \geq 0,\ j \geq 0$, where x^h and x^v are the horizontal and vertical sub-vectors axis and vertical respectively. An alternative model is due to Fornasini and Marchesini [25] and has the form

$$\begin{cases} x(i+1,j+1) = A_0 x(i,j) + A_1(i+1,j) + A_2(i,j+1) + Bu(i,j) \\ y(i,j) = Cx(i,j) \end{cases} \tag{2.34}$$

where in contrast to the Roesser model the state vector x is not partitioned into two sub-vectors [47]. More detail can also be found in [9, 29, 44, 51].

Consider the following ILC law for application to the system described by (2.1)

$$u(p,k+1) = u(p,k) + K_0 e(p,k) + K_1 e(p+1,k) \tag{2.35}$$

where K_0 and K_1 are the control law matrices and $e(p+1,k)$ is a phase-lead term. Defining $\xi(p,k) = e(p,k+1) - [I - BK_1]e(p,k)$ the resulting controlled dynamics can be written as the Roesser state-space model

$$\begin{aligned} \xi(p+1,k) &= A\xi(p,k) + [-BK_0 - ABK_1]e(p,k) \\ e(p,k+1) &= I + [I - BK_1]e(p,k) \end{aligned} \tag{2.36}$$

Using this model [48] showed that error convergence requires $r(I - BK_1) < 1$, where $r(\cdot)$ denotes the spectral radius, i.e., if an $h \times h$ matrix H has eigenvalues λ_i then $r(H) = \max_{1 \leq i \leq h} |\lambda_i|$ (see also [24, 32, 33, 80] for more detail of 2D system theory based ILC design).

From the above analysis, trial-to-trial error convergence occurs independent of the along the trial dynamics (in p) due to the fact that over a finite trial length even an unstable linear system can only produce a bounded output in response to a bounded input. If the dynamics along the trial are not stable the approach is to design a stabilizing feedback control law and then do ILC design for the resulting controlled dynamics. This is a two-step design that can be avoided by using the repetitive process setting, for which the following is the required background.

Repetitive processes are a distinct class of 2D linear systems [30, 31, 39, 73, 78, 81]. Such processes make a series of sweeps, termed passes, through a set of dynamics defined over a finite duration known as the pass length. The output on each pass is known as the pass profile and once each profile is produced the process resets to the starting location ready for the start of the next pass. During each pass the previous pass profile acts as a forcing function and hence contributes to the current pass profile dynamics. The result can be oscillations that increase in amplitude from pass to pass. Such behavior cannot be controlled by standard control action.

Repetitive processes have their origins in modeling and control of long-wall coal cutting dynamics but the repetitive process structure also arises in other applications. These include physical applications, such as metal rolling, and others where the repetitive process setting has advantages for analysis, such as optimal control problems for gas pipelines. The details can again be found in [58, 72, 74].

Of particular interest in this thesis are so-called discrete unit memory linear repetitive processes, where the term unit memory refers to the fact that only the previous pass profile contributes explicitly to the dynamics of the next one. The state-space model is of the form

$$\begin{aligned} x_{k+1}(p+1) &= Ax_{k+1}(p) + Bu_{k+1}(p) + B_0 y_k(p) \\ y_{k+1}(p) &= Cx_{k+1}(p) + Du_{k+1}(p) + D_0 y_k(p) \end{aligned} \tag{2.37}$$

where $x_k(p) \in \mathbb{R}^n$ is the state vector, $y_k(p) \in \mathbb{R}^m$ is the pass profile vector, $u_k(p) \in \mathbb{R}^l$ is the control input vector, $k > 0$ is the trial number, and $0 \leq p \leq \alpha - 1$ where $\alpha < \infty$ denotes the number of samples along the pass (α times the sampling period gives the pass length). To complete the process description it is necessary to specify the boundary conditions, i.e., the state initial vector for each pass and the initial pass profile (i.e., for $k = 0$). The simplest possible form for these is $x_{k+1}(0) = d_{k+1},\ k \geq 0$ where d_{k+1} has known constant entries and $y_0(p) = f(p)$ where the entries in $f(p)$ are known functions of p over the pass length $\alpha < \infty$.

The stability properties and their characterisation for linear repetitive processes is motivated by the unique control problem, i.e., oscillations in the pass profile sequence that increase in amplitude as k increases, This stability theory is of the bounded input bounded output form. In particular a bounded initial pass profile is required to produce a bounded sequence of pass profiles. Moreover, two cases are possible, either this property over the finite and fixed pass length α or independent of the pass length.

The stability theory for linear repetitive processes is defined in terms of an abstract model in a Banach space setting, where this abstract model, given next, includes all examples as special cases.

Definition 2.2. [74] A linear repetitive process of constant pass length $\alpha > 0$ consists of a Banach space E_α, a linear subspace W_α of E_α, and a bounded linear operator L_α mapping E_α into itself (also written $L_\alpha \in B(E_\alpha, E_\alpha)$). The system dynamics are described by linear recursion relations of the form

$$y_{k+1} = L_\alpha y_k + b_{k+1}, \quad k \geq 0 \tag{2.38}$$

where $y_k \in E_\alpha$ is the pass profile on pass k and $b_{k+1} \in W_\alpha$. Here the term $L_\alpha y_k$ represents the contribution from pass k to pass $k+1$ and b_{k+1} represents initial conditions, disturbances and control input effects.

The natural definition of asymptotic stability for these processes is to demand that, given any initial profile y_0 and any disturbance sequence $\{b_k\}_{k\geq 1}$ that 'settles down' to a steady disturbance b_∞ as $k \to 0$, the sequence $\{y_k\}_{k\to 1}$ generated by the abstract model (2.38) 'settles down' to a steady, or so-called limit, profile as $k \to \infty$. This means that abstract model is asymptotic stable if giving any initial pass profile y_0 and strong convergent disturbance b_k the sequence y_k can converges to a limit profile y_∞. In the absence of disturbances the pass profile sequence $\{y_k\}_{k\geq 1}$ converges strongly to zero for all initial profiles if $\|L_\alpha\| < 1$. In the absence

Theorem 2.3. *[74] The linear repetitive process (2.38) of constant pass length $\alpha > 0$ is asymptotically stable if and only if*

$$r(L_\alpha) < 1 \tag{2.39}$$

In the special cases of discrete unit memory processes this property holds if and only if $r(D_0) < 1$.

A more general form of repetitive processes have non-unit memory, i.e., a finite number of pass profiles greater than one explicitly contribute to the current pass profile. In particular, suppose that $M > 1$ pass profiles explicitly contribute to the current one. Then a discrete non-unit memory linear repetitive process is described by the state-space model

$$\begin{aligned} x_{k+1}(p+1) &= Ax_{k+1}(p) + Bu_{k+1}(p) + \sum_{j=1}^{M} B_{j-1} y_{k+1-j}(p) \\ y_{k+1}(p) &= Cx_{k+1}(p) + Du_{k+1}(p) + \sum_{j=1}^{M} D_{j-1} y_{k+1-j}(p) \end{aligned} \tag{2.40}$$

with the boundary conditions

$$\begin{aligned} x_{k+1}(0) &= d_{k+1}, \quad k \geq 0 \\ y_{1-j}(p) &= \hat{y}_{1-j}(p), \ 0 \leq p \leq \alpha - 1, 1 \leq j \leq M \end{aligned} \tag{2.41}$$

where d_{k+1} is an $n \times 1$ vector with known constant entries and the entries in the $m \times 1$ vectors $\hat{y}_{1-j}(p)$ are known functions of p.

The abstract model based stability theory also includes these processes and the following result characterizes asymptotic stability.

Theorem 2.4. *[74] A discrete non-unit memory linear repetitive process described by (2.40) and (2.41) is asymptotically stable if and only if*

$$r(\tilde{D}) < 1 \tag{2.42}$$

where

$$\tilde{D} = \begin{bmatrix} 0 & I & 0 & \cdots & 0 \\ 0 & 0 & I & \cdots & 0 \\ 0 & 0 & 0 & \cdots & 0 \\ \vdots & \vdots & \vdots & \ddots & I \\ D_{M-1} & D_{M-2} & D_{M-3} & \cdots & D_0 \end{bmatrix} \tag{2.43}$$

Asymptotic stability places no restrictions on the along the pass dynamics and this can lead to unacceptable behavior. Guarantee that the sequence of pass profiles y_k converges in norm to the limit profile denoted by y_∞, which, see [74] for the details, is described by a standard linear systems state-space model with for examples described by (2.40) state matrix $A + B_0(I - D_0)^{-1}C$. Now consider the case when $A = -0.5$, $C = 1$ and $B_0 = 0.5 + \beta$ where β is a real scalar. In this case $A + B_0(I - D_0)^{-1}C = \beta$ and hence the limit profile is unstable for $|\beta| \geq 1$.

To avoid such cases arising, stability along the pass can be imposed and treated mathematically by letting $\alpha \to \infty$.

Theorem 2.5. *[74] Suppose that the pair $\{A, B_0\}$ is controllable and the pair $\{C, A\}$ is observable. Then a discrete unit memory linear repetitive process described by (2.37) is stable along the pass if and only if*

(a) $r(D_0) < 1$

(b) $r(A) < 1$

(c) all eigenvalues of the transfer-function matrix $G(z) = C(zI - A)^{-1}B_0 + D_0$ have modulus strictly less than unity $\forall\, |z| = 1$.

The condition (a) is asymptotic stability and enforces pass-to-pass convergence, condition (b) stabilizes the state dynamics along each pass and condition (c), in the SISO case for simplicity, requires that the frequency response generated by the transfer-function $G(z)$ lies inside the unit circle in the complex plane. Equivalently the frequency content of the initial pass profile is attenuated from pass to pass over the complete frequency spectrum.

The corresponding stability conditions for non-unit memory discrete linear repetitive process (2.40) are

Theorem 2.6. *[74] Suppose that the pair $\{A, B_0\}$ is controllable and the pair $\{C, A\}$ is observable. Then the discrete non-unit memory linear repetitive process described by (2.40) and (2.41) is stable along the pass if and only if,*

(a) $r(\tilde{D}) < 1$

(b) $r(A) < 1$

(c) *all eigenvalues of the transfer-function matrix $\tilde{G}(z)$ have modulus strictly less than unity $\forall\, |z| = 1$.*

where $\tilde{D}$ is defined in (2.43) and

$$\tilde{G}(z) = \begin{bmatrix} 0 & I & 0 & \cdots & 0 \\ 0 & 0 & I & \cdots & 0 \\ 0 & 0 & 0 & \cdots & 0 \\ \vdots & \vdots & \vdots & \ddots & I \\ G_M(z) & G_{M-1}(z) & G_{M-2}(z) & \cdots & G_1(z) \end{bmatrix} \tag{2.44}$$

where

$$G_j(z) = C(zI - A)^{-1}B_{j-1} + D_{j-1},\ 1 \le j \le M \tag{2.45}$$

In design, the route via the so-called 2D Lyapunov equation leads to Linear Matrix Inequality (LMI) computations but at the expense of sufficient but not necessary conditions for stability along the pass.

Theorem 2.7. *[74] A discrete unit memory linear repetitive process of the form defined by (2.37) is stable along the pass if, there exists an $(n+m) \times (n+m)$ matrix $P > 0$ such that*

$$Q = \begin{bmatrix} \delta_1 P & 0 \\ 0 & \delta_2 P \end{bmatrix} - \hat{A}^T P \hat{A} > 0 \tag{2.46}$$

for any $\delta_i > 0,\ i = 1, 2,\ \delta_1 + \delta_2 = 1$, and $\hat{A} = \ [A_1\ A_2]$.

where the notation > 0 (respectively < 0 denotes a symmetric positive definite (respectively) negative-definite matrix. The equation (2.46) is one form of the 2D Lyapunov inequality for these processes and the associated condition is necessary and sufficient in the case of single-input single-output examples.

Theorem 2.8. *[74] A discrete unit memory linear repetitive process described by (2.37) is stable along the pass if, there exists matrices $Y > 0$ and $Z > 0$ satisfying the following LMI*

$$\begin{bmatrix} Z - Y & 0 & YA_1^T \\ 0 & -Z & YA_2^T \\ A_1 Y & A_2 Y & -Y \end{bmatrix} < 0 \tag{2.47}$$

where A_1 and A_2 are defined by

$$A_1 = \begin{bmatrix} A & B_0 \\ 0 & 0 \end{bmatrix}, \quad A_2 = \begin{bmatrix} 0 & 0 \\ C & D_0 \end{bmatrix} \tag{2.48}$$

Define the augmented plant matrix Φ as

$$\Phi = \begin{bmatrix} A & B_0 \\ C & D_0 \end{bmatrix} \tag{2.49}$$

Then an alternative theorem for stability along the pass is the following

Theorem 2.9. *[74] A discrete unit memory linear repetitive process described by (2.37) is stable along the pass if, there exists matrices $W_1 > 0$ and $W_2 > 0$ such that the 2D Lyapunov inequality*

$$\Phi^T W \Phi - W < 0 \tag{2.50}$$

where W is the direct sum of W_1 and W_2, i.e. $W = W_1 \oplus W_2$, or

$$W := \begin{bmatrix} W_1 & 0 \\ 0 & W_2 \end{bmatrix} \tag{2.51}$$

Also applying the Schur's complement formula to (2.50) the LMI based stability condition becomes

$$\begin{bmatrix} -W & W\Phi^T \\ \Phi W & -W \end{bmatrix} < 0. \tag{2.52}$$

Consider the state-space model of a differential non-unit memory linear repetitive processes is

$$\begin{aligned} \dot{x}_{k+1}(t) &= Ax_{k+1}(t) + Bu_{k+1}(t) + \sum_{j=1}^{M} B_{j-1} y_{k+1-j}(t) \\ y_{k+1}(t) &= Cx_{k+1}(t) + Du_{k+1}(t) + \sum_{j=1}^{M} D_{j-1} y_{k+1-j}(t) \end{aligned} \tag{2.53}$$

where $x_k(t)$ denotes state, $u_k(t)$ denotes control input, and $y_k(t)$ denotes pass profile, $k > 0$ is the trial number, and $0 < t \leq \alpha$ over the finite pass length α. To complete the process description, it is necessary to specify the boundary conditions, and the simplest possible form is

$$\begin{aligned} x_{k+1}(0) &= d_{k+1}, \quad k \geq 0 \\ y_{1-j}(t) &= \hat{y}_{1-j}(t), \; 0 < t \leq \alpha, 1 \leq j \leq M \end{aligned} \tag{2.54}$$

where d_{k+1} is an $n \times 1$ vector with known constant entries and the entries in the $n \times 1$ vectors $\hat{y}_{1-j}(t)$ are known functions of t. It is stable along the pass when next conditions are hold.

Theorem 2.10. *[74] Suppose that the pair $\{A, B_0\}$ is controllable and the pair $\{C, A\}$ is observable. Then the differential non-unit memory linear repetitive process described by (2.53) and (2.54) is stable along the pass if and only if,*

(a) all eigenvalues of the block companion matrix $\tilde{D}$ of (2.43) have modulus strictly less than unity, i.e. $r(\tilde{D}) < 1$

(b) $det(sI_m - A) \neq 0, Re(s) \geq 0$, and

(c) all eigenvalues of the block companion transfer-function matrix

$$\tilde{G}(s) := \begin{bmatrix} 0 & I & 0 & \cdots & 0 \\ 0 & 0 & I & \cdots & 0 \\ 0 & 0 & 0 & \cdots & 0 \\ \vdots & \vdots & \vdots & \ddots & I \\ G_M(s) & G_{M-1}(s) & G_{M-2}(s) & \cdots & G_1(s) \end{bmatrix} \tag{2.55}$$

have modulus strictly less than unity for $s = i\omega$, $\forall \omega \geq 0$, where

$$G_j(s) = C(sI_m - A)^{-1}B_{j-1} + D_{j-1}, 1 \leq j \leq M \tag{2.56}$$

The model in (2.53) becomes the differential unit memory linear repetitive processes when $M = 1$. Similarly, the $2D$ Lyapunov inequality can be used to analyze the stability of the differential linear repetitive processes and for design. Based on the unit memory linear model.

Theorem 2.11. *[74] The unit memory version of (2.53) is stable along the pass if there exist matrices $W = W_1 \oplus W_2 > 0$ which solve the $2D$ Lyapunov inequality,*

$$\Phi^T W^{1,0} + W^{1,0}\Phi + \Phi^T W^{0,1}\Phi - W^{0,1} < 0 \tag{2.57}$$

where Φ is defined by (2.49) and W_1, W_2 are matrices of dimensions $m \times m$, $n \times n$ respectively, $W^{1,0} = W_1 \oplus 0_{n\times n}$, and $W^{0,1} = 0_{m\times m} \oplus W_2$.

Hladowski et al. [38] have used the repetitive process setting to design an ILC law of the form

$$u_{k+1}(p) = u_k(p) + K_1(x_{k+1}(p) - x_k(p)) + K_2 e_k(p+1) \tag{2.58}$$

where K_1 and K_2 are control matrices in the control law. The first step is to write the dynamics as a discrete linear repetitive process. Introduce $\eta_{k+1}(p+1) = x_{k+1}(p) - x_k(p)$

and combine with (2.1) and (2.58) to obtain the discrete linear repetitive process state space model

$$\begin{aligned} \eta_{k+1}(p+1) &= \hat{A}\eta_{k+1}(p) + \hat{B}e_k(p) \\ e_{k+1}(p) &= \hat{C}\eta_{k+1}(p) + \hat{D}e_k(p) \end{aligned} \tag{2.59}$$

where

$$\begin{aligned} \hat{A} &= A + BK_1, \qquad \hat{B} = BK_2, \\ \hat{C} &= -C(A + BK_1), \qquad \hat{D} = I - CBK_2 \end{aligned} \tag{2.60}$$

Hence the controlled ILC dynamics are a repetitive process with current pass state vector η and pass profile e.

Using the 2D Lyapunov inequality gives the following result.

Theorem 2.12. *[38] The discrete linear repetitive process (2.59) is stable along the pass if and only if there exist matrices $X_1 > 0$, $X_2 > 0$, R_1 and R_2 such that the following LMI is feasible:*

$$\begin{bmatrix} -X_1 & 0 & X_1A^T + R_1^TB^T & -X_1A^TC^T - R_1^TB^TC^T \\ 0 & -X_2 & R_2^TB^T & X_2 - R_2^TB^TC^T \\ AX_1 + BR_1 & BR_2 & -X_1 & 0 \\ -CAX_1 - CBR_1 & X_2 - CBR_2 & 0 & -X_2 \end{bmatrix} < 0 \tag{2.61}$$

If (2.61) holds, the control law matrices K_1 and K_2 can be computed using

$$K_1 = R_1X_1^{-1}, \qquad K_2 = R_2X_2^{-1} \tag{2.62}$$

The control law in the above result requires that the complete state vector is available for measurement. If this is not the case an alternative to the use of an observer is to use a law of the following form which only uses the output vector

$$u_{k+1}(p) = u_k(p) + K_1\zeta_{k+1}(p+1) + K_2\zeta_{k+1}(p) + K_3e_k(p+1) \tag{2.63}$$

where

$$\zeta_{k+1}(p) = y_{k+1}(p-1) - y_k(p-1) = C(x_{k+1}(p-1) - x_k(p-1)) \tag{2.64}$$

where K_1, K_2 and K_3 are the control law matrices. The next step is to design the control matrices. Hence again set $\eta_{k+1}(p+1) = x_{k+1}(p) - x_k(p)$ and let

$$\tilde{\eta}_{k+1}(p+1) = \begin{bmatrix} \eta_{k+1}(p+1) \\ \eta_{k+1}(p) \end{bmatrix} \tag{2.65}$$

The controlled ILC dynamics can be written as

$$\begin{aligned} \tilde{\eta}_{k+1}(p+1) &= \hat{A}\tilde{\eta}_{k+1}(p) + \hat{B}e_k(p) \\ e_{k+1}(p) &= \hat{C}\tilde{\eta}_{k+1}(p) + \hat{D}e_k(p) \end{aligned} \tag{2.66}$$

where

$$\begin{aligned} \hat{A} &= \begin{bmatrix} A+BK_1C & BK_2 \\ I & 0 \end{bmatrix} \\ \hat{B} &= \begin{bmatrix} BK_3 \\ 0 \end{bmatrix} \\ \hat{C} &= \begin{bmatrix} -CA-CBK_1C & -CBK_2C \end{bmatrix} \\ \hat{D} &= I - CBK_3 \end{aligned} \tag{2.67}$$

The following result enables control law design.

Theorem 2.13. *[40] An ILC scheme described by (2.66) is stable along the pass, if there exist matrices $Y > 0$, $Z > 0$, N_1, N_2, and N_3 such that the following LMI with linear constraints holds*

$$\begin{aligned} &\begin{bmatrix} Z-Y & 0 & \Omega_1^T \\ 0 & -Z & \Omega_2^T \\ \Omega_1 & \Omega_2 & -Y \end{bmatrix} < 0 \\ &CY_1 = PC, \; CY_2 = QC \end{aligned} \tag{2.68}$$

where $Y = diag(Y_1,\ Y_2,\ Y_3)$ and

$$\begin{aligned} \Omega_1 &= \begin{bmatrix} AY_1+BN_1C & BN_2C & BN_3 \\ Y_1 & 0 & 0 \\ 0 & 0 & 0 \end{bmatrix} \\ \Omega_1 &= \begin{bmatrix} 0 & 0 & 0 \\ 0 & 0 & 0 \\ -CAY_1-CBN_1C & -CBN_2C & Y_3-CBN_3 \end{bmatrix} \end{aligned} \tag{2.69}$$

and the matrices P and Q are additional decision variables. If the LMI with equality constraints of (2.68) is feasible, the control law matrices calculated using

$$K_1 = N_1P^{-1}, \; K_2 = N_2Q^{-1}, \; K_3 = N_3Y_3^{-1} \tag{2.70}$$

Both of these LMI designs result in a structure that is amenable to implementation. Likewise they have been extended to for example robust control and again this is introduced where relevant in this thesis.

The final points to note that in contrast to designs based on the 2D Roesser model ILC laws have been experimentally verified on a laboratory scale gantry robot that replicates the pick and place operation to which ILC is particularly suited. The details are in [30, 40]. Also the repetitive process setting permits one step design, i.e., regulation of the dynamics along the passes and trial-to-trial error convergence. Also this design method extend directly to differential dynamics, in contrast to lifting based designs.

As discussed above, stability along the trial requires frequency attenuation over the complete frequency spectrum and this could be a very stringent condition. Moreover, in terms of control law design practical experience confirms that often it is only required to impose design conditions over finite frequency ranges. This has led to the development of strong practical stability and design based on the Kalman-Yakubovich-Popov (KYP) lemma. Let $y_\infty(p)$, $x_\infty(p)$ and $u_\infty(p)$ denote the strong limits, if they exist, of $y_k(p)$, $x_k(p)$ and $u_k(p)$. Then strong practical stability [17, 18, 19, 20, 21] requires that these vectors are bounded. In effect, strong practical stability relaxes the bounded input bounded output stability requirement over $P := \{(p,k) : \ k \geq 0, \ p \geq 0\}$ by removing the uniform boundedness requirement as both $k \to \infty$ and $\alpha \to \infty$.

Let $y_k(\infty)$, $x_k(\infty)$ and $u_k(\infty)$ denote the strong limits as $\alpha \to \infty$ of $y_k(p)$, $x_k(p)$ and $u_{k+1}(p)$, respectively. Then the following hold with $D = 0$ in (2.37)

$$\begin{aligned} x_\infty(p+1) &= (A + B_0(I - D_0)^{-1}C)x_\infty(p) + Bu_\infty(p) \\ y_\infty(p) &= (I - D_0)^{-1}Cx_\infty(p) \end{aligned} \tag{2.71}$$

and

$$\begin{aligned} y_{k+1}(\infty) &= (C(I - A)^{-1}B_0 + D_0)y_k(\infty) \\ x_{k+1}(\infty) &= (I - A)^{-1}B_0 y_k(\infty) \end{aligned} \tag{2.72}$$

Hence, if a discrete linear repetitive process described by (2.37) is strong practical stability it must satisfy

[a] $r(D_0) < 1$

[b] $r(A) < 1$

[c] $r(A + B_0(I - D_0)^{-1}C) < 1$

[d] $r(C(I - A)^{-1}B_0 + D_0) < 1$

Consider the control law

$$u_{k+1}(p) = u_k(p) + Ke_k(p+1) \tag{2.73}$$

Using control law (2.73) for (2.1) and the controlled system becomes (2.59) with

$$\hat{A} = A, \qquad \hat{B} = BK,$$
$$\hat{C} = -CA, \qquad \hat{D} = I - CBK \tag{2.74}$$

If the matrix CBK is nonsingular, the condition [c] of strong practical stability always holds.

Theorem 2.14. *[21] The ILC scheme described by (2.59) with $r(A)$ and CBK nonsingular is strong practical stable if there exist $Q > 0$, nonsingular matrix $S = diag\{S_1, S_2\}$ and a regular matrix $\tilde{N} = [0\ N]$, said the following LMI that hold*

$$\begin{bmatrix} -Q & S^T\tilde{A}^T + \tilde{N}^T\tilde{\Pi}^T \\ \tilde{A}S + \tilde{\Pi}\tilde{N} & Q - \hat{E}S - (\hat{E}S)^T \end{bmatrix} < 0 \tag{2.75}$$

where

$$\tilde{A} = \begin{bmatrix} 0 & 0 \\ 0 & \mathrm{I} \end{bmatrix}, \tilde{\Pi} = \begin{bmatrix} B \\ -CB \end{bmatrix}, \hat{E} = \begin{bmatrix} \mathrm{I} - A & 0 \\ CA & \mathrm{I} \end{bmatrix} \tag{2.76}$$

If (2.75) holds, control matrix K is given by $K = NS_2^{-1}$.

In practical, some performance over the finite frequency range is the most important in design. Then generalized KYP lemma [41, 42, 43], which is the basis for many of the new results in the thesis is as follows for the discrete and differential cases respectively.

Lemma 2.15. *[43] For a discrete linear time-invariant system with transfer-function matrix $G(e^{j\theta})$ and frequency response matrix $G(e^{j\theta}) = C(e^{j\theta}\mathrm{I} - A)^{-1}B + D$, the following inequalities are equivalent:*

(i) the frequency domain inequality

$$\begin{bmatrix} G(e^{j\theta}) \\ I \end{bmatrix}^* \Pi \begin{bmatrix} G(e^{j\theta}) \\ I \end{bmatrix} < 0, \ \forall\theta \in \Theta, \tag{2.77}$$

where Π is a given real symmetric matrix and Θ denotes the following frequency ranges

	Low frequency range	Middle frequency range	High frequency range
Θ	$\lvert\theta\rvert \le \theta_l$	$\theta_1 \le \theta \le \theta_2$	$\lvert\theta\rvert \ge \theta_h$

(ii) the LMI

$$\begin{bmatrix} A & B \\ \mathrm{I} & 0 \end{bmatrix}^T \Xi \begin{bmatrix} A & B \\ \mathrm{I} & 0 \end{bmatrix} + \begin{bmatrix} C & D \\ 0 & \mathrm{I} \end{bmatrix}^T \Pi \begin{bmatrix} C & D \\ 0 & \mathrm{I} \end{bmatrix} < 0 \tag{2.78}$$

where $Q > 0$, P is a symmetric matrix and the matrix Ξ is partitioned as

$$\Xi = \begin{bmatrix} \Xi_{11} & \Xi_{12} \\ \Xi_{12}^{*} & \Xi_{22} \end{bmatrix} \tag{2.79}$$

and specified as follows:
for the low frequency range: $|\theta| \leq \theta_l$

$$\Xi = \begin{bmatrix} -P & Q \\ Q & P - 2cos(\theta_l)Q \end{bmatrix} \tag{2.80}$$

for the middle frequency range: $\theta_l \leq \theta \leq \theta_h$

$$\Xi = \begin{bmatrix} -P & e^{j(\theta_1+\theta_2)/2}Q \\ e^{-j(\theta_1+\theta_2)/2}Q & P - (2cos((\theta_2 - \theta_1)/2)Q \end{bmatrix} \tag{2.81}$$

for the high frequency range: $|\theta| \geq \theta_h$

$$\Xi = \begin{bmatrix} -P & -Q \\ -Q & P + 2cos(\theta_h)Q \end{bmatrix} \tag{2.82}$$

and for continuous-time system is

Lemma 2.16. *[43] For a continuous linear time-invariant system with transfer-function matrix $G(j\omega)$ and frequency response matrix*

$$G(j\omega) = C(j\omega I - A)^{-1}B + D$$

the following inequalities are equivalent:

1. *the frequency domain inequality*

$$\begin{bmatrix} G(j\omega) \\ I \end{bmatrix}^{*} \Pi \begin{bmatrix} G(j\omega) \\ I \end{bmatrix} < 0 \tag{2.83}$$

   where Π is a given real symmetric matrix.

2. *the LMI*

$$\begin{bmatrix} A & B \\ I & 0 \end{bmatrix}^{T} \Xi \begin{bmatrix} A & B \\ I & 0 \end{bmatrix} + \begin{bmatrix} C & D \\ 0 & I \end{bmatrix}^{T} \Pi \begin{bmatrix} C & D \\ 0 & I \end{bmatrix} < 0 \tag{2.84}$$

   where $Q > 0$, and P is a positive symmetric matrix and the matrix Ξ is defined as

   - *for the low frequency range $|\omega| \leq \omega_l$*

$$\Xi = \begin{bmatrix} \Xi_{11} & \Xi_{12} \\ \Xi_{12}^{*} & \Xi_{22} \end{bmatrix} = \begin{bmatrix} -Q & P \\ P & -\omega_l^2 Q \end{bmatrix} \tag{2.85}$$

- *for the middle frequency range* $\omega_1 \leq \omega \leq \omega_2$

$$\Xi = \begin{bmatrix} \Xi_{11} & \Xi_{12} \\ \Xi_{12}^* & \Xi_{22} \end{bmatrix} = \begin{bmatrix} -Q & P + j(\omega_1 + \omega_2)/2Q \\ * & -\omega_1\omega_2 Q \end{bmatrix} \tag{2.86}$$

- *for the high frequency range* $|\omega| \neq \omega_h$

$$\Xi = \begin{bmatrix} \Xi_{11} & \Xi_{12} \\ \Xi_{12}^* & \Xi_{22} \end{bmatrix} = \begin{bmatrix} Q & P \\ P & -\omega_h^2 Q \end{bmatrix} \tag{2.87}$$

In [63], the generalized KYP lemma is used to design the control law matrices (more detail can also be found in [64, 65, 66]).

Theorem 2.17. *[63] An ILC scheme described by (2.59) is stable along the trial over the finite frequency ranges in Lemma 2.15 if there exist matrices X_1, X_2, W, $S > 0$, $Q > 0$, $P > 0$ together with real scalars ρ_1 and ρ_2 such that the following LMIs are feasible:*

$$\begin{bmatrix} S + \rho_2 W + \rho_2 W^T & -\rho_2 AW - \rho_2 BX_1 - \rho_1 W^T \\ * & -S + sym\{\rho_1 AW + \rho_1 BX_1\} \end{bmatrix} < 0 \tag{2.88}$$

$$\begin{bmatrix} \Xi_{11} & \Xi_{12} - W^T & 0 & 0 \\ * & \Xi_{22} + sym\{AW + BX_1\} & BX_2 & -W^T A^T C^T - X_1^T B^T C^T \\ * & * & I & I - X_2^T B^T C^T \\ * & * & * & I \end{bmatrix} < 0 \tag{2.89}$$

where the compatibly dimensioned matrices Ξ_{11}, Ξ_{12}, Ξ_{22} form Ξ of (2.79) and ρ_1 and ρ_2 satisfy

$$\rho_1^2 - \rho_2^2 < 0 \tag{2.90}$$

If the LMI (2.88) and (2.89) are feasible, stabilizing control law matrices K_1 and K_2 in (2.58) are given by

$$K_1 = X_1 W^{-1}, \; K_2 = X_2 \tag{2.91}$$

Here the subscript $\{*\}$ denotes block entries in symmetric matrices. Also $sym\{X\}$ is used to denote the symmetric matrix $X + X^T$. One feature of ILC is that all information in the previous trials is known, and it can use them in the control law to update the next trial input. Cichy et al.[16] developed an ILC that uses a weighted sum of phase-lag term and phase-lead term of information in the previous trial (also [15] for stabilize the linear repetitive processes). In the previous control law, the phase-lead term $e_k(p + \lambda)$, $\lambda > 0$ is applied, here the phase-lag term $e_k(p - \lambda)$, $\lambda > 0$ is also used. The control law for system state-space model (2.1) is defined as

$$u_{k+1}(p) = u_k(p) + K_x(x_{k+1}(p) - x_k(p)) + \sum_{i=-\Omega_l}^{\Omega_h} K_i e_k(p+i+1) \tag{2.92}$$

where Ω_l and Ω_h are positive integers and the time interval range from $p-\Omega_l$ to $p+\Omega_h$ denotes the "wave window". Substituting this control law into (2.1), the controlled system is

$$\begin{aligned} \eta_{k+1}(p+1) &= \hat{A}\eta_{k+1}(p) + \sum_{i=-\Omega_l}^{\Omega_h} \hat{B}_i e_k(p+i) \\ e_{k+1}(p) &= \hat{C}\eta_{k+1}(p) + \sum_{i=-\Omega_l}^{\Omega_h} \hat{D}_i e_k(p+i) \end{aligned} \tag{2.93}$$

where

$$\begin{aligned} &\hat{A} = A + BK_x, \quad \hat{B}_0 = BK_0, \quad \hat{B}_i = BK_i, \\ &\hat{C} = -C(A+BK_x), \quad \hat{D}_0 = I - CBK_0, \\ &\hat{D}_i = -CBK_i, \quad i = -\Omega_l, ..., \Omega_h, i \neq 0 \end{aligned} \tag{2.94}$$

The additional boundary condition is

$$e_k(p) = 0, \quad p \in \{-\Omega_l, ..., -1\} \cup \{\alpha, ..., \alpha + \Omega_h - 1\} \tag{2.95}$$

Since this control law applying the weighted sum of phase-lead term and phase-lag term of error information in the control law, the global Lyapunov function is used to obtain the design algorithm, which is shown next

Theorem 2.18. *[16] The ILC scheme described by (2.93) is stable along the trial if there exist matrices $P > 0$, N, $Q_i > 0$ and N_i with $i = -\Omega_l, ..., \Omega_h$, such that the following LMI is feasible:*

$$\begin{bmatrix} -\overline{P} & (\overline{AP} + \overline{BN})^T \\ \overline{AP} + \overline{BN} & -\overline{P} \end{bmatrix} < 0 \tag{2.96}$$

where

$$\overline{A} = \begin{bmatrix} A & 0 & \cdots & 0 & I & 0 & \cdots & 0 \\ -CA & 0 & \cdots & 0 & I & 0 & \cdots & 0 \\ \vdots & \vdots & \ddots & \vdots & \vdots & \vdots & \ddots & \vdots \\ -CA & 0 & \cdots & 0 & I & 0 & \cdots & 0 \end{bmatrix} \tag{2.97}$$

$$\overline{B} = \begin{bmatrix} B & \cdots & B \\ -CB & \cdots & -CB \\ \vdots & \ddots & \vdots \\ -CB & \cdots & -CB \end{bmatrix} \tag{2.98}$$

and

$$\begin{aligned} \overline{P} &= diag\{P, Q_{-\Omega_l}, ..., Q_0, ..., Q_{\Omega_h}\} \\ \overline{N} &= diag\{N, N_{-\Omega_l}, ..., N_0, ..., N_{\Omega_h}\} \end{aligned} \tag{2.99}$$

If the LMI of (2.96) holds, stabilizing matrices in the control law (2.94) are given by

$$\begin{aligned} K_x &= NP^{-1} \\ K_i &= N_i Q_i^{-1}, \quad i = -\Omega_l, ...\Omega_h \end{aligned} \tag{2.100}$$

Robustness is an important issue for ILC design. As in other areas, the approach used is to assume that the uncertainty present is described by a particular model structure. Under the case of norm bounded uncertainty, the state-space model describing the dynamics in the discrete case is

$$\begin{aligned} x_{k+1}(p+1) &= (A+\Delta A)x_{k+1}(p) + (B+\Delta B)u_{k+1}(p) + (B_0+\Delta B_0)y_k(p), \\ y_{k+1}(p) &= (C+\Delta C)x_{k+1}(p) + (D+\Delta D)u_{k+1}(p) + (D_0+\Delta D_0)y_k(p) \end{aligned} \tag{2.101}$$

Here ΔA, ΔB, ΔC, ΔD, ΔB_0, and ΔD_0 are norm-bounded additive perturbations to the state-space model matrices A, B, C, D, B_0 and D_0. The next result is extensively used in the robustness analysis in this thesis.

Theorem 2.19. *[45] For any $\mathcal{F}^T\mathcal{F} \leq \mathrm{I}$, and a scalar $\varepsilon > 0$ the following holds*

$$\Sigma_1\mathcal{F}\Sigma_2 + \Sigma_2^T\mathcal{F}\Sigma_1^T \leq \epsilon^{-1}\Sigma_1\Sigma_1^T + \epsilon\Sigma_2^T\Sigma_2 \tag{2.102}$$

The augmented plant matrix is subject to additive perturbations defined as follows

$$\Phi + \Delta\Phi = \begin{bmatrix} A & B_0 \\ C & D_0 \end{bmatrix} + \begin{bmatrix} \Delta A & \Delta B_0 \\ \Delta C & \Delta D_0 \end{bmatrix} \tag{2.103}$$

If $\mathcal{F}^T\mathcal{F} \leq I$ holds and the uncertainties $\Delta\Phi$ follows the norm bounded structure:

$$\Delta\Phi = \begin{bmatrix} H_1 \\ H_2 \end{bmatrix} \mathcal{F} \begin{bmatrix} E_1 & E_2 \end{bmatrix} = \begin{bmatrix} H_1 \\ H_2 \end{bmatrix} \mathcal{F}E \tag{2.104}$$

Let

$$\Delta A_1 = \begin{bmatrix} \Delta A & \Delta B_0 \\ 0 & 0 \end{bmatrix}, \; \Delta A_2 = \begin{bmatrix} 0 & 0 \\ \Delta C & \Delta D_0 \end{bmatrix} \tag{2.105}$$

hence

$$\Delta\Phi = \Delta A_1 + \Delta A_2 = \hat{H}_1\mathcal{F}E + \hat{H}_2\mathcal{F}E \tag{2.106}$$

where

$$\hat{H}_1 = \begin{bmatrix} H_1 \\ 0 \end{bmatrix}, \ \hat{H}_2 = \begin{bmatrix} 0 \\ H_2 \end{bmatrix} \tag{2.107}$$

The next theorem provides conditions for stability along the pass under norm bounded uncertainty in the discrete case.

Theorem 2.20. *[74] Consider a discrete unit memory linear repetitive process of the form defined by (2.37) in the presence of an uncertainty structure satisfying (2.106) and (2.107). Then this process is stable along the pass if there exist matrices $P > 0$ and $\hat{Q} > 0$ such that*

$$(\hat{A}_0 + \hat{H}\hat{\mathcal{F}}\hat{E})^T P(\hat{A}_0 + \hat{H}\hat{\mathcal{F}}\hat{E}) + \hat{Q} < 0 \tag{2.108}$$

where

$$\hat{A}_0 = \begin{bmatrix} \hat{A}_1 & \hat{A}_2 \end{bmatrix}, \ \hat{Q} = \begin{bmatrix} Q - P & 0 \\ 0 & -Q \end{bmatrix} \tag{2.109}$$

and

$$\hat{H} = \begin{bmatrix} \hat{H}_1 & \hat{H}_2 \end{bmatrix}, \ \hat{\mathcal{F}} := I_2 \otimes \mathcal{F}, \ \hat{E} := I_2 \otimes E \tag{2.110}$$

and $\otimes$ denotes the matrix Kronecker product. By using Theorem 2.19, (2.108) can be written as: for any choice of Q, there exists $P > 0$ such that (2.108) holds if, and only if, there exists a scalar $\epsilon > 0$ such that

$$\begin{bmatrix} -P^{-1} + \epsilon\hat{H}\hat{H}^T & \hat{A}_0 \\ \hat{A}_0^T & \epsilon^{-1}\hat{E}^T\hat{E} + \hat{Q} \end{bmatrix} < 0 \tag{2.111}$$

In [38], two robust ILC design algorithms were developed. The theory is based on the following model with time-varying uncertainty

$$\begin{aligned} x_k(p+1) &= Ax_k(p) + \hat{\mu}E(p)Hx_k(p) + Bu_k(p) \\ y_k(p) &= Cx_k(p), \quad p = 0, 1, ..., \alpha - 1 \end{aligned} \tag{2.112}$$

In the time-varying term $\hat{\mu}E(p)Hx_k(p)$, $\hat{\mu}$ is a constant positive scalar, the normalizing matrix $H \in \mathbb{R}^{h\times n}$ has constant entries and it is $E(p) \in \mathbb{R}^{n\times h}$ that brings in the time-varying dynamics. The last matrix is assumed to satisfy

$$E(p)^T E(p) < 1, \ \forall p = 0, 1, ..., \alpha - 1 \tag{2.113}$$

Using the same notation as above, the controlled dynamics with uncertainty can be written as

$$\begin{aligned} \eta_{k+1}(p+1) &= [\hat{A} + \hat{\mu}\hat{\Psi}(p)]\eta_{k+1}(p) + \hat{B}e_k(p) \\ e_{k+1}(p) &= [\hat{C} - \hat{\mu}\hat{\Gamma}(p)]\eta_{k+1}(p) + \hat{D}e_k(p) \end{aligned} \tag{2.114}$$

where $\hat{A}$, $\hat{B}$, $\hat{C}$ and $\hat{D}$ are defined in (2.59) and

$$\begin{aligned} \hat{\Psi}(p) &:= E(p-1)H \\ \hat{\Gamma}(p) &:= CE(p-1)H \end{aligned} \tag{2.115}$$

Theorem 2.21. *[38] The ILC scheme described by (2.114) is stable along the trial for all time-varying uncertainties satisfying (2.113) if there exist R_1, R_2, $X_1 > 0$, $X_2 > 0$, and scalars $\lambda > 0$ and $\gamma > 0$ such that the following LMI is feasible:*

$$\begin{bmatrix} -X_1 & 0 & X_1A^T+R_1^TB^T & -X_1A^TC^T-R_1^TB^TC^T & X_1H^T \\ 0 & -X_2 & R_2^TB^T & X_2-R_2^TB^TC^T & 0 \\ AX_1+BR_1 & BR_2 & -X_1+\gamma I & 0 & 0 \\ -CAX_1-CBR_1 & X_2-CBR_2 & 0 & -X_2+\gamma CC^T & 0 \\ HX_1 & 0 & 0 & 0 & -0.5\gamma I \end{bmatrix} < 0 \tag{2.116}$$

Also an upper bound for the parameter $\hat{\mu}$ in the time-varying uncertainty description of (2.112) is given by

$$\hat{\mu} = \sqrt{\frac{\gamma}{\lambda}} \tag{2.117}$$

If the condition holds, the control law matrices K_1 and K_2 are given by $K_1 = R_1X_1^{-1}$ and $K_2 = R_2X_2^{-1}$.

This design algorithm provides a compromise between the uncertainty bounds and convergence speed. However, it does not provide K_1 and K_2 for the maximum possible uncertainty bound on $\hat{\mu}$. To remove this difficulty, a second robust design algorithm based on the Generalized Eigenvalue Problem (GEVP) was developed.

Theorem 2.22. *[38] The ILC scheme described by (2.114) is stable along the trial for all time-varying uncertainties satisfying (2.113) if there exist R_1, R_2, $X_1 > 0$, $X_2 > 0$, and a scalar $\lambda > 0$ such that the following GEVP is feasible*

$$\begin{aligned} &minimize\ \eta > 0 \\ &subject\ to: \\ &\begin{bmatrix} 0 & 0 & 0 & 0 & 0 \\ 0 & 0 & 0 & 0 & 0 \\ 0 & 0 & I & 0 & 0 \\ 0 & 0 & 0 & CC^T & 0 \\ 0 & 0 & 0 & 0 & 0 \end{bmatrix} < \eta\Omega \end{aligned} \tag{2.118}$$

where

$$\Omega = \begin{bmatrix} -X_1 & 0 & -X_1A^T - R_1^TB^T & X_1A^TC^T + R_1^TB^TC^T & -X_1H^T \\ 0 & X_2 & -R_2^TB^T & -X_2 + R_2^TB^TC^T & 0 \\ -AX_1 - BR_1 & -BR_2 & X_1 & 0 & 0 \\ CAX_1 + CBR_1 & -X_2 + CBR_2 & 0 & X_2 & 0 \\ -HX_1 & 0 & 0 & 0 & 0.5\gamma I \end{bmatrix} \tag{2.119}$$

and $\Omega > 0$*. Also an upper bound for the parameter* $\hat{\mu}$ *in (2.112) is given by*

$$\hat{\mu}_{max} = \sqrt{\frac{1}{\eta\lambda}} \tag{2.120}$$

If this condition holds, the control law matrices K_1 *and* K_2 *are given by* $K_1 = R_1X_1^{-1}$ *and* $K_2 = R_2X_2^{-1}$*.*

In [63], the case of norm-bounded uncertainty was considered, starting from the state-space model

$$\begin{aligned} x_k(p+1) &= (A + \Delta A)x_k(p) + (B + \Delta B)u_k(p) \\ y_k(p) &= (C + \Delta C)x_k(p) \end{aligned} \tag{2.121}$$

where the perturbations are assumed to be of the norm-bounded form, that is

$$\Delta A = H_1\mathcal{F}(p)E_1, \ \Delta B = H_1\mathcal{F}(p)E_2, \ \Delta C = H_2\mathcal{F}(p)E_1 \tag{2.122}$$

where H_1, H_2, E_1, and E_2 are known real constant matrices of compatible dimensions and $\mathcal{F}(p)$ is an uncertain perturbation satisfying $\mathcal{F}(p)\mathcal{F}^T(p) \leq I$. Applying the control law (2.66), controlled system is in the form of (2.59) with

$$\begin{aligned} &\hat{A} = (A + \Delta A) + (B + \Delta B)K_1, \qquad \hat{B} = (B + \Delta B)K_2, \\ &\hat{C} = -(C + \Delta C)((A + \Delta A) + (B + \Delta B)K_1), \qquad \hat{D} = I - (C + \Delta C)(B + \Delta B)K_2 \end{aligned} \tag{2.123}$$

Apply 2D Lyapunov equation, Schur's complement and Theorem 2.19 to design the control matrices, design robust is as follows.

Theorem 2.23. *[63] An ILC scheme described by (2.59) with uncertainty structure modeled by (2.122) and* $\mathcal{F}(p)\mathcal{F}^T(p) \leq \mathrm{I}$ *is stable along the trial over finite frequency range in Lemma 2.15 if there exist matrices* $S > 0$*,* $Q > 0$*,* $P > 0$*,* X_1*,* X_2*,* $\hat{W}$*,* W_2*,* W_{11}*,* W_{21}*,* W_{31}*,* W_{41} *together with real scalars* ρ_1*,* ρ_2*,* $\epsilon_1 > 0$ *and*

$$\begin{bmatrix} S + sym\{\rho_2\hat{W}\} + \epsilon_1\rho_2^2H_1H_1^T & -\rho_2A\hat{W} - \rho_2BX_1 - \rho_1\hat{W}^T - \epsilon_1\rho_1\rho_2H_1H_1^T & 0 \\ * & -S + sym\{\rho_1A\hat{W} + \rho_1BX_1\} + \epsilon_1\rho_1^2H_1H_1^T & X_1^TE_2^T + \hat{W}^TE_1^T \\ * & * & -\epsilon_1 I \end{bmatrix} < 0 \tag{2.124}$$

$\epsilon_2 > 0$ *such that the following LMIs are feasible:*

$$\begin{bmatrix} \Xi_{11} & \Xi_{12}-\hat{W}^T & 0 & -W_{11}C^T & -W_{11} & W_{11}E_1^T & 0 \\ * & \Omega_{22} & BX_2 & -W_{21}C^T & \Omega_{25} & W_{21}E_1^T & -\hat{W}^T E_1^T+X_1^T E_2^T \\ * & * & I & I-W_{31}C^T & X_2^T B^T-W_{31} & W_{31}E_1^T & X_2^T E_2^T \\ * & * & * & \Omega_{44} & -W_{41}-CW_2^T & W_{41}E_1^T & 0 \\ * & * & * & * & \Omega_{55} & W_2 E_1^T & 0 \\ * & * & * & * & * & -\epsilon_2 I & 0 \\ * & * & * & * & * & -* & -\epsilon_2 I \end{bmatrix} < 0 \qquad (2.125)$$

where

$$\Omega_{22} = \Xi_{22} + sym\{A\hat{W} + BX_1\} + \epsilon_2 H_1 H_1^T, \; \Omega_{25} = \hat{W}^T A^T + X_1^T B^T - W_{21} + \epsilon_2 H_1 H_1^T$$
$$\Omega_{44} = -\mathrm{I} - sym\{W_{41}C^T\} + \epsilon_2 H_2 H_2^T, \; \Omega_{55} = -W_2 - W_2^T + \epsilon_2 H_1 H_1^T \qquad (2.126)$$

and ρ_1 *and* ρ_2 *satisfy (2.90). Consequently, if the LMIs (2.124) and (2.125) are feasible, stabilizing control law matrices* K_1 *and* K_2 *are given by* $K_1 = X_1\hat{W}^{-1}$ *and* $K_2 = X_2$*.*

Moreover, more detail of some robust design for disturbance can be found in [59, 60, 61, 62, 86, 87, 88].

2.7 Higher-order ILC

The novel future of ILC is that all information from the previous trials including error and input are known once they are complete. Therefore an ILC law can use more than one trials information in the control law and such laws are known as higher order. Higher-order ILC was proposed by Gu et al. [34], with application to a PUMA 560 robot. Bien et al. [10] then gave the general form of such a law. Consider system model (2.1), then the higher-order ILC law is of the form

$$u_{k+1}(p) = P_1 u_k(p) + ... + P_N u_{k-N+1}(p) + Q_1 e_k(p) + ... + Q_N e_{k-N+1}(p) \qquad (2.127)$$

where P_i and Q_i, $i \in [1, N]$ are control law matrices, and the condition for trial-to-trial convergence is

$$\sum_{i=1}^{N} P_i = I, \quad \sum_{i=1}^{N} \|P_i - Q_i CB\| < 1 \qquad (2.128)$$

2.8 Summary

This chapter has given a summary of ILC laws and their design with a particular focus on the use of repetitive process stability theory. Also the basics of higher-order ILC has been introduced, where the major aim of this thesis is to extend the use of such control laws. In the next chapter the KYP lemma is used to design a higher-order ILC law using the repetitive process setting.

Chapter 3

New Algorithms for State-Feedback Higher-order Control Law Design Using the KYP Lemma

3.1 Introduction

Higher-order iterative learning control uses error information of several previous trials in control law. In this chapter, a state feedback higher-order ILC control law is used, and an LMI approach is given to design the control law matrices.

When using higher-order control law for a system, the controlled dynamics can be described as a non-unit memory linear repetitive process. Therefore the stability conditions of such process can be used to analyze the ILC performance and design the control law matrices. This chapter gives an LMI design algorithm for the optimal control law matrices. It is difficult to design the control law matrices from stability conditions of non-unit memory linear repetitive process due to the weight summation term of previous trials information. However, by applying the super-vector it can be converted to a unit memory linear repetitive process. Then LMI design algorithm is obtained by using KYP lemma of unit memory linear repetitive process.

In many applications, the systems are modelled with the uncertainties. The classical design methods are much less powerful in such areas. Therefore, a robust control theory is required. In this chapter, the norm-bounded additive uncertainty is considered and the robust design algorithms are developed.

3.2 Higher-order ILC Design for Discrete-time Systems

3.2.1 Problem Setup

Consider the discrete time-invariant linear state-space system model in the ILC setting

$$\begin{aligned} x_k(p+1) &= Ax_k(p) + Bu_k(p), \\ y_k(p) &= Cx_k(p),\ p = 0, 1, ..., \alpha - 1 \end{aligned} \tag{3.1}$$

where $x_k(p) \in \mathbb{R}^n$ is the state vector, $y_k(p) \in \mathbb{R}^m$ is the output vector, $u_k(p) \in \mathbb{R}^l$ is the input vector, k is the trial number, and the finite trial length $\alpha < \infty$. Let $y_d \in \mathbb{R}^m$ be reference trajectory then error on trial k is $e_k(p) = y_d(p) - y_k(p)$. Recognizing the availability of all information generated on the previous trials, a common form of ILC law computes the current trial control input as the sum of that used on the previous trial plus a correction term,i.e., of the form

$$u_{k+1}(p) = u_k(p) + \Delta u_{k+1}(p) \tag{3.2}$$

where $\Delta u_{k+1}(p)$ is a function of the error on trial k but could also be a function of the previous trial control input. A natural extension is to allow $\Delta u_{k+1}(p)$ to be a function of the error and/or control vectors on a finite number of previous trials. In order to use repetitive process theory for ILC design, introduce, for analysis purposes only,

$$\eta_{k+1}(p+1) = x_{k+1}(p) - x_k(p) \tag{3.3}$$

and in (3.2) set

$$\Delta u_{k+1}(p) = K\eta_{k+1}(p+1) + \sum_{j=1}^{M} K_{j-1} e_{k+1-j}(p+1) \tag{3.4}$$

The resulting controlled dynamics state-space model is

$$\begin{aligned} \eta_{k+1}(p+1) &= \hat{A}\eta_{k+1}(p) + \sum_{j=1}^{M} \hat{B}_{j-1} e_{k+1-j}(p) \\ e_{k+1}(p) &= \hat{C}\eta_{k+1}(p) + \sum_{j=1}^{M} \hat{D}_{j-1} e_{k+1-j}(p) \end{aligned} \tag{3.5}$$

where

$$\begin{aligned} &\hat{A} = A + BK, \quad \hat{B}_0 = BK_0, \quad \hat{B}_{j-1} = BK_{j-1}, \\ &\hat{C} = -C(A + BK), \quad \hat{D}_0 = I - CBK_0, \end{aligned}$$

$$\hat{D}_{j-1} = -CBK_{j-1}, \quad j = 2, ..., M \tag{3.6}$$

which is a non-unit memory linear repetitive process, and is stable along the trial if and only if all conditions in Theorem 2.6 are satisfied. Therefore the design algorithm for control law matrices is based on Theorem 2.6. Many researchers have proposed the LMI based design algorithms for such a control law for the unit memory case (Theorem 2.12, Theorem 2.13). However, it is difficult to develop an LMI based design algorithm for higher-order control law since the controlled system is non-unit memory and the summation term of error information on the previous trials cannot be used in the design algorithm directly. This section gives a design algorithm for the higher-order control law matrices which is based on the stability conditions for linear repetitive process.

In some applications, uncertainties will be present in the model structure. For such system models, the general design algorithm cannot guarantee the system stable if it is only based on the normal plant model. Therefore, robust design algorithm is given to solve this problem. In this chapter, the norm-bounded additive uncertainty of the system is considered. A system with norm-bounded uncertainty has the state-space model

$$\begin{aligned} x_k(p+1) &= (A + \Delta A)x_k(p) + (B + \Delta B)u_k(p), \\ y_k(p) &= (C + \Delta C)x_k(p), \quad p = 0, 1, ..., \alpha - 1 \end{aligned} \tag{3.7}$$

and the norm-bounded additive perturbations ΔA, ΔB and ΔC to the state-space model matrices A, B and C are in the form

$$\Delta A = H_1 F E_1, \ \Delta B = H_1 F E_2, \ \Delta C = H_2 F E_1, \tag{3.8}$$

where H_1, H_2, E_1, E_2, and $F \in \mathbb{R}^{r \times r}$ is an unknown matrix that satisfies $F = F^T$ and $FF^T \leq I$. If apply the higher-order control law (3.2) for this model the controlled system is in the form (3.5) with

$$\begin{aligned} &\hat{A} = (A + \Delta A) + (B + \Delta B)K, \quad \hat{B}_0 = (B + \Delta B)K_0, \quad \hat{B}_{j-1} = (B + \Delta B)K_{j-1}, \\ &\hat{C} = -(C + \Delta C)((A + \Delta A) + (B + \Delta B)K), \quad \hat{D}_0 = I - (C + \Delta C)(B + \Delta B)K_0, \\ &\hat{D}_{j-1} = -(C + \Delta C)(B + \Delta B)K_{j-1}, \quad j = 2, ..., M \end{aligned} \tag{3.9}$$

The higher-order ILC control law robust design algorithms are based on the feedback system (3.5) with (3.6) and (3.9), respectively.

3.2.2 LMI Based ILC Design

In the repetitive process setting the state-space model (3.5) is termed non-unit memory, with M denoting the memory length. If $M = 1$ the model of the previous section, termed a unit memory repetitive process, is recovered. The analysis in this part requires (3.5) to be written as a unit memory process, where the result is

$$\begin{aligned}\eta_{k+1}(p+1) &= \hat{A}\eta_{k+1}(p) + \bar{B}\bar{e}_k(p),\\ \bar{e}_{k+1}(p) &= \bar{C}\eta_{k+1}(p) + \bar{D}\bar{e}_k(p),\end{aligned} \tag{3.10}$$

where

$$\begin{aligned}\bar{e}_k(p) &= \begin{bmatrix} e_{k-M+1}^T(p) & \cdots & e_{k-1}^T(p) & e_k^T(p)\end{bmatrix}^T,\\ \bar{B} &= \begin{bmatrix}\hat{B}_{M-1} & \cdots \hat{B}_1 & \hat{B}_0\end{bmatrix},\\ \bar{C} &= \begin{bmatrix}0\\0\\\vdots\\0\\\hat{C}\end{bmatrix},\ \bar{D} = \begin{bmatrix}0 & I & 0 & \cdots & 0\\ 0 & 0 & I & \ddots & 0\\ 0 & 0 & 0 & \cdots & 0\\ \vdots & \vdots & \vdots & \ddots & I\\ \hat{D}_{M-1} & \hat{D}_{M-2} & \hat{D}_{M-3} & \cdots & \hat{D}_0\end{bmatrix},\end{aligned} \tag{3.11}$$

Applying the z-transform, i.e., $zx_k(p) = x_k(p+1)$, (see [74] for the details of how to avoid problems arising from the finite trial length) to (3.10) gives

$$\bar{e}_{k+1}(z) = G(z)\bar{e}_k(z) \tag{3.12}$$

where $G(z) = \bar{C}(zI - \hat{A})^{-1}\bar{B} + \bar{D}$. The term in transfer-function matrix $G(z)$ which relates the convergence performance is only the bottom row, i.e.,

$$e_{k+1}(z) = [G_{M-1}(z), ..., G_1(z), G_0(z)]\bar{e}_k(z) \tag{3.13}$$

The design objective is to select the gains K, $K_{j-1}, j = 1, ..., M$ such that the norm of the above transfer function is sufficiently small and thus convergence can be achieved. First give the following theorem.

Theorem 3.1. *For a given $\gamma > 0$ the discrete linear repetitive process representing the ILC dynamics described by (3.10) is stable along the trial and satisfies*

$$\|[G_{M-1}(z), ..., G_1(z), G_0(z)]\|_\infty < \gamma \tag{3.14}$$

if there exist symmetric matrix $P_1 > 0$, and N_1, N_2 with $\mu = \gamma^2$ such that following LMIs are feasible

$$\begin{bmatrix} -P+Q & * \\ A_1P + B_1N & -P\end{bmatrix} < 0 \tag{3.15}$$

$$\begin{bmatrix} -P & * \\ A_2P + B_2N & -P\end{bmatrix} < 0 \tag{3.16}$$

where

$$A_1 = \begin{bmatrix} A & 0 & 0 & \cdots & 0 \\ -CA & 0 & 0 & \cdots & I \end{bmatrix}, \; B_1 = \begin{bmatrix} B & B \\ -CB & -CB \end{bmatrix},$$
$$A_2 = \begin{bmatrix} A & 0 & 0 & \cdots & 0 \\ 0 & 0 & I & \cdots & 0 \\ \vdots & \vdots & \vdots & \ddots & \vdots \\ 0 & 0 & 0 & \cdots & I \\ -CA & 0 & 0 & \cdots & I \end{bmatrix}, \; B_2 = \begin{bmatrix} B & B \\ 0 & 0 \\ \vdots & \vdots \\ 0 & 0 \\ -CB & -CB \end{bmatrix},$$

and

$$P = diag\{P_1, I\}, \quad Q = diag\{0, (1-\mu)I\}, \quad N = diag\{N_1, N_2\}.$$

The stabilizing control law matrices are given by

$$K = N_1 P_1^{-1}, \; [K_{M-1}, ..., \; K_1, \; K_0] = N_2 \tag{3.17}$$

Proof. The LMI (3.16) can be written as

$$\Phi^T P \Phi - P < 0 \tag{3.18}$$

where

$$\Phi = \begin{bmatrix} \hat{A} & \bar{B} \\ \bar{C} & \bar{D} \end{bmatrix} \tag{3.19}$$

which is 2D Lyapunov inequality for stability of discrete linear repetitive process [74], and the feedback system is stable along the trial. The condition (3.14) can be written as

$$\begin{bmatrix} (zI-\hat{A})^{-1}\bar{B} \\ I \end{bmatrix}^T \begin{bmatrix} \hat{C} & \tilde{D} \\ 0 & I \end{bmatrix}^T \begin{bmatrix} I & 0 \\ 0 & -\mu I \end{bmatrix} \begin{bmatrix} \hat{C} & \tilde{D} \\ 0 & I \end{bmatrix} \begin{bmatrix} (zI-\hat{A})^{-1}\bar{B} \\ I \end{bmatrix} < 0 \tag{3.20}$$

Also by the bounded real lemma [22, 91], this last condition holds if and only if the following LMI holds

$$\begin{bmatrix} \hat{A}^T P_1 \hat{A} - P_1 & \hat{A}^T P_1 \bar{B} \\ \bar{B}^T P_1 \hat{A} & \bar{B}^T P_1 \bar{B} \end{bmatrix} + \begin{bmatrix} \hat{C} & \tilde{D} \\ 0 & I \end{bmatrix}^T \begin{bmatrix} I & 0 \\ 0 & -\mu I \end{bmatrix} \begin{bmatrix} \hat{C} & \tilde{D} \\ 0 & I \end{bmatrix} < 0 \tag{3.21}$$

Where $\tilde{D} = [\hat{D}_{M-1}, ..., \; \hat{D}_0]$, by using the Schur's complement formula, the LMI (3.15) can be obtained from (3.21), and proof is complete. □

The next theorem shows that when γ is small, the tracking error is guaranteed to converge to zero.

Theorem 3.2. *If for $\gamma \in (0, 1/\sqrt{M})$ the design in Theorem 3.1 is feasible, the tracking error converges to zero as $k \to \infty$. Moreover, the convergence is monotonic in the sense that*

$$\max\{\|e_{k+1}\|, ..., \|e_{k-M+2}\|\} < \gamma \max\{\|e_k\|, ..., \|e_{k-M+1}\|\}$$

Proof. When the design algorithm in Theorem 3.1 is feasible,

$$\|e_{k+1}\|_2^2 < \gamma^2 \sum_{i=0}^{M-1} \|e_{k-i}\|_2^2 \tag{3.22}$$

Define $q = \gamma^2 M$. As $\gamma < 1/\sqrt{M}$, $q < 1$. Hence

$$\begin{aligned} \|e_{k+1}\|_2^2 &< \gamma^2 \times \{\|e_{k-M+1}\|_2^2 + ... + \|e_k\|_2^2\} \\ &< q \times \max\{\|e_{k-M+1}\|_2^2, ..., \|e_k\|_2^2\} \end{aligned} \tag{3.23}$$

Furthermore,

$$\begin{aligned} \|e_{k+2}\|_2^2 &< q \times \{\|e_{k-M+2}\|_2^2 + ... + \|e_{k+1}\|_2^2\} \\ &< q \times \max\{\|e_{k-M+1}\|_2^2, ..., \|e_k\|_2^2\} \end{aligned} \tag{3.24}$$

Following a similar argument

$$\begin{aligned} &\max\{\|e_{k+1}\|_2^2, ..., \|e_{k-M+2}\|_2^2\} \\ &\quad < q \times \max\{\|e_{k-M+1}\|_2^2, ..., \|e_k\|_2^2\} \\ &\quad < q^k \times \max\{\|e_{M-1}\|_2^2, ..., \|e_0\|_2^2\} \end{aligned} \tag{3.25}$$

Since $q < 1$, the value of $q^k \to 0$ as $k \to \infty$, and hence $\|e_\infty\|_2 = 0$, which completes the proof. □

From the above theorem it can be seen that γ characterizes how quickly the trial-to-trial error converges to zero under the higher order ILC design. In practice, a faster convergence is usually desirable. This can be achieved by finding the minimum γ value by solving the following minimization problem.

$$\min_{P_1>0, \gamma<1, N_1, N_2} \mu \tag{3.26}$$

where μ is defined in the Theorem 3.1.

3.2.3 Robust Design Algorithm

In this section, a robust design algorithm can solve this problem for the norm-bounded uncertainty in the system. The uncertainty based feedback system model can be converted to the unit-memory repetitive processes (3.10), (3.11) with (3.9), and the robust design result can now be established.

Theorem 3.3. *For a given $\gamma > 0$ the discrete linear repetitive process representing the ILC dynamics of (3.5) with additive uncertainties ΔA, ΔB, and ΔC in (3.9) is stable along the trial and satisfies (3.14) if there exist matrices $P_1 > 0$, N_1, N_2, W_{1x}, W_{2x}, W_{1j} for $j = 0, ..., M-1$, W_{20}, W_3, W_{4x}, W_{5x}, W_{4j}, W_{5j} for $j = 0, ..., M-1$, W_6 with appropriate dimensions and real scalar $\epsilon_1 > 0$, $\epsilon_2 > 0$ and $\mu = \gamma^2$ such that the following LMI is feasible*

$$\begin{bmatrix} -P+Q & * & * & * & * \\ A_2P+B_2N & \Delta_{22} & * & * & * \\ \Delta_{31} & \Delta_{32} & \Delta_{33} & * & * \\ \Delta_{41} & \Delta_{42} & \Delta_{43} & \Delta_{44} & * \\ \Delta_{51} & \Delta_{52} & \Delta_{53} & \Delta_{54} & \Delta_{55} \end{bmatrix} < 0 \tag{3.27}$$

$$\begin{bmatrix} -P & * & * & * & * \\ A_3P+B_3N & \Delta_{62} & * & * & * \\ \Delta_{71} & \Delta_{72} & \Delta_{73} & * & * \\ \Delta_{81} & \Delta_{82} & \Delta_{83} & \Delta_{84} & * \\ \Delta_{91} & \Delta_{92} & \Delta_{93} & \Delta_{94} & \Delta_{95} \end{bmatrix} < 0 \tag{3.28}$$

where P, Q, and N are defined in the Theorem 3.1 and

$$A_2 = \begin{bmatrix} A & 0 & 0 & \cdots & 0 \end{bmatrix}, \quad B_2 = \begin{bmatrix} B & B \end{bmatrix}, \quad I_2 = \begin{bmatrix} 0 & \cdots & 0 & I \end{bmatrix},$$

$$A_3 = \begin{bmatrix} A & 0 & 0 & \cdots & 0 \\ 0 & 0 & I & \cdots & 0 \\ \vdots & \vdots & 0 & \ddots & \vdots \\ 0 & 0 & 0 & \cdots & I \end{bmatrix}, \quad B_3 = \begin{bmatrix} B & B \\ 0 & 0 \\ \vdots & \vdots \\ 0 & 0 \end{bmatrix}, \quad I_1 = \begin{bmatrix} 0 & I & \cdots & 0 \\ \vdots & \vdots & \ddots & \vdots \\ 0 & 0 & \cdots & I \end{bmatrix},$$

and

$$\begin{aligned} \Delta_{22} &= -P_1 + \epsilon_1 H_1 H_1^T, \\ \Delta_{31} &= [-CW_{1x}^T, -CW_{1M-1}^T, ..., -CW_{11}^T, I - CW_{10}^T], \\ \Delta_{32} &= -CW_{2x}^T, \\ \Delta_{33} &= -I - CW_{20}^T - W_{20}C^T + \epsilon_1 H_2 H_2^T, \end{aligned}$$

$$\Delta_{41} = A_2P + B_2N + [-W_{1x}^T, -W_{1M-1}^T, ..., -W_{10}^T],$$
$$\Delta_{42} = -W_{2x}^T,$$
$$\Delta_{43} = -W_{20}^T - W_3C^T,$$
$$\Delta_{44} = -W_3 - W_3^T + \epsilon_1 H_1 H_1^T,$$
$$\bar{E}_1 = [E_1 \ 0 \ 0, ..., \ 0], \ \bar{E}_2 = [E_2 \ E_2],$$
$$\Delta_{51} = \begin{bmatrix} & \bar{E}_1P + \bar{E}_2N & & \\ -E_1W_{1x}^T & -E_1W_{1M-1}^T & \cdots & -E_1W_{10}^T \\ & \bar{E}_1P + \bar{E}_2N & & \end{bmatrix},$$
$$\Delta_{52} = \begin{bmatrix} 0 \\ -E_1W_{2x}^T \\ 0 \end{bmatrix}, \quad \Delta_{53} = \begin{bmatrix} 0 \\ -E_1W_{20}^T \\ 0 \end{bmatrix},$$
$$\Delta_{54} = \begin{bmatrix} 0 \\ -E_1W_3^T \\ 0 \end{bmatrix}, \quad \Delta_{55} = \begin{bmatrix} -\epsilon_1 I & 0 & 0 \\ 0 & -\epsilon_1 I & 0 \\ 0 & 0 & -\epsilon_1 I \end{bmatrix},$$
$$\Delta_{62} = diag\{-P_1 + \epsilon_2 H_1 H_1^T, -I\},$$
$$\Delta_{71} = [-CW_{4x}^T, -CW_{4M-1}^T, ..., -CW_{41}^T, I - CW_{40}^T],$$
$$\Delta_{72} = [-CW_{5x}^T, -CW_{5M-1}^T, ..., -CW_{51}^T],$$
$$\Delta_{73} = -I - CW_{50}^T - W_{50}C^T + \epsilon_2 H_2 H_2^T,$$
$$\Delta_{81} = A_2P + B_2N + [-W_{4x}^T, -W_{4M-1}^T, ..., -W_{40}^T],$$
$$\Delta_{82} = [-W_{5x}^T, -W_{5M-1}^T, ..., -W_{51}^T],$$
$$\Delta_{83} = -W_{50}^T - W_6C^T,$$
$$\Delta_{84} = -W_6 - W_6^T + \epsilon_2 H_1 H_1^T,$$
$$\Delta_{91} = \begin{bmatrix} & \bar{E}_1P + \bar{E}_2N & & \\ -E_1W_{4x}^T & -E_1W_{4M-1}^T & \cdots & -E_1W_{40}^T \\ & \bar{E}_1P + \bar{E}_2N & & \end{bmatrix},$$
$$\Delta_{92} = \begin{bmatrix} 0 & 0 & \cdots & 0 \\ -E_1W_{5x}^T & -E_1W_{5M-1}^T & \cdots & -E_1W_{51}^T \\ 0 & 0 & \cdots & 0 \end{bmatrix},$$
$$\Delta_{93} = \begin{bmatrix} 0 \\ -E_1W_{50}^T \\ 0 \end{bmatrix}, \quad \Delta_{94} = \begin{bmatrix} 0 \\ -E_1W_6^T \\ 0 \end{bmatrix},$$
$$\Delta_{95} = \begin{bmatrix} -\epsilon_2 I & 0 & 0 \\ 0 & -\epsilon_2 I & 0 \\ 0 & 0 & -\epsilon_2 I \end{bmatrix},$$

If the LMI (3.27) and (3.28) are feasible, stabilizing control law matrices are given by

$$K = N_1P_1^{-1}, \ [K_{M-1}, \ ..., \ K_1, \ K_0] = N_2 \tag{3.29}$$

with use of the linear objective minimization procedure (3.26).

Proof. Direct substitution of (3.9) into (3.15) and (3.16) introduces nonlinear terms. To avoid these and obtain LMIs, apply Theorem 2.19 to these two LMIs, and then the Schur's complement formula gives (3.27) and proof is complete. □

Theorem 3.4. *If for $\gamma \in (0, 1/\sqrt{M})$ the design in Theorem 3.3 is feasible, the tracking error converges to zero as $k \to \infty$ even with the presence of model uncertainty ΔA, ΔB and ΔC. Moreover, the convergence is monotonic in the sense that*

$$\max\{\|e_{k+1}\|, ..., \|e_{k-M+2}\|\} < \gamma \max\{\|e_k\|, ..., \|e_{k-M+1}\|\}$$

Proof. This follows identical steps to that of Theorem 3.2 and here the details are omitted. □

3.3 Higher-order ILC Design for Continuous-time Systems

3.3.1 Problem Setup

Consider the continuous time-invariant linear state-space system model in the ILC setting

$$\begin{aligned} \dot{x}_k(t) &= Ax_k(t) + Bu_k(t), \\ y_k(t) &= Cx_k(t), 0 < t \leq \alpha \end{aligned} \tag{3.30}$$

where x_k, y_k, and u_k are state, output and input vector, respectively, and k is the trial number, and the finite trial length $\alpha < \infty$. If y_d denote the reference trajectory then the error on trial k is $e_k(t) = y_d(t) - y_k(t)$. The ILC law is

$$u_{k+1}(t) = u_k(t) + \Delta u_{k+1}(t) \tag{3.31}$$

where $\Delta u_{k+1}(t)$ is a function of the error on trial k but could also be a function of the previous trial control input. A natural extension is to allow $\Delta u_{k+1}(t)$ to be a function of the error and/or control vectors on a finite number of previous passes. In order to use repetitive process theory for ILC design, introduce, for analysis purposes only,

$$\eta_{k+1}(t) = \int_0^t (x_{k+1}(t) - x_k(t))dt \tag{3.32}$$

and in (3.31) set

$$\Delta u_{k+1}(t) = K\eta_{k+1}(t) + \sum_{j=1}^{M} K_{j-1}\dot{e}_{k+1-j}(t) \tag{3.33}$$

The resulting controlled dynamics state-space model is

$$\begin{aligned}\dot{\eta}_{k+1}(t) &= \hat{A}\eta_{k+1}(t) + \sum_{j=1}^{M} \hat{B}_{j-1} e_{k+1-j}(t),\\ e_{k+1}(t) &= \hat{C}\eta_{k+1}(t) + \sum_{j=1}^{M} \hat{D}_{j-1} e_{k+1-j}(t),\end{aligned} \tag{3.34}$$

where

$$\begin{aligned}&\hat{A} = A + BK, \quad \hat{B}_0 = BK_0, \quad \hat{B}_{j-1} = BK_{j-1},\\ &\hat{C} = -C(A+BK), \quad \hat{D}_0 = I - CBK_0,\end{aligned}$$

$$\hat{D}_{j-1} = -CBK_{j-1}, \quad j = 2, ..., M \tag{3.35}$$

This non-unit memory linear repetitive process. It is stable along the pass if and only if all conditions in Theorem 2.10 are satisfied. In a similar manner to the discrete case, the model with uncertainty present is

$$\begin{aligned}\dot{x}_k(t) &= (A + \Delta A)x_k(t) + (B + \Delta B)u_k(t),\\ y_k(t) &= (C + \Delta C)x_k(t), \quad 0 < t \leq \alpha\end{aligned} \tag{3.36}$$

and the norm-bounded additive perturbations ΔA, ΔB and ΔC to the state-space model matrices A, B and C are of the form

$$\Delta A = H_1 F E_1, \ \Delta B = H_1 F E_2, \ \Delta C = H_2 F E_1 \tag{3.37}$$

where H_1, H_2, E_1, E_2, and $F \in \mathbb{R}^{r\times r}$ is an unknown matrix that satisfies $F = F^T$ and $FF^T \leq I$. If apply the control law (3.31) for this model the controlled system is in the form (3.34) with

$$\begin{aligned}&\hat{A} = (A + \Delta A) + (B + \Delta B)K, \quad \hat{B}_0 = (B + \Delta B)K_0, \quad \hat{B}_{j-1} = (B + \Delta B)K_{j-1},\\ &\hat{C} = -(C + \Delta C)((A + \Delta A) + (B + \Delta B)K), \quad \hat{D}_0 = I - (C + \Delta C)(B + \Delta B)K_0,\\ &\hat{D}_{j-1} = -(C + \Delta C)(B + \Delta B)K_{j-1}, \quad j = 2, ..., M\end{aligned} \tag{3.38}$$

3.3.2 LMI Based ILC Design

Since the state-space model (3.34) is non-unit memory , with M denoting the memory length, the analysis in this section requires (3.34) to be written as a unit memory process, where the result is

$$\begin{aligned}\dot{\eta}_{k+1}(t) &= \hat{A}\eta_{k+1}(t) + \bar{B}\bar{e}_k(t),\\ \bar{e}_{k+1}(t) &= \bar{C}\eta_{k+1}(t) + \bar{D}\bar{e}_k(t),\end{aligned} \tag{3.39}$$

where

$$\begin{aligned}\bar{e}_k(t) &= \begin{bmatrix} e^T_{k-M+1}(t) & \cdots & e^T_{k-1}(t) & e^T_k(t)\end{bmatrix}^T,\\ \bar{B} &= \begin{bmatrix}\hat{B}_{M-1} & \cdots \hat{B}_1 & \hat{B}_0\end{bmatrix},\\ \bar{C} &= \begin{bmatrix}0\\0\\ \vdots \\ 0\\ \hat{C}\end{bmatrix},\ \bar{D} = \begin{bmatrix}0 & I & 0 & \cdots & 0\\ 0 & 0 & I & \ddots & 0\\ 0 & 0 & 0 & \cdots & 0\\ \vdots & \vdots & \vdots & \ddots & I\\ \hat{D}_{M-1} & \hat{D}_{M-2} & \hat{D}_{M-3} & \cdots & \hat{D}_0\end{bmatrix},\end{aligned} \tag{3.40}$$

Using Laplace transform, i.e., $L[\dot{x}_k(t)] = sL[x_k(t)] - x_k(0)$, (see [74] for the details of how to avoid problems arising from the finite trial length) to (3.39) gives

$$\bar{e}_{k+1}(s) = G(s)\bar{e}_k(s) \tag{3.41}$$

where $G(s) = \bar{C}(sI - \hat{A})^{-1}\bar{B} + \bar{D}$. The term in transfer-function matrix $G(s)$ which relates the convergence performance is only the bottom row, i.e.,

$$e_{k+1}(s) = [G_{M-1}(s), ..., G_1(s), G_0(s)]\bar{e}_k(s) \tag{3.42}$$

and the objective is to select the gains K, $K_{j-1}, j = 1, ..., M$ such that the norm of the above transfer function is small and thus convergence can be achieved.

Theorem 3.5. *For a given $\gamma > 0$ the differential linear repetitive process representing the ILC dynamics described by (3.39) is stable along the trial and satisfies*

$$\|[G_{M-1}(s), ..., G_1(s), G_0(s)]\|_\infty < \gamma \tag{3.43}$$

if there exist symmetric matrix $P_1 > 0$, and N_1, N_2 with $\mu = \gamma^2$ such that following LMIs are feasible

$$\begin{bmatrix} sym\{AP_1 + BN_1\} & BN_2 & -P_1A^TC^T - N_1^TB^TC^T\\ N_2^TB^T & -\mu I & I_0^T - N_2^TB^TC^T\\ -CAP_1 - CBN_1 & I_0 - CBN_2 & -I\end{bmatrix} < 0 \tag{3.44}$$

$$\begin{bmatrix} sym\{AP_1 + BN_1\} & BN_2 & -P_1A^TC_1^T - N_1^TB^TC_1^T\\ N_2^TB^T & -I & I_1^T - N_2^TB^TC_1^T\\ -C_1AP_1 - C_1BN_1 & I_1 - C_1BN_2 & -I\end{bmatrix} < 0 \tag{3.45}$$

where

$$C_1 = \begin{bmatrix} 0 \\ 0 \\ \vdots \\ 0 \\ C \end{bmatrix}, I_1 = \begin{bmatrix} 0 & I & 0 & \cdots & 0 \\ 0 & 0 & I & \cdots & 0 \\ \vdots & \vdots & \vdots & \ddots & \vdots \\ 0 & 0 & 0 & \cdots & I \\ 0 & 0 & 0 & \cdots & I \end{bmatrix}, I_0 = \begin{bmatrix} 0 & 0 & 0 & \cdots & I \end{bmatrix}, \tag{3.46}$$

The stabilizing control law matrices are given by

$$K = N_1 P_1^{-1}, \ [K_{M-1}, ..., \ K_1, \ K_0] = N_2 \tag{3.47}$$

Proof. The LMI (3.45) can be written as

$$\Phi^T \begin{bmatrix} P_1 & 0 \\ 0 & 0 \end{bmatrix} + \begin{bmatrix} P_1 & 0 \\ 0 & 0 \end{bmatrix} \Phi + \Phi^T \begin{bmatrix} 0 & 0 \\ 0 & I \end{bmatrix} \Phi - \begin{bmatrix} 0 & 0 \\ 0 & I \end{bmatrix} < 0 \tag{3.48}$$

where

$$\Phi = \begin{bmatrix} \hat{A} & \bar{B} \\ \bar{C} & \bar{D} \end{bmatrix} \tag{3.49}$$

which is 2D Lyapunov inequality for stability of differential linear repetitive process [74], and the feedback system is stable along the trial. The condition (3.44) can be written as

$$\begin{bmatrix} (j\omega I - \hat{A})^{-1}\bar{B} \\ I \end{bmatrix}^T \begin{bmatrix} \hat{C} & \tilde{D} \\ 0 & I \end{bmatrix}^T \begin{bmatrix} I & 0 \\ 0 & -\mu I \end{bmatrix} \begin{bmatrix} \hat{C} & \tilde{D} \\ 0 & I \end{bmatrix} \begin{bmatrix} (j\omega I - \hat{A})^{-1}\bar{B} \\ I \end{bmatrix} < 0 \tag{3.50}$$

Also by the bounded real lemma [91], this last condition holds if and only if the following LMI holds

$$\begin{bmatrix} \hat{A}^T P_1 + P_1 \hat{A} & P_1 \bar{B} \\ \bar{B}^T P_1 & 0 \end{bmatrix} + \begin{bmatrix} \hat{C}^T \hat{C} & \hat{C}^T \tilde{D} \\ \tilde{D}^T \hat{C} & \tilde{D}^T \tilde{D} - \mu I \end{bmatrix} < 0 \tag{3.51}$$

Where $\tilde{D} = [\hat{D}_{M-1}, ..., \ \hat{D}_0]$, by using Schur's complement formula, the LMI (3.44) is obtained from (3.51), and proof is complete. □

The next theorem shows that when γ is small, the tracking error is guaranteed to convergence to zero.

Theorem 3.6. *If for $\gamma \in (0, 1/\sqrt{M})$ the design in Theorem 3.5 is feasible, the tracking error converges to zero as $k \to \infty$. Moreover, the convergence is monotonic in the sense that*

$$\max\{\|e_{k+1}\|, ..., \|e_{k-M+2}\|\} < \gamma \max\{\|e_k\|, ..., \|e_{k-M+1}\|\}$$

Proof. When the design algorithm in Theorem 3.5 is feasible,

$$\|e_{k+1}\|_2^2 < \gamma^2 \sum_{i=0}^{M-1} \|e_{k-i}\|_2^2 \tag{3.52}$$

Define $q = \gamma^2 M$. As $\gamma < 1/\sqrt{M}$, $q < 1$. Hence

$$\begin{aligned} \|e_{k+1}\|_2^2 &< \gamma^2 \times \{\|e_{k-M+1}\|_2^2 + ... + \|e_k\|_2^2\} \\ &< q \times \max\{\|e_{k-M+1}\|_2^2, ..., \|e_k\|_2^2\} \end{aligned} \tag{3.53}$$

Furthermore,

$$\begin{aligned} \|e_{k+2}\|_2^2 &< q \times \{\|e_{k-M+2}\|_2^2 + ... + \|e_{k+1}\|_2^2\} \\ &< q \times \max\{\|e_{k-M+1}\|_2^2, ..., \|e_k\|_2^2\} \end{aligned} \tag{3.54}$$

Similarly

$$\begin{aligned} &\max\{\|e_{k+1}\|_2^2, ..., \|e_{k-M+2}\|_2^2\} \\ &\quad < q \times \max\{\|e_{k-M+1}\|_2^2, ..., \|e_k\|_2^2\} \\ &\quad < q^k \times \max\{\|e_{M-1}\|_2^2, ..., \|e_0\|_2^2\} \end{aligned} \tag{3.55}$$

Since $q < 1$, the value of $q^k \to 0$ as $k \to \infty$, and hence $\|e_\infty\|_2 = 0$, which completes the proof. □

From the above theorem it can be seen that γ characterizes how quickly the tracking error converges to zero under the higher order ILC design. In practice, a faster convergence is usually desirable. This can be achieved by solving the following minimization problem.

$$\min_{P_1>0, \gamma<1, N_1, N_2} \mu \tag{3.56}$$

where $\mu = \gamma^2$, which is defined in the Theorem 3.5.

3.3.3 Robust Design Algorithm

Following the same argument on the discrete case in section 3.2.3, gives the theorem,

Theorem 3.7. *For a given $\gamma > 0$ the differential linear repetitive process representing the ILC dynamics of (3.39) with additive uncertainties ΔA, ΔB, and ΔC in (3.37) is stable along the trial and satisfies (3.43) if there exist matrices $P_1 > 0$, N_1, N_2, W_{1x}, W_{2x}, W_{1j} for $j = 0, ..., M-1$, W_2, W_{3x}, W_{4x}, W_{3j}, W_4 for $j = 0, ..., M-1$, W_6 with appropriate dimensions and real scalar $\epsilon_1 > 0$, $\epsilon_2 > 0$ and $\mu = \gamma^2$ such that the following*

LMI is feasible

$$\begin{bmatrix} \Delta_{11} & * & * & * & * & * & * \\ N_2^T B^T & -\mu I & * & * & * & * & * \\ -CW_{1x}^T & I_0 - CW_1^T & \Delta_{33} & * & * & * & * \\ AP_1 + BN_1 - W_{1x}^T & BN_2 - W_1^T & -W_{2x}^T - W_2 C^T & \Delta_{44} & * & * & * \\ E_1 P_1 + E_2 N_1 & E_2 N_2 & 0 & 0 & -\epsilon_1 I & * & * \\ -E_1 W_{1x}^T & -E_1 W_1^T & -E_1 W_{2x}^T & -E_1 W_2^T & 0 & -\epsilon_1 I & * \\ E_1 P_1 + E_2 N_1 & E_2 N_2 & 0 & 0 & 0 & 0 & -\epsilon_1 I \end{bmatrix} < 0 \tag{3.57}$$

$$\begin{bmatrix} \Delta_{51} & * & * & * & * & * & * \\ N_2^T B^T & -I & * & * & * & * & * \\ -C_1 W_{3x}^T & I_1 - C_1 W_3^T & \Delta_{63} & * & * & * & * \\ AP_1 + BN_1 - W_{3x}^T & BN_2 - W_3^T & -W_{4x}^T - W_4 C_1^T & \Delta_{74} & * & * & * \\ E_1 P_1 + E_2 N_1 & E_2 N_2 & 0 & 0 & -\epsilon_2 I & * & * \\ -E_1 W_{3x}^T & -E_1 W_3^T & -E_1 W_{4x}^T & -E_1 W_4^T & 0 & -\epsilon_2 I & * \\ E_1 P_1 + E_2 N_1 & E_2 N_2 & 0 & 0 & 0 & 0 & -\epsilon_2 I \end{bmatrix} < 0 \tag{3.58}$$

where I_0, I_1, and C_1 are defined in (3.46) and

$$\begin{aligned} \Delta_{11} &= sym\{AP_1 + BN_1\} + \epsilon_1 H_1 H_1^T, \\ \Delta_{33} &= -I - CW_{2x}^T - W_{2x} C^T + \epsilon_1 H_2 H_2^T, \\ \Delta_{44} &= -W_2 - W_2^T + \epsilon_1 H_1 H_1^T, \\ \Delta_{51} &= sym\{AP_1 + BN_1\} + \epsilon_2 H_1 H_1^T, \\ \Delta_{63} &= -I - CW_{4x}^T - W_{4x} C^T + \epsilon_2 H_3 H_3^T, \\ \Delta_{74} &= -W_4 - W_4^T + \epsilon_2 H_1 H_1^T, \end{aligned}$$

and $W_1 = [W_{1M-1}, ..., W_{11}]$, $W_3 = [W_{3M-1}, ..., W_{31}]$, $H_3 = [0, ..., 0, H_2]^T$.

If the LMIs (3.57) and (3.58) are satisfied, the stabilizing control law matrices are given by

$$K = N_1 P_1^{-1}, \ [K_{M-1}, ..., \ K_1, \ K_0] = N_2 \tag{3.59}$$

with use of the linear objective minimization procedure (3.56).

Proof. Direct substitution of (3.9) into (3.44) and (3.45) introduces nonlinear terms. To avoid these and obtain LMIs, apply Theorem 2.19 to these two LMIs, and then the Schur's complement formula gives the LMI (3.57) and (3.58) and proof is complete. □

and the next theorem gives the condition for error convergence to zero as trial increase to infinity.

Theorem 3.8. *If for $\gamma \in (0, 1/\sqrt{M})$ the design in Theorem 3.7 is feasible, the tracking error converges to zero as $k \to \infty$ even with the presence of model uncertainty ΔA, ΔB and ΔC. Moreover, the convergence is monotonic in the sense that*

$$\max\{\|e_{k+1}\|, ..., \|e_{k-M+2}\|\} < \gamma \max\{\|e_k\|, ..., \|e_{k-M+1}\|\}$$

Proof. This follows identical steps to that of Theorem 3.6 and here the details are omitted. □

3.4 Numerical Examples

In this section, numerical examples are used to test the design algorithms developed earlier in this chapter. In this simulation, the value of memory length M is from 1 to 5, and the number of trials is 40, the trial length is 2 sec. In the simulation, the reference trajectory is the same for the discrete-time systems and continuous-time system example, and is shown in figure 3.1.

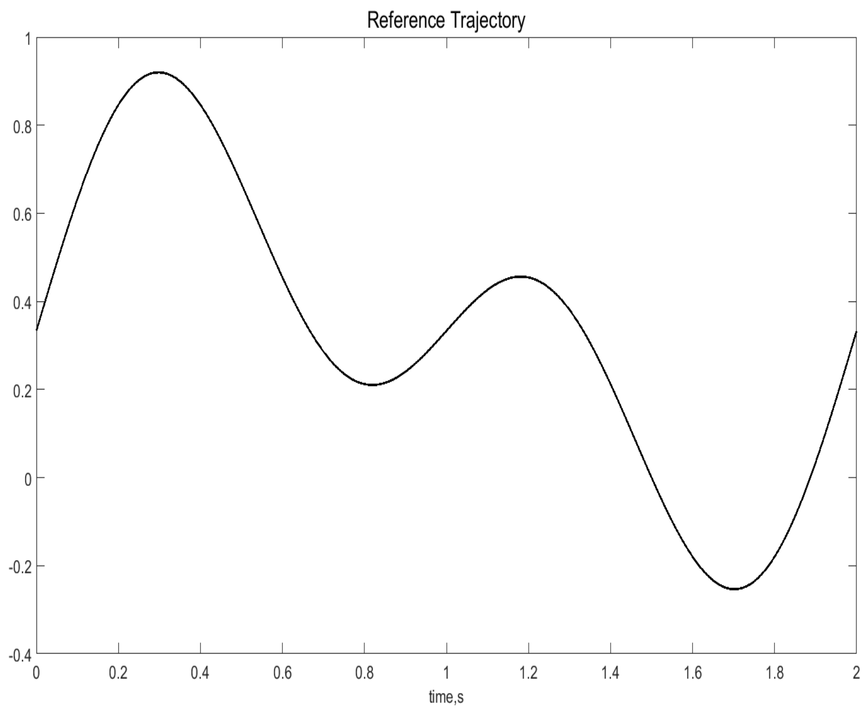

Figure 3.1: The tracking reference trajectory.

This part shows the numerical simulation for discrete-time system model, the example is a simple 2th-order system, after the sampling by sample frequency 100Hz. The state-space model matrices are

$$A = \begin{bmatrix} 0.9970 & 0 \\ 0.0035 & 0.9978 \end{bmatrix},$$
$$B = \begin{bmatrix} 0.0015 & 0 \end{bmatrix}^T,$$
$$C = \begin{bmatrix} 0.15 & 0 \end{bmatrix},$$

and on completion of each trial the 2-norm of the error signal is computed as

$$\|e_k\|_2 = \sqrt{\sum_{p=1}^{N} e_k^2(p)}$$

The first simulation study investigated the effect of the memory length M on the trial-to-trial error convergence performance. Using Theorem 3.1, and the relation between values of M and γ is given in table 3.1. These confirm that as M increases, i.e., more information from the past is used, the value of γ decreases and the tracking error converges faster, see also figure 3.2. For example, the control law matrices when $M = 2$ are $K = [-628.3001\ 0.5001]$ and $K_1 = 1.1825$, $K_0 = 1428.08$. As the figure shows, the error convergence is faster with larger M.

M	γ
1	0.7081
2	0.6953
3	0.5164
4	0.4564
5	0.4140

Table 3.1: Relation between value of M and γ for LMI design result by using algorithm in Theorem 3.1.

To examine the effectiveness of the robust design developed in Theorem 3.3, consider the case when the matrices defining the uncertainty model are

$$H_1 = \begin{bmatrix} 0.1 & 0 \end{bmatrix}^T, H_2 = 0.01, E_2 = 0.01,$$
$$E_1 = \begin{bmatrix} 0.1 & -0.1 \end{bmatrix}.$$

The results for different M are shown in figure 3.3, and confirm that: 1) the tracking error decreases monotonically and 2) increasing M improves the convergence speed. Table 3.2 shows the relationship between M and value of γ, and error convergence based different value of M is in figure 3.3. Moreover, γ satisfies $\gamma \in [0, 1)$ and since the

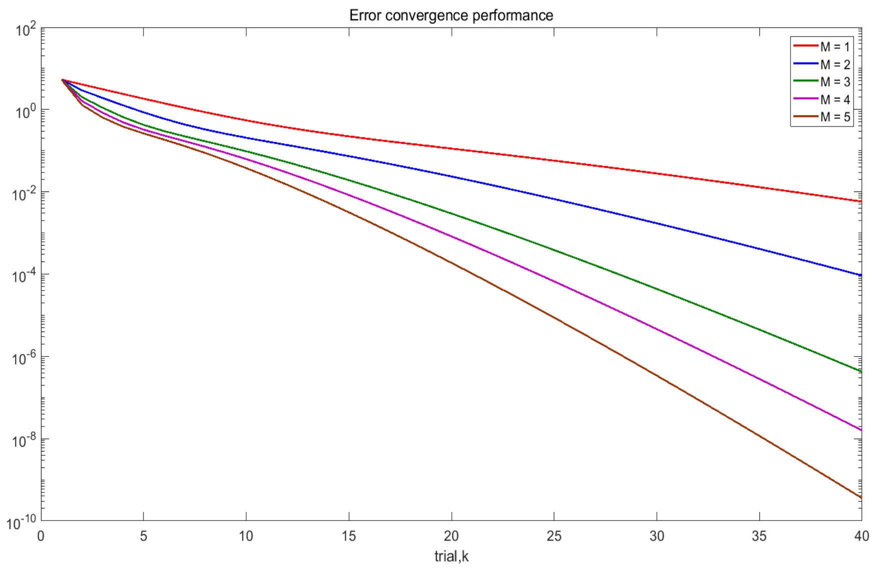

Figure 3.2: Error convergence performance along the trial by using algorithm in Theorem 3.1.

M	γ
1	0.7018
2	0.7012
3	0.5370
4	0.4871
5	0.4312

Table 3.2: Relation between value of M and γ for robust design result by using algorithm in Theorem 3.3.

design is applied to an uncertain system, the value of γ with model uncertainty is larger than that without, which is the price paid for robust design.

This part shows the numerical simulation for continuous-time system model, the example is a simple 2th-order system model with state-space model matrices

$$A = \begin{bmatrix} -0.3 & 0 \\ 0.35 & -0.22 \end{bmatrix},$$
$$B = \begin{bmatrix} 0.15 & 0 \end{bmatrix}^T,$$
$$C = \begin{bmatrix} 0.15 & 0 \end{bmatrix},$$

and the completion of each trial the 2-norm of the error signal is

$$\|e_k\|_2 = \sqrt{\int_{t=1}^{N} e_k^2(t)dt}$$

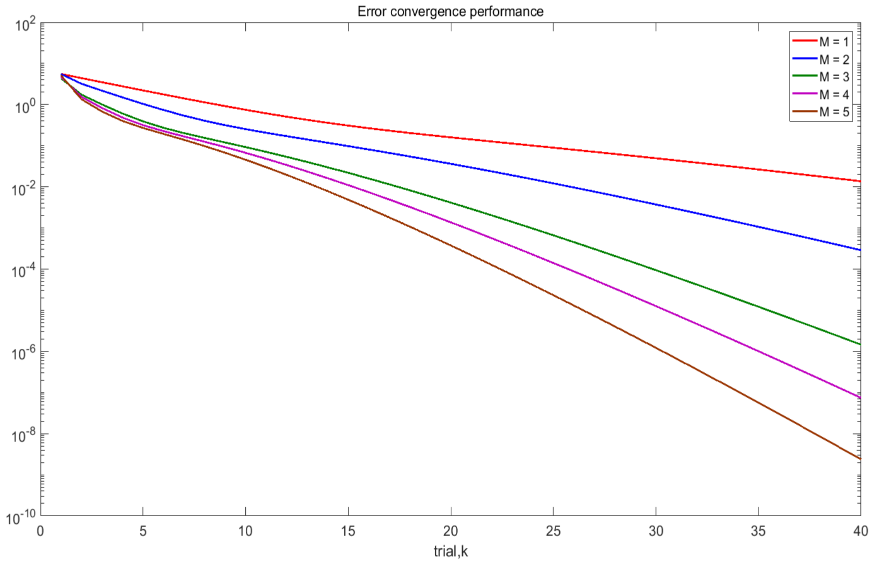

Figure 3.3: Error convergence performance along the trial by using algorithm in Theorem 3.3.

M	γ
1	0.7101
2	0.6978
3	0.5211
4	0.4672
5	0.4214

Table 3.3: Relation between value of M and γ for LMI design result by using algorithm in Theorem 3.5.

The first simulation study investigated the effect of the memory length M on the trial-to-trial error convergence performance. Using the design method of Theorem 3.5, and the relation between value of M and γ is given in table 3.3. These confirm that as M increases, i.e., more information from the past is used, the value of γ decreases and the tracking error converges faster, see also figure 3.4. For example, the control law matrices when $M = 2$ are $K = [-24.7632\ 1.8631]$ and $K_1 = 0.1243$, $K_0 = 46.3028$. As the figure shows, the error convergence is faster with larger M.

To examine the effectiveness of the robust design developed in Theorem 3.7, consider the case when the matrices defining the same uncertainty model as for the discrete-time example. The results for different M are shown in figure 3.5, and confirm that: 1) the tracking error decreases monotonically and 2) increasing M improves the convergence speed. Table 3.4 shows the relationship between M and value of γ, and the result of error convergence based different value of M is in figure 3.5. In table 3.4, γ satisfies $\gamma \in [0, 1)$ and since the design is applied to an uncertain system, the value of γ with model uncertainty is larger than that without, which is the price paid for robust design.

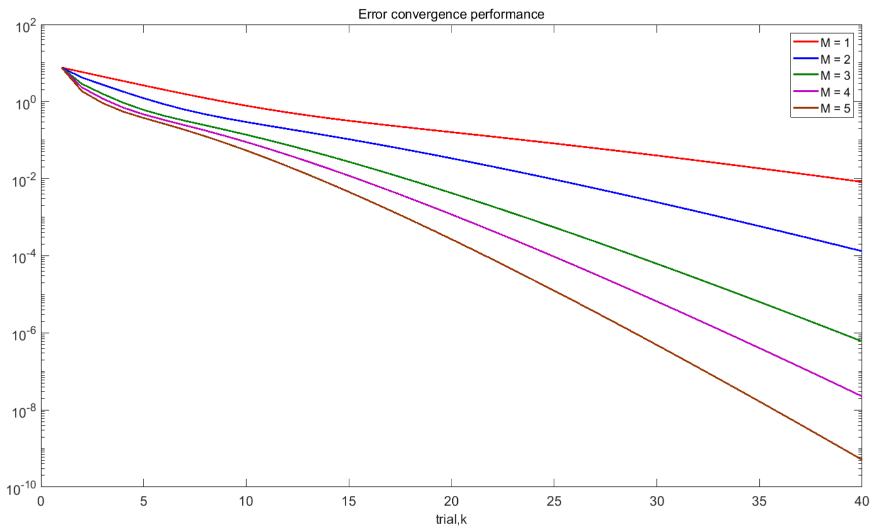

Figure 3.4: Error convergence performance along the trial by using algorithm in Theorem 3.5.

M	γ
1	0.7115
2	0.7016
3	0.5391
4	0.4921
5	0.4334

Table 3.4: Relation between value of M and γ for robust design result by using algorithm in Theorem 3.7.

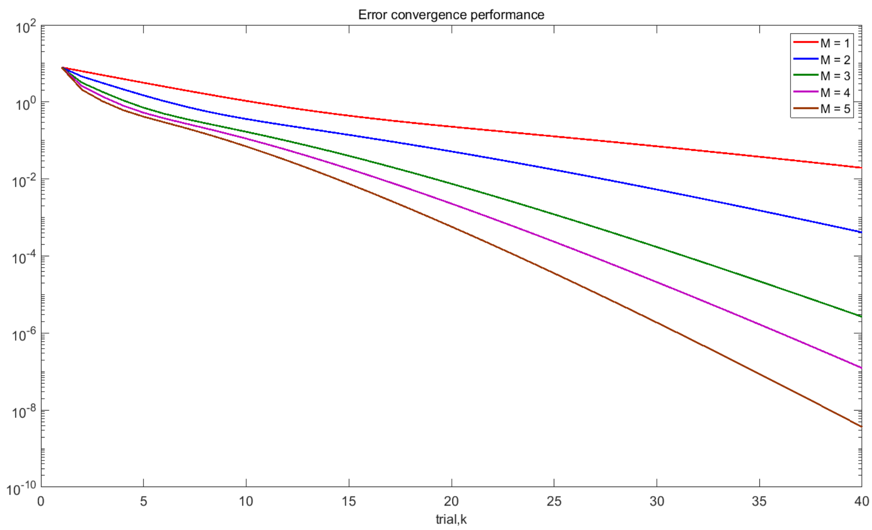

Figure 3.5: Error convergence performance along the trial by using algorithm in Theorem 3.7.

3.5 Summary

In this chapter, a new design algorithm has been developed for higher-order ILC control law matrices. The higher-order control law uses state-feedback, and design is based on the KYP lemma. This new design requires attenuation of the frequency content of the previous trial error over the complete trial length. In some applications, however, only a finite frequency range need to be considered. In other applications, it may be required to impose different frequency specifications over various frequency ranges. The next chapter uses the generalized KYP lemma to develop algorithms for control law design in such case.

Chapter 4

New Algorithms for State-Feedback Control Law Design Using the Generalized KYP Lemma

4.1 Introduction

This chapter develops new design algorithms for state feedback higher-order control law design which described in the previous Chapter. The design algorithms are based on the generalized Kalman-Yakubovich-Popov (GKYP) lemma.

4.2 Higher-order ILC Design for Discrete-time Systems

4.2.1 Problem Setup

Consider the discrete time-invariant linear state-space system model in the ILC setting

$$\begin{aligned} x_k(p+1) &= Ax_k(p) + Bu_k(p), \\ y_k(p) &= Cx_k(p),\ p = 0, 1, ..., \alpha - 1 \end{aligned} \tag{4.1}$$

where $x_k(p) \in \mathbb{R}^n$ is the state vector, $y_k(p) \in \mathbb{R}^m$ is the output vector, $u_k(p) \in \mathbb{R}^l$ is the input vector, k is the trial number, and the finite trial length $\alpha < \infty$. Let $y_d \in \mathbb{R}^m$ be reference trajectory then error on trial k is $e_k(p) = y_d(p) - y_k(p)$. The ILC control law is

$$u_{k+1}(p) = u_k(p) + \Delta u_{k+1}(p) \tag{4.2}$$

where $\Delta u_{k+1}(p)$ is a function of the error on trial k but could also be a function of the previous trial control input. Introduce, for analysis purposes only,

$$\eta_{k+1}(p+1) = x_{k+1}(p) - x_k(p) \tag{4.3}$$

and in (4.2) set

$$\Delta u_{k+1}(p) = K\eta_{k+1}(p+1) + \sum_{j=1}^{M} K_{j-1}e_{k+1-j}(p+1) \tag{4.4}$$

as the higher-order ILC control law. The resulting controlled dynamics state-space model is

$$\begin{aligned} \eta_{k+1}(p+1) &= \hat{A}\eta_{k+1}(p) + \sum_{j=1}^{M} \hat{B}_{j-1}e_{k+1-j}(p) \\ e_{k+1}(p) &= \hat{C}\eta_{k+1}(p) + \sum_{j=1}^{M} \hat{D}_{j-1}e_{k+1-j}(p) \end{aligned} \tag{4.5}$$

where

$$\begin{aligned} &\hat{A} = A + BK, \quad \hat{B}_0 = BK_0, \quad \hat{B}_{j-1} = BK_{j-1}, \\ &\hat{C} = -CA - CBK, \quad \hat{D}_0 = I - CBK_0, \end{aligned}$$

$$\hat{D}_{j-1} = -CBK_{j-1}, \quad j = 2, ..., M \tag{4.6}$$

which again is a non-unit memory linear repetitive process, and is stable along the trial if and only if all conditions in Theorem 2.6 are satisfied. Therefore the design algorithm for control law matrices is based on Theorem 2.6. However, it is difficult to develop the LMI based design algorithm for higher-order control law since the controlled system is non-unit memory and the summation term of error information on the previous trials cannot be used in the design algorithm directly. This section develops a design algorithm for the higher-order control law matrices which is based on the stability conditions for linear repetitive process.

In some applications, the systems are in the presence of uncertainties will be present in the model structure. For such system models, the general design algorithm cannot guarantee the system stable if it is only based on the normal plant model. Therefore, robust design algorithm is given to solve this problem. The norm-bounded additive uncertainty of the system is in considered. A system with norm-bounded uncertainty has the state-space model

$$x_k(p+1) = (A + \Delta A)x_k(p) + (B + \Delta B)u_k(p),$$
$$y_k(p) = (C + \Delta C)x_k(p), \quad p = 0, 1, ..., \alpha - 1 \tag{4.7}$$

and the norm-bounded additive perturbations ΔA, ΔB and ΔC to the state-space model matrices A, B and C are in the form

$$\Delta A = H_1 F E_1, \ \Delta B = H_1 F E_2, \ \Delta C = H_2 F E_1 \tag{4.8}$$

where H_1, H_2, E_1, E_2, and $F \in \mathbb{R}^{r \times r}$ is an unknown matrix that satisfies $F = F^T$ and $FF^T \leq I$. If apply the higher-order control law (4.2) for this model the controlled system is in the form (4.5) with

$$\hat{A} = (A + \Delta A) + (B + \Delta B)K, \quad \hat{B}_0 = (B + \Delta B)K_0, \quad \hat{B}_{j-1} = (B + \Delta B)K_{j-1},$$
$$\hat{C} = -(C + \Delta C)((A + \Delta A) + (B + \Delta B)K), \quad \hat{D}_0 = I - (C + \Delta C)(B + \Delta B)K_0,$$

$$\hat{D}_{j-1} = -(C + \Delta C)(B + \Delta B)K_{j-1}, \quad j = 2, ..., M \tag{4.9}$$

The higher-order ILC control law robust design algorithm are based on the feedback system (4.5) with (4.6) and (4.9), respectively.

4.2.2 LMI Based ILC Design

In the repetitive process setting the state-space model (4.5) is termed non-unit memory, with M denoting the memory length. The analysis in this section requires (4.5) to be written as a unit memory process, where the result is

$$\eta_{k+1}(p+1) = \bar{A}\eta_{k+1}(p) + \bar{B}\bar{e}_k(p),$$
$$\bar{e}_{k+1}(p) = \bar{C}\eta_{k+1}(p) + \bar{D}\bar{e}_k(p), \tag{4.10}$$

where

$$\bar{e}_k(p) = \begin{bmatrix} e_{k-M+1}^T(p) & \cdots & e_{k-1}^T(p) & e_k^T(p) \end{bmatrix}^T,$$
$$\bar{B} = \begin{bmatrix} \hat{B}_{M-1} & \cdots \hat{B}_1 & \hat{B}_0 \end{bmatrix},$$

$$\bar{C} = \begin{bmatrix} 0 \\ 0 \\ \vdots \\ 0 \\ \hat{C} \end{bmatrix}, \; \bar{D} = \begin{bmatrix} 0 & I & 0 & \cdots & 0 \\ 0 & 0 & I & \ddots & 0 \\ 0 & 0 & 0 & \cdots & 0 \\ \vdots & \vdots & \vdots & \ddots & I \\ \hat{D}_{M-1} & \hat{D}_{M-2} & \hat{D}_{M-3} & \cdots & \hat{D}_0 \end{bmatrix}, \tag{4.11}$$

Applying the z-transform, i.e., $zx_k(p) = x_k(p+1)$ to (4.10) gives

$$\bar{e}_{k+1}(z) = G(z)\bar{e}_k(z) \tag{4.12}$$

where $G(z) = \bar{C}(zI - \hat{A})^{-1}\bar{B} + \bar{D}$. The term in transfer-function matrix $G(z)$ which relates the convergence performance is only the bottom row, i.e.,

$$e_{k+1}(z) = [G_{M-1}(z), ..., G_1(z), G_0(z)]\bar{e}_k(z) \tag{4.13}$$

In [63], one design algorithm which uses the generalized KYP lemma for design the control law matrices of the ILC controlled system, and a standard state-feedback control law is used then the ILC controlled system is unit memory linear repetitive processes. In this section, it is extended for higher-order ILC control law. The generalized KYP lemma which is described in Lemma 2.15, and the design algorithm is

Theorem 4.1. *For a given $\gamma > 0$ the discrete linear repetitive process representing the ILC dynamics of (4.10) is stable along the trial and satisfies*

$$\max \sigma([G_{M-1}(e^{j\theta}), ..., G_1(e^{j\theta}), G_0(e^{j\theta})]) < \gamma \tag{4.14}$$

over the finite frequency range $\theta \in \Theta$ defined in Lemma 2.15, and $z = e^{j\theta}$, and there exist matrices $S > 0$, $P_1 > 0$, $Q_1 > 0$, $P_2 > 0$, $Q_2 > 0$, X_1, X_2, and W_1, and real scalar ρ_1, ρ_2 and $\mu = \gamma^2$ such that the following LMIs are feasible:

$$\begin{bmatrix} \Xi_{11} & \Xi_{12} - W_1^T & 0 & 0 \\ * & \Xi_{22} + sym\{AW_1 + BX_1\} & BX_2 & -W_1^T A^T C^T - X_1^T B^T C^T \\ * & * & -\mu I & I_0^T - X_2^T B^T C^T \\ * & * & * & -I \end{bmatrix} < 0 \tag{4.15}$$

$$\begin{bmatrix} \bar{\Xi}_{11} & \bar{\Xi}_{12} - W_1^T & 0 & 0 \\ * & \bar{\Xi}_{22} + sym\{AW_1 + BX_1\} & BX_2 & -W_1^T A^T C_1^T - X_1^T B^T C_1^T \\ * & * & -I & I_1^T - X_2^T B^T C_1^T \\ * & * & * & -I \end{bmatrix} < 0 \tag{4.16}$$

$$\begin{bmatrix} S + \rho_2 W_1 + \rho_2 W_1^T & -\rho_2 AW_1 - \rho_2 BX_1 - \rho_1 W_1^T \\ * & -S + sym\{\rho_1 AW_1 + \rho_1 BX_1\} \end{bmatrix} < 0 \tag{4.17}$$

where the compatibly dimensioned matrices Ξ_{11}, Ξ_{12}, Ξ_{22}, *and* $\bar{\Xi}_{11}$, $\bar{\Xi}_{12}$, $\bar{\Xi}_{22}$ *form* Ξ *and* $\bar{\Xi}$ *in Lemma 2.15 and* ρ_1, ρ_2 *satisfy*

$$\rho_1^2 - \rho_2^2 < 0 \tag{4.18}$$

and

$$I_0 = [0, \quad ..., \quad 0 \quad I]$$

,

$$I_1 = \begin{bmatrix} 0 & I & \cdots & 0 \\ 0 & \vdots & \ddots & \vdots \\ 0 & 0 & \cdots & I \\ 0 & 0 & \cdots & I \end{bmatrix}, \quad C_1 = \begin{bmatrix} 0 \\ \vdots \\ 0 \\ C \end{bmatrix}, \tag{4.19}$$

If the (4.15), (4.16) and (4.17) are satisfied, stabilizing control law matrices are given by

$$K = X_1 W_1^{-1}, \; [K_{M-1}, ..., \; K_1, \; K_0] = X_2 \tag{4.20}$$

Proof. The generalized KYP lemma given in this thesis as Lemma 2.15, then applied with $\hat{A}$, $\bar{B}$, $\bar{C}$, and $\bar{D}$, the resulting LMI is

$$\begin{bmatrix} \hat{A} & \bar{B} \\ I & 0 \end{bmatrix}^T \bar{\Xi} \begin{bmatrix} \hat{A} & \bar{B} \\ I & 0 \end{bmatrix} + \begin{bmatrix} \bar{C} & \bar{D} \\ 0 & I \end{bmatrix}^T \Pi \begin{bmatrix} \bar{C} & \bar{D} \\ 0 & I \end{bmatrix} < 0 \tag{4.21}$$

Then after some processes include Schur's complement, LMI (4.16) can be obtained from (4.21). However, the controlled system is stable along the trial if it satisfies the next Lyapunov inequality:

$$\hat{A}^T S \hat{A} - S < 0 \tag{4.22}$$

Then after routine manipulations (4.17) can be obtained, and proof is complete. □

The next result shows that when γ is small, the tracking error is guaranteed to converges to zeros.

Theorem 4.2. *If for* $\gamma \in [0, 1/\sqrt{M})$ *the design in Theorem 4.1 is feasible, the tracking error converges to zero as* $k \to \infty$ *over the finite frequency range* $\theta \in \Theta$ *defined in Lemma 2.15. Moreover, the convergence is monotonic in the sense that*

$$\max\{\|e_{k+1}\|, ..., \|e_{k-M+2}\|\} < \gamma \max\{\|e_k\|, ..., \|e_{k-M+1}\|\}$$

Proof. When the design algorithm in Theorem 4.1 is feasible,

$$\|e_{k+1}\|_2^2 < \gamma^2 \sum_{i=0}^{M-1} \|e_{k-i}\|_2^2 \tag{4.23}$$

Define $q = \gamma^2 M$. As $\gamma < 1/\sqrt{M}$, $q < 1$. Hence

$$\begin{aligned}\|e_{k+1}\|_2^2 &< \gamma^2 \times \{\|e_{k-M+1}\|_2^2 + ... + \|e_k\|_2^2\} \\ &< q \times \max\{\|e_{k-M+1}\|_2^2, ..., \|e_k\|_2^2\}\end{aligned} \tag{4.24}$$

Furthermore,

$$\begin{aligned}\|e_{k+2}\|_2^2 &< q \times \{\|e_{k-M+2}\|_2^2 + ... + \|e_{k+1}\|_2^2\} \\ &< q \times \max\{\|e_{k-M+1}\|_2^2, ..., \|e_k\|_2^2\}\end{aligned} \tag{4.25}$$

Following a similar argument

$$\begin{aligned}&\max\{\|e_{k+1}\|_2^2, ..., \|e_{k-M+2}\|_2^2\} \\ &\quad < q \times \max\{\|e_{k-M+1}\|_2^2, ..., \|e_k\|_2^2\} \\ &\quad < q^k \times \max\{\|e_{M-1}\|_2^2, ..., \|e_0\|_2^2\}\end{aligned} \tag{4.26}$$

Since $q < 1$, the value of $q^k \to 0$ as $k \to \infty$, and hence $\|e_\infty\|_2 = 0$, which completes the proof. □

From the above theorem it can be seen that γ characterizes how quickly the tracking error converges to zero under the higher order ILC design. In practice, a faster convergence is usually desirable. This can be achieved by finding the minimum γ value by solving the following minimization problem.

$$\min_{S>0, P_1>0, Q_1>0, P_2>0, Q_2>0, \gamma<1,, W_1, X_1, X_2} \mu \tag{4.27}$$

4.2.3 Robust Design Algorithm

In this section, a robust design algorithm can solve this problem for the norm-bounded uncertainty in the system. The uncertainty based feedback system model can be converted to the unit-memory repetitive processes (4.10), (4.11) with (4.9), with linear objective minimization procedure (4.27) the robust design result can now be established.

Theorem 4.3. *For a given $\gamma > 0$ the discrete linear repetitive process representing the ILC dynamics of (4.10) with additive uncertainties ΔA, ΔB, and ΔC in (4.9) is stable along the trial and satisfies (4.14) over the finite frequency range $\theta \in \Theta$ defined in Lemma 2.15, and there exist matrices $S > 0$, $P_1 > 0$, $Q_1 > 0$, $P_2 > 0$, $Q_2 > 0$, X_1, X_2, and W_1, W_{11}, W_{12}, W_{13}, W_{14}, W_2 and W_{31}, W_{32}, W_{33}, W_{34}, W_4, and real scalar*

ρ_1, ρ_2, $\epsilon_1 > 0$, $\epsilon_2 > 0$ and $\epsilon_3 > 0$ such that the following LMIs are feasible

$$\begin{bmatrix} \Xi_{11} & \Xi_{12}-W_1^T & 0 & -W_{11}C^T & -W_{11} & 0 & -W_{11}E_1^T & 0 \\ * & \Delta_{22} & BX_2 & -W_{12}C^T & \Delta_{25} & \Delta_{26} & -W_{12}E_1^T & \Delta_{28} \\ * & * & -\mu I & I_0^T-W_{13}C^T & X_2^TB^T-W_{13} & X_2^TE_2^T & -W_{13}E_1^T & X_2^TE_2^T \\ * & * & * & \Delta_{44} & -CW_2^T-W_{14} & 0 & -W_{14}E_1^T & 0 \\ * & * & * & * & \Delta_{55} & 0 & -W_2E_1^T & 0 \\ * & * & * & * & * & -\epsilon_1 I & 0 & 0 \\ * & * & * & * & * & * & -\epsilon_1 I & 0 \\ * & * & * & * & * & * & * & -\epsilon_1 I \end{bmatrix} < 0 \tag{4.28}$$

$$\begin{bmatrix} \bar{\Xi}_{11} & \bar{\Xi}_{12}-W_1^T & 0 & -W_{31}C_1^T & -W_{31} & 0 & -W_{31}E_1^T & 0 \\ * & \Delta_{62} & BX_2 & -W_{32}C_1^T & \Delta_{65} & \Delta_{66} & -W_{32}E_1^T & \Delta_{68} \\ * & * & -I & I_1^T-W_{33}C_1^T & X_2^TB^T-W_{33} & X_2^TE_2^T & -W_{33}E_1^T & X_2^TE_2^T \\ * & * & * & \Delta_{74} & -CW_2^T-W_{34} & 0 & -W_{34}E_1^T & 0 \\ * & * & * & * & \Delta_{85} & 0 & -W_4E_1^T & 0 \\ * & * & * & * & * & -\epsilon_2 I & 0 & 0 \\ * & * & * & * & * & * & -\epsilon_2 I & 0 \\ * & * & * & * & * & * & * & -\epsilon_2 I \end{bmatrix} < 0 \tag{4.29}$$

$$\begin{bmatrix} \Delta_{91} & \Delta_{92} & 0 & 0 \\ * & -S+sym\{\rho_1 AW+\rho_1 BX_1\}+\epsilon_3 H_1H_1^T & -W_1^TE_1^T-X_1^TE_2^T & W_1^TE_1^T+X_1^TE_2^T \\ * & * & -\epsilon_3 I & 0 \\ * & * & * & -\epsilon_3 I \end{bmatrix} < 0 \tag{4.30}$$

where

$$\begin{aligned}
\Delta_{22} &= \Xi_{22} + sym\{AW + BX_1\} + \epsilon_1 H_1 H_1^T, \\
\Delta_{25} &= W_1^T A^T + X_1^T B^T - W_{12}, \\
\Delta_{26} &= \Delta_{28} = W_1^T E_1^T + X_1^T E_2^T, \\
\Delta_{44} &= -I - sym\{CW_{14}^T\} + \epsilon_1 H_2 H_2^T, \\
\Delta_{55} &= -W_2 - W_2^T + \epsilon_1 H_1 H_1^T, \\
\Delta_{62} &= \bar{\Xi}_{22} + sym\{AW + BX_1\} + \epsilon_2 H_1 H_1^T, \\
\Delta_{65} &= W_1^T A^T + X_1^T B^T - W_{32}, \\
\Delta_{66} &= \Delta_{68} = W_1^T E_1^T + X_1^T E_2^T, \\
\Delta_{74} &= -I - sym\{CW_{34}^T\} + \epsilon_2 H_2 H_2^T, \\
\Delta_{85} &= -W_4 - W_4^T + \epsilon_2 H_1 H_1^T, \\
\Delta_{91} &= S + sym\{\rho_2 W_1\} + \epsilon_3 \rho_2^2 H_1 H_1^T, \\
\Delta_{92} &= -\rho_2 AW - \rho_2 BX_1 - \rho_1 W_1^T,
\end{aligned}$$

and I_0, I_1, C_1 are defined in (4.19), and ρ_1, ρ_2 satisfy (4.18), Ξ_{22}, and $\bar{\Xi}_{11}$, $\bar{\Xi}_{12}$, $\bar{\Xi}_{22}$ form Ξ and $\bar{\Xi}$ in Lemma 2.15. If the LMIs (4.27), (4.28) and (4.29) are satisfied, stabilizing control law matrices are given by

$$K = X_1 W_1^{-1}, \ [K_{M-1}, \ldots, \ K_1, \ K_0] = X_2 \tag{4.31}$$

with use of the linear objective minimization procedure (4.27).

Proof. Direct substitution of (4.9) into (4.15), (4.16) and (4.17) introduces nonlinear terms, applying Theorem 2.19 to these two LMIs and the Schur's complement formula gives (4.28), (4.29) and (4.30) and proof is complete. □

Theorem 4.4. *If for $\gamma \in (0, 1/\sqrt{M})$ the design in Theorem 4.3 is feasible, the tracking error converges to zero as $k \to \infty$ over the finite frequency range $\theta \in \Theta$ defined in Lemma 2.15 even with the presence of model uncertainties ΔA, ΔB and ΔC. Moreover, the convergence is monotonic in the sense that*

$$\max\{\|e_{k+1}\|, ..., \|e_{k-M+2}\|\} < \gamma \max\{\|e_k\|, ..., \|e_{k-M+1}\|\}$$

Proof. This follows identical steps to that of Theorem 4.2 and here the details are omitted. □

4.3 Higher-order ILC Design for Continuous-time Systems

4.3.1 Problem Setup

Consider the continuous time-invariant linear state-space system model in the ILC setting

$$\begin{aligned} \dot{x}_k(t) &= Ax_k(t) + Bu_k(t), \\ y_k(t) &= Cx_k(t), 0 < t \leq \alpha \end{aligned} \tag{4.32}$$

where x_k, y_k, and u_k are state, output and input vector, respectively, and k is the trial number, and the finite trial length $\alpha < \infty$. If y_d denotes the reference trajectory then error on trial k is $e_k(t) = y_d(t) - y_k(t)$. The ILC law is

$$u_{k+1}(t) = u_k(t) + \Delta u_{k+1}(t) \tag{4.33}$$

where $\Delta u_{k+1}(t)$ is a function of the error on trial k but could also be a function of the previous trial control input. A natural extension is to allow $\Delta u_{k+1}(t)$ to be a function of the error and/or control vectors on a finite number of previous passes. In order to use repetitive process theory for ILC design, introduce, for analysis purposes only,

$$\eta_{k+1}(t) = \int_0^t (x_{k+1}(t) - x_k(t))dt \tag{4.34}$$

and in (4.33) set

$$\Delta u_{k+1}(t) = K\eta_{k+1}(t) + \sum_{j=1}^{M} K_{j-1}\dot{e}_{k+1-j}(t) \tag{4.35}$$

The resulting controlled dynamics state-space model is

$$\dot{\eta}_{k+1}(t) = \hat{A}\eta_{k+1}(t) + \sum_{j=1}^{M} \hat{B}_{j-1}e_{k+1-j}(t)$$
$$e_{k+1}(t) = \hat{C}\eta_{k+1}(t) + \sum_{j=1}^{M} \hat{D}_{j-1}e_{k+1-j}(t) \tag{4.36}$$

where

$$\hat{A} = A + BK, \quad \hat{B}_0 = BK_0, \quad \hat{B}_{j-1} = BK_{j-1},$$
$$\hat{C} = -C(A + BK), \quad \hat{D}_0 = I - CBK_0,$$

$$\hat{D}_{j-1} = -CBK_{j-1}, \quad j = 2, ..., M \tag{4.37}$$

This is a non-unit memory linear repetitive process. It is stable along the pass if and only if all conditions in Theorem 2.10 are satisfied. In a similar manner to the discrete case in section 4.2.1, the model with uncertainty present is

$$\dot{x}_k(t) = (A + \Delta A)x_k(t) + (B + \Delta B)u_k(t),$$
$$y_k(t) = (C + \Delta C)x_k(t), \quad 0 < t \leq \alpha \tag{4.38}$$

and the norm-bounded additive perturbations ΔA, ΔB and ΔC to the state-space model matrices A, B and C are of the form

$$\Delta A = H_1FE_1, \; \Delta B = H_1FE_2, \; \Delta C = H_2FE_1 \tag{4.39}$$

where H_1, H_2, E_1, E_2, and $F \in \mathbb{R}^{r\times r}$ is an unknown matrix that satisfies $F = F^T$ and $FF^T \leq I$. If apply the control law (4.33) for this model the controlled system is in the form (4.36) with

$$\hat{A} = (A + \Delta A) + (B + \Delta B)K, \quad \hat{B}_0 = (B + \Delta B)K_0, \quad \hat{B}_{j-1} = (B + \Delta B)K_{j-1},$$
$$\hat{C} = -(C + \Delta C)((A + \Delta A) + (B + \Delta B)K), \quad \hat{D}_0 = I - (C + \Delta C)(B + \Delta B)K_0,$$
$$\hat{D}_{j-1} = -(C + \Delta C)(B + \Delta B)K_{j-1}, \quad j = 2, ..., M \tag{4.40}$$

4.3.2 LMI Based ILC Design

Since the state-space model (4.36) is termed non-unit memory, with M denoting the memory length, the analysis in this section requires (4.36) to be written as a unit memory process, where the result is

$$\begin{aligned}\dot{\eta}_{k+1}(t) &= \hat{A}\eta_{k+1}(t) + \bar{B}\bar{e}_k(t),\\ \bar{e}_{k+1}(t) &= \bar{C}\eta_{k+1}(t) + \bar{D}\bar{e}_k(t),\end{aligned} \tag{4.41}$$

where

$$\begin{aligned}\bar{e}_k(t) &= \begin{bmatrix} e_{k-M+1}^T(t) & \cdots & e_{k-1}^T(t) & e_k^T(t)\end{bmatrix}^T,\\ \bar{B} &= \begin{bmatrix}\hat{B}_{M-1} & \cdots \hat{B}_1 & \hat{B}_0\end{bmatrix},\\ \bar{C} &= \begin{bmatrix}0\\0\\\vdots\\0\\\hat{C}\end{bmatrix},\ \bar{D} = \begin{bmatrix}0 & I & 0 & \cdots & 0\\ 0 & 0 & I & \ddots & 0\\ 0 & 0 & 0 & \cdots & 0\\ \vdots & \vdots & \vdots & \ddots & I\\ \hat{D}_{M-1} & \hat{D}_{M-2} & \hat{D}_{M-3} & \cdots & \hat{D}_0\end{bmatrix},\end{aligned} \tag{4.42}$$

Using Laplace transform, i.e., $L[\dot{x}_k(t)] = sL[x_k(t)] - x_k(0)$, (see [74] for the details of how to avoid problems arising from the finite trial length) to (4.41) gives

$$\bar{e}_{k+1}(s) = G(s)\bar{e}_k(s) \tag{4.43}$$

where $G(s) = \bar{C}(sI - \hat{A})^{-1}\bar{B} + \bar{D}$. The term in transfer-function matrix $G(s)$ which relates the convergence performance is only the bottom row. It is

$$e_{k+1}(s) = [G_{M-1}(s), ..., G_1(s), G_0(s)]\bar{e}_k(s) \tag{4.44}$$

and the design objective is to select the gains K, $K_{j-1}, i = 1, ..., M$ such that the norm of the above transfer function is small and thus convergence can be achieved.

Theorem 4.5. *For a given $\gamma > 0$ the differential linear repetitive process representing the ILC dynamics of (4.41) is stable along the trial and satisfies*

$$\max \sigma([G_{M-1}(j\theta), ..., G_1(j\theta), G_0(j\theta)]) < \gamma \tag{4.45}$$

over the finite frequency range defined in Lemma 2.16, and there exist matrices $S > 0$, $P_1 > 0$, $Q_1 > 0$, $P_2 > 0$, $Q_2 > 0$, X_1, X_2, and W_1, and $\mu = \gamma^2$ such that the following LMIs are feasible:

$$\begin{bmatrix}\Xi_{11} & \Xi_{12} - W_1^T & 0 & 0\\ * & \Xi_{22} + sym\{AW_1 + BX_1\} & BX_2 & -W_1^TA^TC^T - X_1^TB^TC^T\\ * & * & -\mu I & I_0^T - X_2^TB^TC^T\\ * & * & * & -I\end{bmatrix} < 0 \tag{4.46}$$

$$\begin{bmatrix} \bar{\Xi}_{11} & \bar{\Xi}_{12} - W_1^T & 0 & 0 \\ * & \bar{\Xi}_{22} + sym\{AW_1 + BX_1\} & BX_2 & -W_1^T A^T C_1^T - X_1^T B^T C_1^T \\ * & * & -I & I_1^T - X_2^T B^T C_1^T \\ * & * & * & -I \end{bmatrix} < 0 \quad (4.47)$$

$$\begin{bmatrix} -W_1 - W_1^T & S + AW_1 + BX_1 - W_1^T \\ * & sym\{AW_1 + BX_1\} \end{bmatrix} < 0 \quad (4.48)$$

where the compatibly dimensioned matrices Ξ_{11}, Ξ_{12}, Ξ_{22}, and $\bar{\Xi}_{11}$, $\bar{\Xi}_{12}$, $\bar{\Xi}_{22}$ form Ξ and $\bar{\Xi}$ in Lemma 2.16 and I_0, I_1, and C_1 are defined in (4.19). If the (4.46), (4.47) and (4.48) are satisfied, stabilizing control law matrices are given by

$$K = X_1 W_1^{-1}, \; [K_{M-1}, ..., \; K_1, \; K_0] = X_2 \quad (4.49)$$

Proof. The generalized KYP lemma of Lemma 2.16, when applied with $\hat{A}$, $\bar{B}$, $\bar{C}$, and $\bar{D}$ in it, the equal LMI is

$$\begin{bmatrix} \hat{A} & \bar{B} \\ I & 0 \end{bmatrix}^T \bar{\Xi} \begin{bmatrix} \hat{A} & \bar{B} \\ I & 0 \end{bmatrix} + \begin{bmatrix} \bar{C} & \bar{D} \\ 0 & I \end{bmatrix}^T \Pi \begin{bmatrix} \bar{C} & \bar{D} \\ 0 & I \end{bmatrix} < 0 \quad (4.50)$$

Then after some processes include Schur's complement formula, the LMI (4.47) is obtained from (4.50). However, the controlled system is stable along the trial if it satisfies next Lyapunov inequality:

$$\hat{A}^T S + S\hat{A} < 0 \quad (4.51)$$

Then after routine manipulations LMI (4.48) can be obtained. □

The next theorem shows that when γ is small, the tracking error is guaranteed to converges to zeros.

Theorem 4.6. *If for $\gamma \in (0, 1/\sqrt{M})$ the design in Theorem 4.5 is feasible, the tracking error converges to zero as $k \to \infty$ over the finite frequency range defined in Lemma 2.16. Moreover, the convergence is monotonic in the sense that*

$$\max\{\|e_{k+1}\|, ..., \|e_{k-M+2}\|\} < \gamma \max\{\|e_k\|, ..., \|e_{k-M+1}\|\}$$

Proof. When the design algorithm in Theorem 4.5 is feasible,

$$\|e_{k+1}\|_2^2 < \gamma^2 \sum_{i=0}^{M-1} \|e_{k-i}\|_2^2 \quad (4.52)$$

Define $q = \gamma^2 M$. As $\gamma < 1/\sqrt{M}$, $q < 1$. Hence

$$\begin{aligned} \|e_{k+1}\|_2^2 &< \gamma^2 \times \{\|e_{k-M+1}\|_2^2 + ... + \|e_k\|_2^2\} \\ &< q \times \max\{\|e_{k-M+1}\|_2^2, ..., \|e_k\|_2^2\} \end{aligned} \quad (4.53)$$

Furthermore,

$$\begin{aligned}\|e_{k+2}\|_2^2 &< q \times \{\|e_{k-M+2}\|_2^2 + ... + \|e_{k+1}\|_2^2\} \\ &< q \times \max\{\|e_{k-M+1}\|_2^2, ..., \|e_k\|_2^2\}\end{aligned} \tag{4.54}$$

Similarly,

$$\begin{aligned}&\max\{\|e_{k+1}\|_2^2, ..., \|e_{k-M+2}\|_2^2\} \\ &\quad < q \times \max\{\|e_{k-M+1}\|_2^2, ..., \|e_k\|_2^2\} \\ &\quad < q^k \times \max\{\|e_{M-1}\|_2^2, ..., \|e_0\|_2^2\}\end{aligned} \tag{4.55}$$

Since $q < 1$, the value of $q^k \to 0$ as $k \to \infty$, and hence $\|e_\infty\|_2 = 0$, which completes the proof. □

From the above theorem it can be seen that γ characterizes how quickly the tracking error converges to zero under the higher order ILC design. In practice, a faster convergence is usually desirable. This can be achieved by finding the minimum γ value by solving the following linear minimization objective procedure.

$$\min_{S>0,P_1>0,Q_1>0,P_2>0,Q_2>0,\gamma<1,,W_1,X_1,X_2} \mu \tag{4.56}$$

4.3.3 Robust Design Algorithm

Following the same argument on the discrete case in section 4.2.3, gives the theorem,

Theorem 4.7. *For a given $\gamma > 0$ the differential linear repetitive process representing the ILC dynamics of (4.41) with additive uncertainties ΔA, ΔB, and ΔC in (4.9) is stable along the trial and satisfies (4.45) over the finite frequency range defined in Lemma 2.16, and there exist matrices $S > 0$, $P_1 > 0$, $Q_1 > 0$, $P_2 > 0$, $Q_2 > 0$, X_1, X_2, and W_1, W_{11}, W_{12}, W_{13}, W_{14}, W_2 and W_{31}, W_{32}, W_{33}, W_{34}, W_4, $\epsilon_1 > 0$, $\epsilon_2 > 0$ and $\epsilon_3 > 0$ such that the following LMIs are feasible*

$$\begin{bmatrix} \Xi_{11} & \Xi_{12}-W_1^T & 0 & -W_{11}C^T & -W_{11} & 0 & -W_{11}E_1^T & 0 \\ * & \Delta_{22} & BX_2 & -W_{12}C^T & \Delta_{25} & \Delta_{26} & -W_{12}E_1^T & \Delta_{28} \\ * & * & -\mu I & I_0^T-W_{13}C^T & X_2^TB^T-W_{13} & X_2^TE_2^T & -W_{13}E_1^T & X_2^TE_2^T \\ * & * & * & \Delta_{44} & -CW_2^T-W_{14} & 0 & -W_{14}E_1^T & 0 \\ * & * & * & * & \Delta_{55} & 0 & -W_2E_1^T & 0 \\ * & * & * & * & * & -\epsilon_1 I & 0 & 0 \\ * & * & * & * & * & * & -\epsilon_1 I & 0 \\ * & * & * & * & * & * & * & -\epsilon_1 I \end{bmatrix} < 0 \tag{4.57}$$

$$\begin{bmatrix} \bar{\Xi}_{11} & \bar{\Xi}_{12}-W_1^T & 0 & -W_{31}C_1^T & -W_{31} & 0 & -W_{31}E_1^T & 0 \\ * & \Delta_{62} & BX_2 & -W_{32}C_1^T & \Delta_{65} & \Delta_{66} & -W_{32}E_1^T & \Delta_{68} \\ * & * & -I & I_1^T-W_{33}C_1^T & X_2^TB^T-W_{33} & X_2^TE_2^T & -W_{33}E_1^T & X_2^TE_2^T \\ * & * & * & \Delta_{74} & -CW_2^T-W_{34} & 0 & -W_{34}E_1^T & 0 \\ * & * & * & * & \Delta_{85} & 0 & -W_4E_1^T & 0 \\ * & * & * & * & * & -\epsilon_2 I & 0 & 0 \\ * & * & * & * & * & * & -\epsilon_2 I & 0 \\ * & * & * & * & * & * & * & -\epsilon_2 I \end{bmatrix} < 0 \tag{4.58}$$

$$\begin{bmatrix} -W_1-W_1^T & \Delta_{92} & 0 & 0 \\ * & sym\{AW_1+BX_1\}+\epsilon_3 H_1 H_1^T & -W_1^T E_1^T - X_1^T E_2^T & W_1^T E_1^T + X_1^T E_2^T \\ * & * & -\epsilon_3 I & 0 \\ * & * & * & -\epsilon_3 I \end{bmatrix} < 0 \tag{4.59}$$

where

$$\Delta_{22} = \Xi_{22} + sym\{AW + BX_1\} + \epsilon_1 H_1 H_1^T,$$
$$\Delta_{25} = W_1^T A^T + X_1^T B^T - W_{12},$$
$$\Delta_{26} = \Delta_{28} = W_1^T E_1^T + X_1^T E_2^T,$$
$$\Delta_{44} = -I - sym\{CW_{14}^T\} + \epsilon_1 H_2 H_2^T,$$
$$\Delta_{55} = -W_2 - W_2^T + \epsilon_1 H_1 H_1^T,$$

$$\Delta_{62} = \bar{\Xi}_{22} + sym\{AW + BX_1\} + \epsilon_2 H_1 H_1^T,$$
$$\Delta_{65} = W_1^T A^T + X_1^T B^T - W_{32},$$
$$\Delta_{66} = \Delta_{68} = W_1^T E_1^T + X_1^T E_2^T,$$
$$\Delta_{74} = -I - sym\{CW_{34}^T\} + \epsilon_2 H_2 H_2^T,$$
$$\Delta_{85} = -W_4 - W_4^T + \epsilon_2 H_1 H_1^T,$$
$$\Delta_{92} = S + AW_1 + BX_1 - W_1^T,$$

and I_0, I_1, C_1 are defined in (4.19), and Ξ_{22}, and $\bar{\Xi}_{11}$, $\bar{\Xi}_{12}$, $\bar{\Xi}_{22}$ form Ξ and $\bar{\Xi}$ in Lemma 2.16. If the LMIs (4.57), (4.58) and (4.59) are satisfied, stabilizing control law matrices are given by

$$K = X_1 W_1^{-1},\ [K_{M-1}, ...,\ K_1,\ K_0] = X_2 \tag{4.60}$$

with use of the linear objective minimization procedure (4.56).

Proof. Direct substitution of (4.39) into (4.46), (4.47) and (4.48) would introduce non-linear terms, applying Theorem 2.19 to these two LMIs, plus the Schur's complement formula gives the LMIs (4.57), (4.58) and (4.59) and proof is complete. □

Theorem 4.8. *If for $\gamma \in (0, 1/\sqrt{M})$ the design in Theorem 4.7 is feasible, the tracking error converges to zero as $k \to \infty$ over the finite frequency range defined in Lemma 2.16 even with the presence of model uncertainties ΔA, ΔB and ΔC. Moreover, the convergence is monotonic in the sense that*

$$\max\{\|e_{k+1}\|, ..., \|e_{k-M+2}\|\} < \gamma \max\{\|e_k\|, ..., \|e_{k-M+1}\|\}$$

Proof. This follows identical steps to that for Theorem 4.6 and that the detail are omitted. □

4.4 Numerical Examples

In this section, numerical examples are used to test the new design algorithms developed earlier in this chapter. In this simulation, the value of memory length M is from 1 to 5, and the number of trials is 40, the trial length is 2 sec. The special frequency range is focused, by using fourier transform for the reference trajectory, and as the figure 4.1 shown, the useful frequency range for the reference trajectory is within 2Hz, in the simulation, the cut-off frequency range chosen for design algorithm is 2Hz.

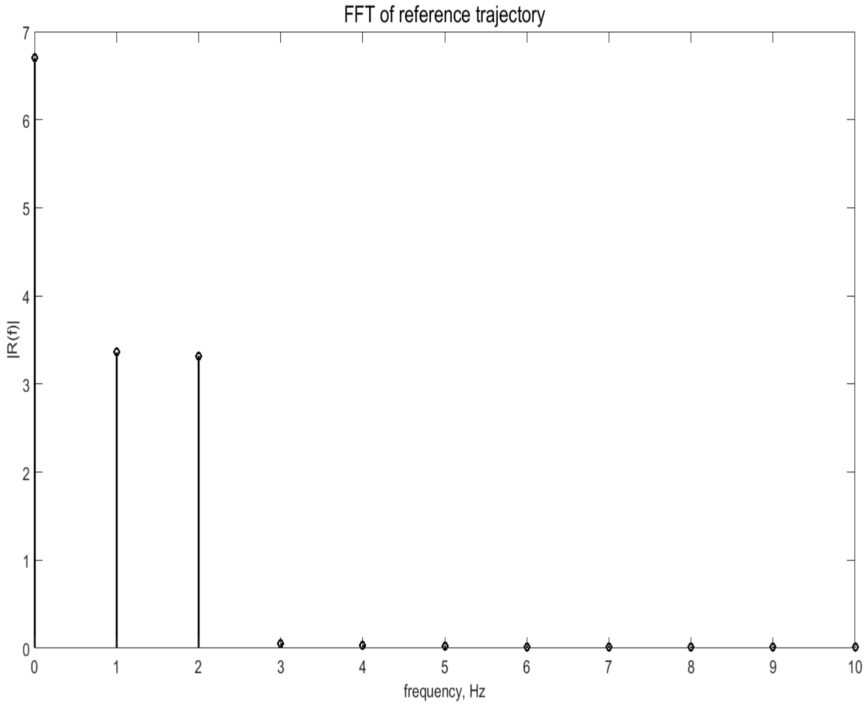

Figure 4.1: The FFT of the tracking reference trajectory.

This part shows the numerical simulation for discrete-time system model, the example is a simple 2th-order system model which after the sampling by sample frequency 100Hz, the state-space model matrices are

$$A = \begin{bmatrix} 0.9970 & 0 \\ 0.0035 & 0.9978 \end{bmatrix},$$
$$B = \begin{bmatrix} 0.0015 & 0 \end{bmatrix}^T,$$
$$C = \begin{bmatrix} 0.15 & 0 \end{bmatrix}$$

M	γ
1	0.6631
2	0.6154
3	0.5022
4	0.4313
5	0.4038

Table 4.1: Relation between value of M and γ for LMI design result by using algorithm in Theorem 4.1.

, and on completion of each trial the 2-norm of the error signal is computed as

$$\|e_k\|_2 = \sqrt{\sum_{p=1}^{N} e_k^2(p)}$$

The first simulation study investigated the effect of the memory length M on the trial-to-trial error convergence performance. Using Theorem 4.1, and the relation between values of M and γ is given in table 4.1. These confirm that as M increases, i.e., more information from the past is used, the value of γ decreases and the tracking error converges faster, see also figure 4.2. For example, the control law matrices when $M = 2$ are $K = [-617.4002\ 0.5021]$ and $K_1 = 1.0826$, $K_0 = 1828.08$. As the figure shown, when choose the bigger value of M, the speed of error convergence becomes faster, and the result of error convergence based different value of M is in figure 4.2.

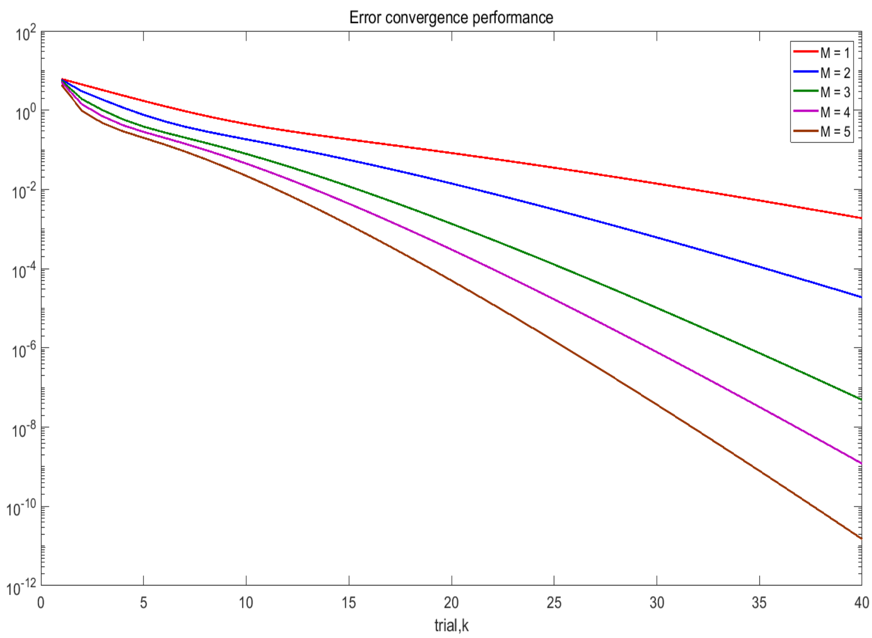

Figure 4.2: Error convergence performance along the trial by using algorithm in Theorem 4.1.

M	γ
1	0.6742
2	0.6240
3	0.5252
4	0.4414
5	0.4133

Table 4.2: Relation between value of M and γ for robust design result by using algorithm in Theorem 4.3.

To examine the effectiveness of the robust design developed in Theorem 4.3, consider the case when the matrices defining the uncertainty model are

$$H_1 = \begin{bmatrix} 0.1 & 0 \end{bmatrix}^T, H_2 = 0.01, E_2 = 0.01,$$
$$E_1 = \begin{bmatrix} 0.1 & -0.1 \end{bmatrix}.$$

The results for different M are shown in figure 4.3, which confirm that: 1) the tracking error decreases monotonically and 2) increasing M improves the convergence speed. table 4.2 shows the relationship between M and value of γ, and the result of error convergence based different value of M is in figure 4.3. Moreover, γ satisfies $\gamma \in [0, 1)$

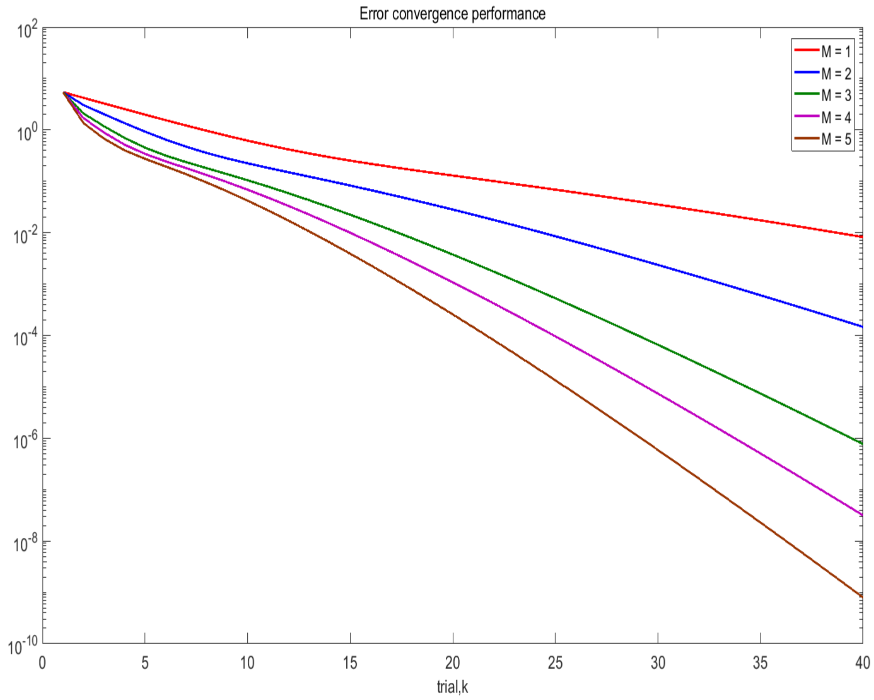

Figure 4.3: Error convergence performance along the trial by using algorithm in Theorem 4.3.

and since the design is applied to an uncertain system, the value of γ with model uncertainty is larger than that without, which is the price paid for robust design.

M	γ
1	0.6602
2	0.6011
3	0.5139
4	0.4456
5	0.4014

Table 4.3: Relation between value of M and γ for LMI design result by using algorithm in Theorem 4.5.

M	γ
1	0.6694
2	0.6214
3	0.5317
4	0.4631
5	0.4322

Table 4.4: Relation between value of M and γ for robust design result by using algorithm in Theorem 4.7.

This part shows the numerical simulation for discrete-time system model, the example is a simple 2th-order system with state-space model matrices

$$A = \begin{bmatrix} -0.3 & 0 \\ 0.35 & -0.22 \end{bmatrix},$$
$$B = \begin{bmatrix} 0.15 & 0 \end{bmatrix}^T,$$
$$C = \begin{bmatrix} 0.15 & 0 \end{bmatrix}$$

, and the completion of each trial the 2-norm of the error signal is

$$\|e_k\|_2 = \sqrt{\int_{t=1}^{N} e_k^2(t)dt}$$

The first simulation study investigated the effect of the memory length M on the trial-to-trial error convergence performance. Using the design method of Theorem 4.5, and the relation between value of M and γ is given in table 4.3. These confirm that as M increases, i.e., more information from the past is used, the value of γ decreases and the tracking error converges faster, see also figure 4.4. For example, the control law matrices when $M = 2$ are $K = [-28.8912 \ 6.6053]$ and $K_1 = 0.5111$, $K_0 = 62.8082$, and the result of error convergence based different value of M is in figure 4.4.

To examine the effectiveness of the robust design developed in Theorem 4.7, consider the case when the matrices defining the same uncertainty model as for the discrete-time example. The results for different M are shown in figure 4.5, which confirm that: 1) the tracking error decreases monotonically and 2) increasing M improves the convergence speed. Table 4.4 shows the relationship between M and value of γ, and the result of

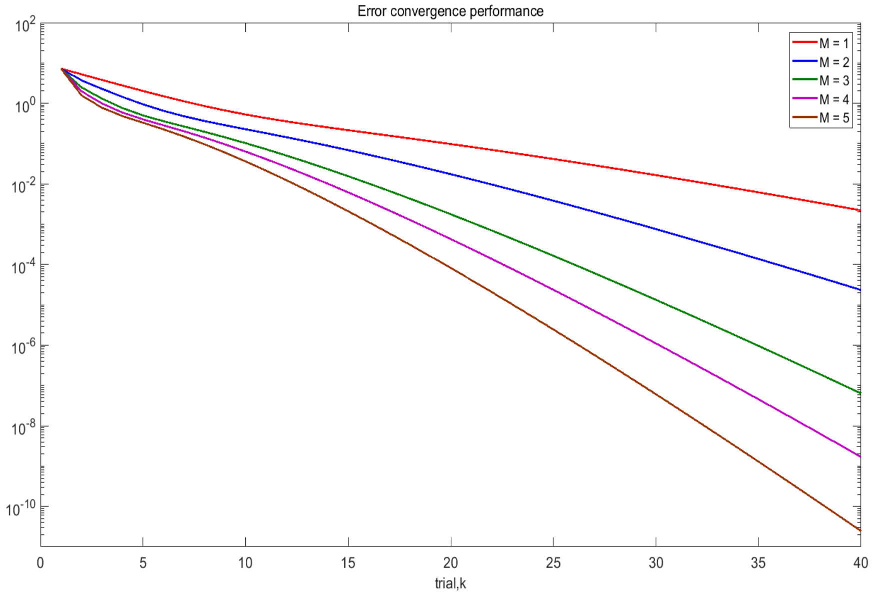

Figure 4.4: Error convergence performance along the trial by using algorithm in Theorem 4.5.

error convergence based different value of M is in table 4.4, γ satisfies $\gamma \in [0, 1)$ and

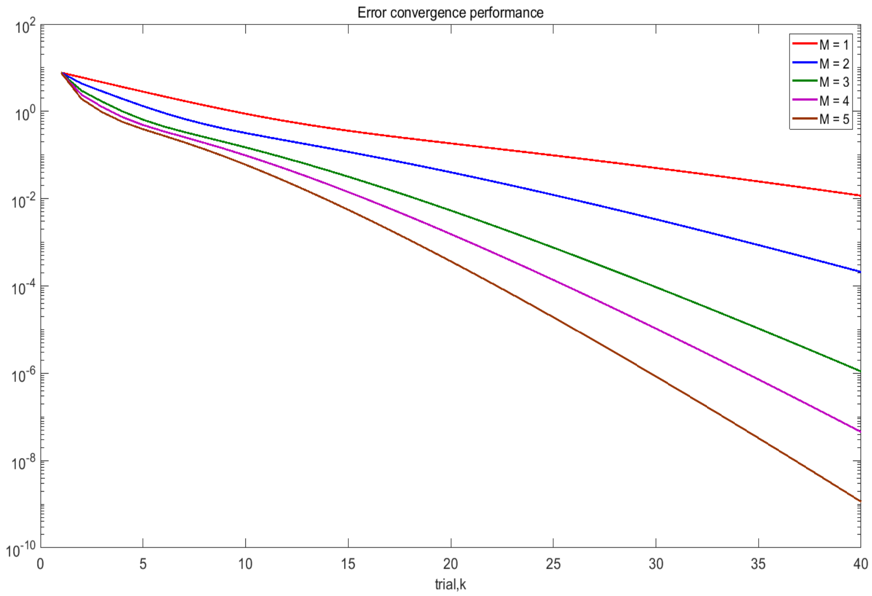

Figure 4.5: Error convergence performance along the trial by using algorithm in Theorem 4.7.

since the design is applied to an uncertain system, the value of γ with model uncertainty is larger than that without, which is the price paid for robust design.

4.5 Summary

In this chapter, the generalized KYP lemma has used to develop new the higher-order ILC control law matrices design algorithms. Compared with the ILC design of the previous chapter, the design algorithm by using generalized KYP lemma can pay more attention on the stability performance within the finite frequency range, such as 'low' frequency. In chapter 3 and chapter 4, the state-feedback control scheme is applied. By using state-feedback control scheme, the feedback system can obtain 'good' transient performance along each trial. However, in practice, the state of system is not always observed, and at this time only output-feedback control scheme is useful for system control. The next chapter gives design algorithm by using output-feedback scheme.

Chapter 5

New Design Algorithms for Output-Feedback Control Laws

5.1 Introduction

In this chapter, the output feedback higher order ILC control law is used. As in the last two, this chapter gives the design algorithms which are based on KYP lemma and its generalized version. Finally, simulation results are also given to show the similar relation between the speed of error convergence and value of memory length.

5.2 Higher-order ILC Design for Discrete-time System

5.2.1 Problem Setup

Consider the discrete time-invariant linear state-space system model in the ILC setting

$$\begin{aligned} x_k(p+1) &= Ax_k(p) + Bu_k(p), \\ y_k(p) &= Cx_k(p),\ \ p = 0, 1, ..., \alpha - 1 \end{aligned} \tag{5.1}$$

where $x_k(p) \in \mathbb{R}^n$ is the state vector, $y_k(p) \in \mathbb{R}^m$ is the output vector, $u_k(p) \in \mathbb{R}^l$ is the input vector, k is the trial number, and the finite trial length $\alpha < \infty$. Let $y_d \in \mathbb{R}^m$ be reference trajectory then error on trial k is $e_k = y_d - y_k$. The ILC control law is

$$u_{k+1}(p) = u_k(p) + \Delta u_{k+1}(p) \tag{5.2}$$

where $\Delta u_{k+1}(p)$ is a function of the error on trial k but could also be a function of the previous trial control input. In order to use repetitive process theory for ILC design, consider

$$\Delta u_{k+1}(p) = \sum_{j=1}^{M} K_{j-1} e_{k+1-j}(p+1) \tag{5.3}$$

as the higher-order ILC control law, and introduce

$$\eta_{k+1}(p+1) = x_{k+1}(p) - x_k(p) \tag{5.4}$$

The resulting controlled dynamics state-space model is

$$\begin{aligned} \eta_{k+1}(p+1) &= A\eta_{k+1}(p) + \sum_{j=1}^{M} \hat{B}_{j-1} e_{k+1-j}(p) \\ e_{k+1}(p) &= \hat{C}\eta_{k+1}(p) + \sum_{j=1}^{M} \hat{D}_{j-1} e_{k+1-j}(p) \end{aligned} \tag{5.5}$$

where

$$\begin{aligned} \hat{B}_0 &= BK_0, \quad \hat{B}_{j-1} = BK_{j-1}, \\ \hat{C} &= -CA, \quad \hat{D}_0 = I - CBK_0, \end{aligned}$$

$$\hat{D}_{j-1} = -CBK_{j-1}, \quad j = 2, ..., M \tag{5.6}$$

which is a discrete non-unit memory linear repetitive process. It is stable along the trial if and only if stability conditions in Theorem 2.6 are satisfied. Therefore the design algorithm for control law matrices is based on Theorem 2.6. In this chapter, the KYP lemma and its generalized version are used.

In some applications, the systems are in the presence of uncertainties in the model structure. For such system models, the general design algorithm cannot make the system stable if it is only based on the certainty part of the model. Therefore, robust design algorithm is given to solve this problem. The norm-bounded additive uncertainty of the system is in consideration. The norm-bounded additive perturbations ΔA, ΔB and ΔC to the state-space model matrices A, B and C are in the form

$$\Delta A = H_1 F E_1, \ \Delta B = H_1 F E_2, \ \Delta C = H_2 F E_1 \tag{5.7}$$

where H_1, H_2, E_1, E_2, and $\mathcal{F}$ are defined in section 3.2.1. Applying the control law (5.2) and (5.3), the model the controlled system is in the form (5.5) and (5.6) with

$$\begin{aligned} &\hat{A} = (A + \Delta A), \quad \hat{B}_0 = (B + \Delta B)K_0, \quad \hat{B}_{j-1} = (B + \Delta B)K_{j-1}, \\ &\hat{C} = -(C + \Delta C)(A + \Delta A), \quad \hat{D}_0 = I - (C + \Delta C)(B + \Delta B)K_0, \end{aligned}$$

$$\hat{D}_{j-1} = -(C + \Delta C)(B + \Delta B)K_{j-1}, \quad j = 2, ..., M \tag{5.8}$$

5.2.2 KYP Lemma Based Design Algorithms

The controlled system (5.5) is not in the standard term of the linear repetitive processes. In order to design the control law matrices, it is necessary to convert it to the unit memory linear repetitive process, i.e.,

$$\begin{aligned} \eta_{k+1}(p+1) &= A\eta_{k+1}(p) + \bar{B}\bar{e}_k(p) \\ \bar{e}_{k+1}(p) &= \bar{C}\eta_{k+1}(p) + \bar{D}\bar{e}_k(p) \end{aligned} \tag{5.9}$$

where

$$\begin{aligned} \bar{e}_k(p) &= \begin{bmatrix} e^T_{k-M+1}(p) & \cdots & e^T_{k-1}(p) & e^T_k(p) \end{bmatrix}^T, \\ \bar{B} &= \begin{bmatrix} \hat{B}_{M-1} & \cdots \hat{B}_1 & \hat{B}_0 \end{bmatrix}, \\ \bar{C} = \begin{bmatrix} 0 \\ 0 \\ \vdots \\ 0 \\ \hat{C} \end{bmatrix}&, \ \bar{D} = \begin{bmatrix} 0 & I & 0 & \cdots & 0 \\ 0 & 0 & I & \ddots & 0 \\ 0 & 0 & 0 & \cdots & 0 \\ \vdots & \vdots & \vdots & \ddots & I \\ \hat{D}_{M-1} & \hat{D}_{M-2} & \hat{D}_{M-3} & \cdots & \hat{D}_0 \end{bmatrix}, \end{aligned} \tag{5.10}$$

Using the z-transform, i.e., $zx_k(p) = x_k(p+1)$, gives

$$\bar{e}_{k+1}(z) = G(z)\bar{e}_k(z) \tag{5.11}$$

where $G(z) = \bar{C}(zI - A)^{-1}\bar{B} + \bar{D}$. The term in transfer-function matrix $G(z)$ which relates to the convergence performance is only the bottom row, i.e.,

$$e_{k+1}(z) = [G_{M-1}(z), ..., G_1(z), G_0(z)]\bar{e}_k(z) \tag{5.12}$$

The design objective is to select the gains $K_{j-1}, j = 1, ..., M$ such that the norm of the above transfer function is sufficiently small and thus convergence can be achieved.

Theorem 5.1. *For a given $\gamma > 0$ and assume the A is stable. Then the discrete linear repetitive process representing the ILC dynamics described by (5.9) is stable along the pass and satisfies*

$$\|[G_{M-1}(z), ..., G_1(z), G_0(z)]\|_\infty < \gamma \tag{5.13}$$

if there exist symmetric matrix $P_1 > 0$, and N_2 with $\mu = \gamma^2$ such that following LMIs are feasible

$$\begin{bmatrix} -P + Q & * \\ A_1P + B_1N & -P \end{bmatrix} < 0 \tag{5.14}$$

$$\begin{bmatrix} -P & * \\ A_2P + B_2N & -P \end{bmatrix} < 0 \tag{5.15}$$

where

$$A_1 = \begin{bmatrix} A & 0 & 0 & \cdots & 0 \\ -CA & 0 & 0 & \cdots & I \end{bmatrix}, \ B_1 = \begin{bmatrix} 0 & B \\ 0 & -CB \end{bmatrix},$$

$$A_2 = \begin{bmatrix} A & 0 & 0 & \cdots & 0 \\ 0 & 0 & I & \cdots & 0 \\ \vdots & \vdots & \vdots & \ddots & \vdots \\ 0 & 0 & 0 & \cdots & I \\ -CA & 0 & 0 & \cdots & I \end{bmatrix}, \ B_2 = \begin{bmatrix} 0 & B \\ 0 & 0 \\ \vdots & \vdots \\ 0 & 0 \\ 0 & -CB \end{bmatrix},$$

and

$$P = diag\{P_1, I\}, \quad Q = diag\{0, (1-\mu)I\}, \quad N = diag\{0, N_2\}.$$

If the LMIs (5.14), and (5.15) are satisfied, stabilizing control law matrices are given by

$$[K_{M-1}, ..., \ K_1, \ K_0] = N_2 \tag{5.16}$$

Proof. The LMI (5.15) can be written as

$$\Phi^T P \Phi - P < 0 \tag{5.17}$$

where

$$\Phi = \begin{bmatrix} A & \bar{B} \\ \bar{C} & \bar{D} \end{bmatrix} \tag{5.18}$$

which is 2D Lyapunov inequality for stability of discrete linear repetitive process, and the feedback system is stable along the trial. The condition (5.13) can be written as

$$\begin{bmatrix} (zI-A)^{-1}\bar{B} \\ I \end{bmatrix}^T \begin{bmatrix} \hat{C} & \tilde{D} \\ 0 & I \end{bmatrix}^T \begin{bmatrix} I & 0 \\ 0 & -\mu I \end{bmatrix} \begin{bmatrix} \hat{C} & \tilde{D} \\ 0 & I \end{bmatrix} \begin{bmatrix} (zI-A)^{-1}\bar{B} \\ I \end{bmatrix} < 0 \tag{5.19}$$

Also by the bounded real lemma, this last condition holds if and only if the following LMI holds

$$\begin{bmatrix} A^TP_1A - P_1 & A^TP_1\bar{B} \\ \bar{B}^TP_1A & \bar{B}^TP_1\bar{B} \end{bmatrix} + \begin{bmatrix} \hat{C} & \tilde{D} \\ 0 & I \end{bmatrix}^T \begin{bmatrix} I & 0 \\ 0 & -\mu I \end{bmatrix} \begin{bmatrix} \hat{C} & \tilde{D} \\ 0 & I \end{bmatrix} < 0 \tag{5.20}$$

Where $\tilde{D} = [\hat{D}_{M-1}, ..., \ \hat{D}_0]$, by using the Schur's complement formula, the LMI (5.12) can be obtained from (5.20), and proof is complete. □

The next theorem shows that when γ is small, the tracking error is guaranteed to convergence to zero.

Theorem 5.2. *If for $\gamma \in [0, 1/\sqrt{M})$ the design in Theorem 5.1 is feasible, the tracking error converges to zero as $k \to \infty$. Moreover, the convergence is monotonic in the sense that*

$$\max\{\|e_{k+1}\|, ..., \|e_{k-M+2}\|\} < \gamma \max\{\|e_k\|, ..., \|e_{k-M+1}\|\}$$

Proof. When the design algorithm in Theorem 5.1 is feasible,

$$\|e_{k+1}\|_2^2 < \gamma^2 \sum_{i=0}^{M-1} \|e_{k-i}\|_2^2 \tag{5.21}$$

Define $q = \gamma^2 M$. As $\gamma < 1/\sqrt{M}$, $q < 1$. Hence

$$\begin{aligned} \|e_{k+1}\|_2^2 &< \gamma^2 \times \{\|e_{k-M+1}\|_2^2 + ... + \|e_k\|_2^2\} \\ &< q \times \max\{\|e_{k-M+1}\|_2^2, ..., \|e_k\|_2^2\} \end{aligned} \tag{5.22}$$

Furthermore,

$$\begin{aligned} \|e_{k+2}\|_2^2 &< q \times \{\|e_{k-M+2}\|_2^2 + ... + \|e_{k+1}\|_2^2\} \\ &< q \times \max\{\|e_{k-M+1}\|_2^2, ..., \|e_k\|_2^2\} \end{aligned} \tag{5.23}$$

Following a similar argument,

$$\begin{aligned} &\max\{\|e_{k+1}\|_2^2, ..., \|e_{k-M+2}\|_2^2\} \\ &\quad < q \times \max\{\|e_{k-M+1}\|_2^2, ..., \|e_k\|_2^2\} \\ &\quad < q^k \times \max\{\|e_{M-1}\|_2^2, ..., \|e_0\|_2^2\} \end{aligned} \tag{5.24}$$

Since $q < 1$, the value of $q^k \to 0$ as $k \to \infty$, and hence $\|e_\infty\|_2 = 0$, which completes the proof. □

From the above theorem it can be seen that γ characterizes how quickly the tracking error converges to zero under the higher order ILC design. In practice, a faster convergence is usually desirable. This can be achieved by solving the following minimization problem.

$$\min_{P_1>0, \gamma<1, N_2} \mu \tag{5.25}$$

If (5.7) is substituted into the general LMI design algorithm, there exists the nonlinear term. In that problem, a solution that avoid this problem is developed. Firstly, using the same output feedback higher-order ILC control law (5.2) for this system (5.1), the controlled ILC system is given by (5.5) and (5.8). This non-unit memory linear repetitive processes can be written as the unit memory linear repetitive processes (5.9). The robust design algorithm is given by the following result.

Theorem 5.3. *For a given $\gamma > 0$ and assume the A is stable. Then the discrete linear repetitive process representing the ILC dynamics of (5.9) with additive uncertainties ΔA, ΔB, and ΔC in (5.7) is stable along the pass and satisfies (5.13) if there exist matrices $P_1 > 0$, N_2, W_{1x}, W_{2x}, W_{1j} for $j = 0, ..., M-1$, W_{20}, W_3, W_{4x}, W_{5x}, W_{4j}, W_{5j} for $j = 0, ..., M-1$, W_6 with appropriate dimensions and real scalars $\epsilon_1 > 0$, $\epsilon_2 > 0$ and $\mu = \gamma^2$ such that the following LMIs are feasible*

$$\begin{bmatrix} -P+Q & * & * & * & * \\ A_2P+B_2N & \Delta_{22} & * & * & * \\ \Delta_{31} & \Delta_{32} & \Delta_{33} & * & * \\ \Delta_{41} & \Delta_{42} & \Delta_{43} & \Delta_{44} & * \\ \Delta_{51} & \Delta_{52} & \Delta_{53} & \Delta_{54} & \Delta_{55} \end{bmatrix} < 0 \tag{5.26}$$

$$\begin{bmatrix} -P & * & * & * & * \\ A_3P+B_3N & \Delta_{62} & * & * & * \\ \Delta_{71} & \Delta_{72} & \Delta_{73} & * & * \\ \Delta_{81} & \Delta_{82} & \Delta_{83} & \Delta_{84} & * \\ \Delta_{91} & \Delta_{92} & \Delta_{93} & \Delta_{94} & \Delta_{95} \end{bmatrix} < 0 \tag{5.27}$$

where P, Q, and N are defined in the Theorem 5.1 and

$$A_2 = \begin{bmatrix} A & 0 & 0 & \cdots & 0 \end{bmatrix}, \quad B_2 = \begin{bmatrix} 0 & B \end{bmatrix},$$

$$A_3 = \begin{bmatrix} A & 0 & 0 & \cdots & 0 \\ 0 & 0 & I & \cdots & 0 \\ \vdots & \vdots & 0 & \ddots & \vdots \\ 0 & 0 & 0 & \cdots & I \end{bmatrix}, \quad B_3 = \begin{bmatrix} 0 & B \\ 0 & 0 \\ \vdots & \vdots \\ 0 & 0 \end{bmatrix},$$

$$I_1 = \begin{bmatrix} 0 & I & \cdots & 0 \\ \vdots & \vdots & \ddots & \vdots \\ 0 & 0 & \cdots & I \end{bmatrix}, \quad I_2 = \begin{bmatrix} 0 & \cdots & 0 & I \end{bmatrix}.$$

$$\Delta_{22} = -P_1 + \epsilon_1 H_1 H_1^T,$$
$$\Delta_{31} = [-CW_{1x}^T, -CW_{1M-1}^T, ..., -CW_{11}^T, I - CW_{10}^T],$$
$$\Delta_{32} = -CW_{2x}^T,$$
$$\Delta_{33} = -I - CW_{20}^T - W_{20}C^T + \epsilon_1 H_2 H_2^T,$$
$$\Delta_{41} = A_2 P + B_2 N + [-W_{1x}^T, -W_{1M-1}^T, ..., -W_{10}^T],$$
$$\Delta_{42} = -W_{2x}^T,$$
$$\Delta_{43} = -W_{20}^T - W_3 C^T,$$
$$\Delta_{44} = -W_3 - W_3^T + \epsilon_1 H_1 H_1^T,$$
$$\bar{E}_1 = [E_1 \ 0 \ 0, ..., \ 0], \ \bar{E}_2 = [E_2 \ E_2],$$
$$\Delta_{51} = \begin{bmatrix} & \bar{E}_1 P + \bar{E}_2 N & & \\ -E_1 W_{1x}^T & -E_1 W_{1M-1}^T & \cdots & -E_1 W_{10}^T \\ & \bar{E}_1 P + \bar{E}_2 N & & \end{bmatrix},$$
$$\Delta_{52} = \begin{bmatrix} 0 \\ -E_1 W_{2x}^T \\ 0 \end{bmatrix}, \quad \Delta_{53} = \begin{bmatrix} 0 \\ -E_1 W_{20}^T \\ 0 \end{bmatrix},$$
$$\Delta_{54} = \begin{bmatrix} 0 \\ -E_1 W_3^T \\ 0 \end{bmatrix}, \quad \Delta_{55} = \begin{bmatrix} -\epsilon_1 I & 0 & 0 \\ 0 & -\epsilon_1 I & 0 \\ 0 & 0 & -\epsilon_1 I \end{bmatrix},$$
$$\Delta_{62} = diag\{-P_1 + \epsilon_2 H_1 H_1^T, -I\},$$
$$\Delta_{71} = [-CW_{4x}^T, -CW_{4M-1}^T, ..., -CW_{41}^T, I - CW_{40}^T],$$
$$\Delta_{72} = [-CW_{5x}^T, -CW_{5M-1}^T, ..., -CW_{51}^T],$$
$$\Delta_{73} = -I - CW_{50}^T - W_{50}C^T + \epsilon_2 H_2 H_2^T,$$
$$\Delta_{81} = A_2 P + B_2 N + [-W_{4x}^T, -W_{4M-1}^T, ..., -W_{40}^T],$$
$$\Delta_{82} = [-W_{5x}^T, -W_{5M-1}^T, ..., -W_{51}^T],$$
$$\Delta_{83} = -W_{50}^T - W_6 C^T,$$
$$\Delta_{84} = -W_6 - W_6^T + \epsilon_2 H_1 H_1^T,$$
$$\Delta_{91} = \begin{bmatrix} & \bar{E}_1 P + \bar{E}_2 N & & \\ -E_1 W_{4x}^T & -E_1 W_{4M-1}^T & \cdots & -E_1 W_{40}^T \\ & \bar{E}_1 P + \bar{E}_2 N & & \end{bmatrix},$$
$$\Delta_{92} = \begin{bmatrix} 0 & 0 & \cdots & 0 \\ -E_1 W_{5x}^T & -E_1 W_{5M-1}^T & \cdots & -E_1 W_{51}^T \\ 0 & 0 & \cdots & 0 \end{bmatrix},$$
$$\Delta_{93} = \begin{bmatrix} 0 \\ -E_1 W_{50}^T \\ 0 \end{bmatrix}, \quad \Delta_{94} = \begin{bmatrix} 0 \\ -E_1 W_6^T \\ 0 \end{bmatrix},$$
$$\Delta_{95} = \begin{bmatrix} -\epsilon_2 I & 0 & 0 \\ 0 & -\epsilon_2 I & 0 \\ 0 & 0 & -\epsilon_2 I \end{bmatrix},$$

If the LMIs (5.26) and (5.27) are satisfied, stabilizing control law matrices are given by

$$[K_{M-1},\ ...,\ K_1,\ K_0] = N_2 \tag{5.28}$$

with use of the linear objective minimization procedure (5.25).

Proof. Direct substitution of (5.8) into (5.14) and (5.15) introduces nonlinear terms. To avoid these and obtain LMIs, applying Theorem 2.19 to these two LMIs, and then the Schur's complement formula gives (5.26) and (5.27) and proof is complete. □

The next theorem gives the condition for monotonic error convergence to zeros as $k \to \infty$.

Theorem 5.4. *If for $\gamma \in (0, 1/\sqrt{M})$ the design in Theorem 5.3 is feasible, the tracking error converges to zero as $k \to \infty$ in the presence of model uncertainties ΔA, ΔB and ΔC. Moreover, the convergence is monotonic in the sense that*

$$\max\{\|e_{k+1}\|, ..., \|e_{k-M+2}\|\} < \gamma \max\{\|e_k\|, ..., \|e_{k-M+1}\|\}$$

Proof. This follows identical steps to that of Theorem 5.2 and here the details are omitted. □

5.2.3 Generalized KYP Lemma Based Design Algorithms

This section develops a new design algorithm for output feedback higher-order control law in the section 5.2.1. The design algorithm is based on the generalized Kalman-Yakubovich-Popov (GKYP) lemma, and is given in the next result.

Theorem 5.5. *For a given $\gamma > 0$ and assume the A is stable. Then the discrete linear repetitive process representing the ILC dynamics described by (5.9) is stable along the pass and satisfies*

$$\max \sigma([G_{M-1}(e^{j\theta}), ..., G_1(e^{j\theta}), G_0(e^{j\theta})]) < \gamma \tag{5.29}$$

over the finite frequency range $\theta \in \Theta$ defined in Lemma 2.15, if there exist matrices $P_1 > 0$, $Q_1 > 0$, $P_2 > 0$, $Q_2 > 0$, X_2, and W_1, and $\mu = \gamma^2$ such that the following LMIs are feasible:

$$\begin{bmatrix} \Xi_{11} & \Xi_{12} - W_1^T & 0 & 0 \\ * & \Xi_{22} + sym\{AW_1\} & BX_2 & -W_1^T A^T C^T \\ * & * & -\mu I & I_0^T - X_2^T B^T C^T \\ * & * & * & -I \end{bmatrix} < 0 \tag{5.30}$$

$$\begin{bmatrix} \bar{\Xi}_{11} & \bar{\Xi}_{12} - W_1^T & 0 & 0 \\ * & \bar{\Xi}_{22} + sym\{AW_1\} & BX_2 & -W_1^T A^T C_1^T \\ * & * & -I & I_1^T - X_2^T B^T C_1^T \\ * & * & * & -I \end{bmatrix} < 0 \tag{5.31}$$

where the compatibly dimensioned matrices Ξ_{11}, Ξ_{12}, Ξ_{22}, *and* $\bar{\Xi}_{11}$, $\bar{\Xi}_{12}$, $\bar{\Xi}_{22}$ *form* Ξ *and* $\bar{\Xi}$ *in Lemma 2.15 and*

$$I_0 = [0, \quad ..., \quad 0 \quad I]$$

,

$$I_1 = \begin{bmatrix} 0 & I & \cdots & 0 \\ 0 & \vdots & \ddots & \vdots \\ 0 & 0 & \cdots & I \\ 0 & 0 & \cdots & I \end{bmatrix}, \quad C_1 = \begin{bmatrix} 0 \\ \vdots \\ 0 \\ C \end{bmatrix}, \tag{5.32}$$

If the (5.30), (5.31) are satisfied, stabilizing control law matrices are given by

$$[K_{M-1}, ..., \ K_1, \ K_0] = X_2 \tag{5.33}$$

Proof. The generalized KYP lemma given in this thesis as Lemma 2.15, then applied with A, $\bar{B}$, $\bar{C}$, and $\bar{D}$, the resulting LMI is

$$\begin{bmatrix} A & \bar{B} \\ I & 0 \end{bmatrix}^T \bar{\Xi} \begin{bmatrix} A & \bar{B} \\ I & 0 \end{bmatrix} + \begin{bmatrix} \bar{C} & \bar{D} \\ 0 & I \end{bmatrix}^T \Pi \begin{bmatrix} \bar{C} & \bar{D} \\ 0 & I \end{bmatrix} < 0 \tag{5.34}$$

Then after some processes include Schur's complement formula, LMI (5.31) is obtained from (5.34), and proof is complete. □

Theorem 5.6. *If for* $\gamma \in [0, 1/\sqrt{M})$ *the design in Theorem 5.5 is feasible, the tracking error converges to zero as* $k \to \infty$ *over the finite frequency range* $\theta \in \Theta$ *defined in Lemma 2.15. Moreover, the convergence is monotonic in the sense that*

$$\max\{\|e_{k+1}\|, ..., \|e_{k-M+2}\|\} < \gamma \max\{\|e_k\|, ..., \|e_{k-M+1}\|\}$$

Proof. This follows identical steps to that of Theorem 5.2 and here the details are omitted. □

In the practice, in order to improve the speed of the error convergence, the next minimization problem is solved to minimize the value of γ,

$$\min_{P_1>0, Q_1>0, P_2>0, Q_2>0, \gamma<1, W_1, X_2} \mu \tag{5.35}$$

Applying the same uncertainties in section 5.2.1, and gives the robust design,

Theorem 5.7. *For a given $\gamma > 0$ and assume the A is stable. Then the discrete linear repetitive process representing the ILC dynamics of (5.9) is stable along the pass and satisfies (5.29) over the finite frequency range $\theta \in \Theta$ defined in Lemma 2.15, and there exist matrices $P_1 > 0$, $Q_1 > 0$, $P_2 > 0$, $Q_2 > 0$, X_2, and W_1, W_{11}, W_{12}, W_{13}, W_{14}, W_2 and W_{31}, W_{32}, W_{33}, W_{34}, W_4, and real scalars ρ_1, ρ_2, $\epsilon_1 > 0$, $\epsilon_2 > 0$ such that the following LMIs are feasible*

$$\begin{bmatrix} \Xi_{11} & \Xi_{12}-W_1^T & 0 & -W_{11}C^T & -W_{11} & 0 & -W_{11}E_1^T & 0 \\ * & \Delta_{22} & BX_2 & -W_{12}C^T & \Delta_{25} & \Delta_{26} & -W_{12}E_1^T & \Delta_{28} \\ * & * & -\mu I & I_0^T-W_{13}C^T & X_2^TB^T-W_{13} & X_2^TE_2^T & -W_{13}E_1^T & X_2^TE_2^T \\ * & * & * & \Delta_{44} & -CW_2^T-W_{14} & 0 & -W_{14}E_1^T & 0 \\ * & * & * & * & \Delta_{55} & 0 & -W_2E_1^T & 0 \\ * & * & * & * & * & -\epsilon_1 I & 0 & 0 \\ * & * & * & * & * & * & -\epsilon_1 I & 0 \\ * & * & * & * & * & * & * & -\epsilon_1 I \end{bmatrix} < 0 \tag{5.36}$$

$$\begin{bmatrix} \bar{\Xi}_{11} & \bar{\Xi}_{12}-W_1^T & 0 & -W_{31}C_1^T & -W_{31} & 0 & -W_{31}E_1^T & 0 \\ * & \Delta_{62} & BX_2 & -W_{32}C_1^T & \Delta_{65} & \Delta_{66} & -W_{32}E_1^T & \Delta_{68} \\ * & * & -I & I_1^T-W_{33}C_1^T & X_2^TB^T-W_{33} & X_2^TE_2^T & -W_{33}E_1^T & X_2^TE_2^T \\ * & * & * & \Delta_{74} & -CW_2^T-W_{34} & 0 & -W_{34}E_1^T & 0 \\ * & * & * & * & \Delta_{85} & 0 & -W_4E_1^T & 0 \\ * & * & * & * & * & -\epsilon_2 I & 0 & 0 \\ * & * & * & * & * & * & -\epsilon_2 I & 0 \\ * & * & * & * & * & * & * & -\epsilon_2 I \end{bmatrix} < 0 \tag{5.37}$$

where

$$\begin{aligned}
\Delta_{22} &= \Xi_{22} + sym\{AW\} + \epsilon_1 H_1 H_1^T, \\
\Delta_{25} &= W_1^T A^T + X_1^T B^T - W_{12}, \\
\Delta_{26} &= \Delta_{28} = W_1^T E_1^T, \\
\Delta_{44} &= -I - sym\{CW_{14}^T\} + \epsilon_1 H_2 H_2^T, \\
\Delta_{55} &= -W_2 - W_2^T + \epsilon_1 H_1 H_1^T \\
\Delta_{62} &= \bar{\Xi}_{22} + sym\{AW\} + \epsilon_2 H_1 H_1^T, \\
\Delta_{65} &= W_1^T A^T - W_{32}, \\
\Delta_{66} &= \Delta_{68} = W_1^T E_1^T, \\
\Delta_{74} &= -I - sym\{CW_{34}^T\} + \epsilon_2 H_2 H_2^T, \\
\Delta_{85} &= -W_4 - W_4^T + \epsilon_2 H_1 H_1^T,
\end{aligned}$$

and I_0, I_1, C_1 are defined in (5.32), and Ξ_{22}, $\bar{\Xi}_{11}$, $\bar{\Xi}_{12}$, $\bar{\Xi}_{22}$ form Ξ and $\bar{\Xi}$ in Lemma 2.15. If the LMIs (5.36), (5.37) are satisfied, stabilizing control law matrices are given by

$$[K_{M-1}, ..., \ K_1, \ K_0] = X_2 \tag{5.38}$$

with use of the linear objective minimization procedure (5.35).

Proof. Direct substitution of (5.8) into (5.30), (5.31) introduces nonlinear terms, applying Theorem 2.19 to these two LMIs and the Schur's complement formula gives the

LMIs (5.36), (5.37), and proof is complete. □

Theorem 5.8. *If for* $\gamma \in (0, 1/\sqrt{M})$ *the design in Theorem 5.7 is feasible, the tracking error converges to zero as* $k \to \infty$ *over the finite frequency range* $\theta \in \Theta$ *defined in Lemma 2.15 even with the presence of model uncertainties* ΔA*,* ΔB *and* ΔC*. Moreover, the convergence is monotonic in the sense that*

$$\max\{\|e_{k+1}\|, ..., \|e_{k-M+2}\|\} < \gamma \max\{\|e_k\|, ..., \|e_{k-M+1}\|\}$$

Proof. This follows identical steps to that of Theorem 5.2 and here the details are omitted. □

5.3 Design Algorithms For Continuous-time Systems

5.3.1 Problem Setup

Consider the discrete time-invariant linear state-space system model in the ILC setting

$$\begin{aligned} \dot{x}_k(t) &= Ax_k(t) + Bu_k(t), \\ y_k(t) &= Cx_k(t),\ 0 < t \leq \alpha \end{aligned} \tag{5.39}$$

and the ILC control law is

$$u_{k+1}(t) = u_k(t) + \Delta u_{k+1}(t) \tag{5.40}$$

where $\Delta u_{k+1}(t)$ is a function of the error on trial k but could also be a function of the previous trial control input and is given by

$$\Delta u_{k+1}(t) = \sum_{j=1}^{M} K_{j-1}\dot{e}_{k+1-j}(t) \tag{5.41}$$

Introduce

$$\eta_{k+1}(t) = \int_0^t (x_{k+1}(t) - x_k(t))dt \tag{5.42}$$

gives resulting controlled dynamics state-space model as

$$\begin{aligned} \dot{\eta}_{k+1}(t) &= A\eta_{k+1}(t) + \sum_{j=1}^{M} \hat{B}_{j-1}e_{k+1-j}(t) \\ ek+1(t) &= \hat{C}\eta_{k+1}(t) + \sum_{j=1}^{M} \hat{D}_{j-1}e_{k+1-j}(t) \end{aligned} \tag{5.43}$$

where

$$\hat{B}_0 = BK_0, \quad \hat{B}_{j-1} = BK_{j-1},$$
$$\hat{C} = -CA, \quad \hat{D}_0 = I - CBK_0,$$

$$\hat{D}_{j-1} = -CBK_{j-1}, \quad j = 2, ..., M \tag{5.44}$$

Applying the same uncertainties in section 5.2.1, the state-space model is

$$\begin{aligned} \dot{x}_k(t) &= (A + \Delta A)x_k(t) + (B + \Delta B)u_k(t), \\ y_k(t) &= (C + \Delta C)x_k(t), \quad p = 0, 1, ..., \alpha - 1 \end{aligned} \tag{5.45}$$

and the norm-bounded additive perturbations ΔA, ΔB and ΔC to the state-space model matrices A, B and C are in the form

$$\Delta A = H_1 F E_1, \ \Delta B = H_1 F E_2, \ \Delta C = H_2 F E_1 \tag{5.46}$$

where H_1, H_2, E_1, E_2, and F are defined in section 3.2.1. If apply the higher-order control law (5.40) for this model the controlled system is in the form (3.5) with

$$\begin{aligned} &\hat{A} = (A + \Delta A), \quad \hat{B}_0 = (B + \Delta B)K_0, \quad \hat{B}_{j-1} = (B + \Delta B)K_{j-1}, \\ &\hat{C} = -(C + \Delta C)(A + \Delta A), \quad \hat{D}_0 = I - (C + \Delta C)(B + \Delta B)K_0, \\ &\hat{D}_{j-1} = -(C + \Delta C)(B + \Delta B)K_{j-1}, \quad j = 2, ..., M \end{aligned} \tag{5.47}$$

5.3.2 KYP Lemma Based Design Algorithms

As similar, the differential linear repetitive process (5.43) is not unit memory, in order to obtain the design algorithm based KYP lemma, convert it to the unit memory linear repetitive process

$$\begin{aligned} \dot{\eta}_{k+1}(t) &= A\eta_{k+1}(t) + \bar{B}\bar{e}_k(t) \\ \bar{e}_{k+1}(t) &= \bar{C}\eta_{k+1}(t) + \bar{D}\bar{e}_k(t) \end{aligned} \tag{5.48}$$

where

$$\bar{e}_k(t) = \begin{bmatrix} e^T_{k-M+1}(t) & \cdots & e^T_{k-1}(t) & e^T_k(t) \end{bmatrix}^T,$$
$$\bar{B} = \begin{bmatrix} \hat{B}_{M-1} & \cdots \hat{B}_1 & \hat{B}_0 \end{bmatrix},$$

$$\bar{C} = \begin{bmatrix} 0 \\ 0 \\ \vdots \\ 0 \\ \hat{C} \end{bmatrix}, \ \bar{D} = \begin{bmatrix} 0 & I & 0 & \cdots & 0 \\ 0 & 0 & I & \ddots & 0 \\ 0 & 0 & 0 & \cdots & 0 \\ \vdots & \vdots & \vdots & \ddots & I \\ \hat{D}_{M-1} & \hat{D}_{M-2} & \hat{D}_{M-3} & \cdots & \hat{D}_0 \end{bmatrix}, \tag{5.49}$$

applying Laplace transform, i.e., $L[\dot{x}_k(t)] = sL[x_k(t)] - x_k(0)$ to (5.49) and gives

$$\bar{e}_{k+1}(s) = G(s)\bar{e}_k(s) \tag{5.50}$$

where $G(s) = \bar{C}(sI - A)^{-1}\bar{B} + \bar{D}$. The term in transfer-function matrix $G(s)$ which relates the convergence performance is only the bottom row. i.e.,

$$e_{k+1}(s) = [G_{M-1}(s), ..., G_1(s), G_0(s)]\bar{e}_k(s) \tag{5.51}$$

and the objective is to select the gains $K_{i-1}, i = 1, ..., M$ such that the norm of the above transfer function is sufficiently small and thus convergence can be achieved.

Theorem 5.9. *For a given $\gamma > 0$ and assume the A is stable. Then the differential linear repetitive process representing the ILC dynamics described by (5.49) is stable along the pass and satisfies*

$$\|[G_{M-1}(s), ..., G_1(s), G_0(s)]\|_\infty < \gamma \tag{5.52}$$

if there exist symmetric matrix $P_1 > 0$, and N_2, $\mu = \gamma^2$ such that following LMIs are feasible

$$\begin{bmatrix} sym\{AP_1\} & BN_2 & -P_1A^TC^T \\ N_2^TB^T & -\mu I & I_0^T - N_2^TB^TC^T \\ -CAP_1 & I_0 - CBN_2 & -I \end{bmatrix} < 0 \tag{5.53}$$

$$\begin{bmatrix} sym\{AP_1\} & BN_2 & -P_1A^TC_1^T \\ N_2^TB^T & -I & I_1^T - N_2^TB^TC_1^T \\ -C_1AP_1 & I_1 - C_1BN_2 & -I \end{bmatrix} < 0 \tag{5.54}$$

where I_0, I_1, and C_1 are defined in (5.32). The stabilizing control law matrices are given by

$$[K_{M-1}, ..., \ K_1, \ K_0] = N_2 \tag{5.55}$$

Proof. The LMI (5.54) can be written as

$$\Phi^T \begin{bmatrix} P_1 & 0 \\ 0 & 0 \end{bmatrix} + \begin{bmatrix} P_1 & 0 \\ 0 & 0 \end{bmatrix} \Phi + \Phi^T \begin{bmatrix} 0 & 0 \\ 0 & I \end{bmatrix} \Phi - \begin{bmatrix} 0 & 0 \\ 0 & I \end{bmatrix} < 0 \tag{5.56}$$

where

$$\Phi = \begin{bmatrix} A & \bar{B} \\ \bar{C} & \bar{D} \end{bmatrix} \tag{5.57}$$

which satisfies the 2D Lyapunov inequality for differential linear repetitive process, The condition (5.52) can be written as

$$\begin{bmatrix} (j\omega I - A)^{-1}\bar{B} \\ I \end{bmatrix}^T \begin{bmatrix} \hat{C} & \tilde{D} \\ 0 & I \end{bmatrix}^T \begin{bmatrix} I & 0 \\ 0 & -\mu I \end{bmatrix} \begin{bmatrix} \hat{C} & \tilde{D} \\ 0 & I \end{bmatrix} \begin{bmatrix} (j\omega I - A)^{-1}\bar{B} \\ I \end{bmatrix} < 0 \tag{5.58}$$

Also by the bounded real lemma, this last condition holds if and only if the following LMI holds

$$\begin{bmatrix} A^T P_1 + P_1 A & P_1 \bar{B} \\ \bar{B}^T P_1 & 0 \end{bmatrix} + \begin{bmatrix} \hat{C}^T \bar{C} & \hat{C}^T \tilde{D} \\ \tilde{D}^T \hat{C} & \tilde{D}^T \tilde{D} - \mu I \end{bmatrix} < 0 \tag{5.59}$$

Where $\tilde{D} = [\hat{D}_{M-1}, ..., \ \hat{D}_0]$, by using Schur's complement formula, the LMI (5.53) can be obtained from (5.59), and proof is complete. □

and the next theorem shows that when γ is small, the tracking error is guaranteed to converge to zeros.

Theorem 5.10. *If for $\gamma \in [0, 1/\sqrt{M})$ the design in Theorem 5.9 is feasible, the tracking error converges to zero as $k \to \infty$. Moreover, the convergence is monotonic in the sense that*

$$\max\{\|e_{k+1}\|, ..., \|e_{k-M+2}\|\} < \gamma \max\{\|e_k\|, ..., \|e_{k-M+1}\|\}$$

Proof. This follows identical steps to that of Theorem 5.2 and here the details are omitted. □

From the above theorem it can be seen that γ characterizes how quickly the tracking error converges to zero under the higher order ILC design. In practice, a faster convergence is usually desirable. This can be achieved by solving the following minimization problem.

$$\min_{P_1 > 0, \gamma < 1, N_2} \mu \tag{5.60}$$

Consider the uncertainties in the state-space model, the robust design is

Theorem 5.11. *For a given $\gamma > 0$ and assume the A is stable. Then the differential linear repetitive process representing the ILC dynamics of (5.48) with additive uncertainty part ΔA, ΔB, and ΔC in (5.7) is stable along the pass and satisfies (5.52) if there exist matrices $P_1 > 0$, N_2, W_{1x}, W_{2x}, W_{1j} for $j = 0, ..., M-1$, W_2, W_{3x}, W_{4x},*

W_{3j}, W_4 for $j = 0, ..., M-1$, W_6 with appropriate dimensions and real scalars $\epsilon_1 > 0$, $\epsilon_2 > 0$ and $\mu = \gamma^2$ such that the following LMI is feasible

$$\begin{bmatrix} \Delta_{11} & * & * & * & * & * & * \\ N_2^T B^T & -\mu I & * & * & * & * & * \\ -CW_{1x}^T & I_0 - CW_1^T & \Delta_{33} & * & * & * & * \\ AP_1 - W_{1x}^T & BN_2 - W_1^T & -W_{2x}^T - W_2 C^T & \Delta_{44} & * & * & * \\ E_1 P_1 & E_2 N_2 & 0 & 0 & -\epsilon_1 I & * & * \\ -E_1 W_{1x}^T & -E_1 W_1^T & -E_1 W_{2x}^T & -E_1 W_2^T & 0 & -\epsilon_1 I & * \\ E_1 P_1 & E_2 N_2 & 0 & 0 & 0 & 0 & -\epsilon_1 I \end{bmatrix} < 0 \tag{5.61}$$

$$\begin{bmatrix} \Delta_{51} & * & * & * & * & * & * \\ N_2^T B^T & -I & * & * & * & * & * \\ -C_1 W_{3x}^T & I_1 - C_1 W_3^T & \Delta_{63} & * & * & * & * \\ AP_1 - W_{3x}^T & BN_2 - W_3^T & -W_{4x}^T - W_4 C_1^T & \Delta_{74} & * & * & * \\ E_1 P_1 & E_2 N_2 & 0 & 0 & -\epsilon_2 I & * & * \\ -E_1 W_{3x}^T & -E_1 W_3^T & -E_1 W_{4x}^T & -E_1 W_4^T & 0 & -\epsilon_2 I & * \\ E_1 P_1 & E_2 N_2 & 0 & 0 & 0 & 0 & -\epsilon_2 I \end{bmatrix} < 0 \tag{5.62}$$

where I_0, I_1, and C_1 are defined in (5.32) and

$$\begin{aligned} \Delta_{11} &= sym\{AP_1\} + \epsilon_1 H_1 H_1^T, \\ \Delta_{33} &= -I - CW_{2x}^T - W_{2x} C^T + \epsilon_1 H_2 H_2^T, \\ \Delta_{44} &= -W_2 - W_2^T + \epsilon_1 H_1 H_1^T, \\ \Delta_{51} &= sym\{AP_1\} + \epsilon_2 H_1 H_1^T, \\ \Delta_{63} &= -I - CW_{4x}^T - W_{4x} C^T + \epsilon_2 H_3 H_3^T, \\ \Delta_{74} &= -W_4 - W_4^T + \epsilon_2 H_1 H_1^T, \end{aligned}$$

and $W_1 = [W_{1M-1}, ..., W_{11}]$, $W_3 = [W_{3M-1}, ..., W_{31}]$, and $H_3 = [0, ..., 0, H_2]^T$. If (5.61) and (5.62) are satisfied, the stabilizing control law matrices are given by

$$[K_{M-1}, ..., \ K_1, \ K_0] = N_2 \tag{5.63}$$

with use of the linear objective minimization procedure (5.60).

Proof. This follows identical steps to that of Theorem 5.3 and here the details are omitted. □

Theorem 5.12. *If for $\gamma \in (0, 1/\sqrt{M})$ the design in Theorem 5.11 is feasible, the tracking error converges to zero as $k \to \infty$ even with the presence of model uncertainties ΔA,*

ΔB and ΔC. Moreover, the convergence is monotonic in the sense that

$$\max\{\|e_{k+1}\|, ..., \|e_{k-M+2}\|\} < \gamma \max\{\|e_k\|, ..., \|e_{k-M+1}\|\}$$

Proof. This follows identical steps to that of Theorem 5.2 and here the details are omitted. □

5.3.3 Generalized KYP Lemma Based Design Algorithms

Applying the generalized KYP lemma to design the control law matrices in (5.41), the theorem is

Theorem 5.13. *For a given $\gamma > 0$ and assume the A is stable. Then the differential linear repetitive process representing the ILC dynamics of (5.48) is stable along the pass and satisfies*

$$\max \sigma([G_{M-1}(j\theta), ..., G_1(j\theta), G_0(j\theta)]) < \gamma \tag{5.64}$$

over the finite frequency range defined in Lemma 2.16, and there exist matrices $P_1 > 0$, $Q_1 > 0$, $P_2 > 0$, $Q_2 > 0$, X_2, and W_1, and $\mu = \gamma^2$ such that the following LMIs are feasible:

$$\begin{bmatrix} \Xi_{11} & \Xi_{12} - W_1^T & 0 & 0 \\ * & \Xi_{22} + sym\{AW_1\} & BX_2 & -W_1^T A^T C^T \\ * & * & -\mu I & I_0^T - X_2^T B^T C^T \\ * & * & * & -I \end{bmatrix} < 0 \tag{5.65}$$

$$\begin{bmatrix} \bar{\Xi}_{11} & \bar{\Xi}_{12} - W_1^T & 0 & 0 \\ * & \bar{\Xi}_{22} + sym\{AW_1\} & BX_2 & -W_1^T A^T C_1^T \\ * & * & -I & I_1^T - X_2^T B^T C_1^T \\ * & * & * & -I \end{bmatrix} < 0 \tag{5.66}$$

where the compatibly dimensioned matrices Ξ_{11}, Ξ_{12}, Ξ_{22}, and $\bar{\Xi}_{11}$, $\bar{\Xi}_{12}$, $\bar{\Xi}_{22}$ form Ξ and $\bar{\Xi}$ in Lemma 2.16 and I_0, I_1, C_1 are defined in (5.32). If the (5.65), (5.66) are satisfied, stabilizing control law matrices are given by

$$[K_{M-1}, ..., \ K_1, \ K_0] = X_2 \tag{5.67}$$

Proof. The generalized KYP lemma of Lemma 2.16, when applied with A, $\bar{B}$, $\bar{C}$, and $\bar{D}$ in it, the equal LMI is

$$\begin{bmatrix} A & \bar{B} \\ I & 0 \end{bmatrix}^T \bar{\Xi} \begin{bmatrix} A & \bar{B} \\ I & 0 \end{bmatrix} + \begin{bmatrix} \bar{C} & \bar{D} \\ 0 & I \end{bmatrix}^T \Pi \begin{bmatrix} \bar{C} & \bar{D} \\ 0 & I \end{bmatrix} < 0 \tag{5.68}$$

Then after some processes include Schur's complement, finally, LMI (5.66) can be obtained from (5.68). □

When γ in the design algorithm is small, the tracking error is guaranteed to converges to zeros.

Theorem 5.14. *If for $\gamma \in [0, 1/\sqrt{M})$ the design in Theorem 5.13 is feasible, the tracking error converges to zero as $k \to \infty$ for some finite frequency range defined in Lemma 2.16. Moreover, the convergence is monotonic in the sense that*

$$\max\{\|e_{k+1}\|, ..., \|e_{k-M+2}\|\} < \gamma \max\{\|e_k\|, ..., \|e_{k-M+1}\|\}$$

Proof. This follows identical steps to that of Theorem 5.2 and here the details are omitted. □

In practice, a faster convergence can be achieved by solving next linear objective minimization procedure,

$$\min_{P_1>0, Q_1>0, P_2>0, Q_2>0, \gamma<1, W_1, X_2} \mu \tag{5.69}$$

and the robust design for uncertainties in the system is

Theorem 5.15. *For a given $\gamma > 0$ and assume the A is stable. Then the differential linear repetitive process representing the ILC dynamics of (5.48)is stable along the pass and satisfies (5.64) over the finite frequency range defined in Lemma 2.16, and there exist matrices $P_1 > 0$, $Q_1 > 0$, $P_2 > 0$, $Q_2 > 0$, X_2, and W_1, W_{11}, W_{12}, W_{13}, W_{14}, W_2 and W_{31}, W_{32}, W_{33}, W_{34}, W_4, $\epsilon_1 > 0$, $\epsilon_2 > 0$ such that the following LMIs are feasible*

$$\begin{bmatrix} \Xi_{11} & \Xi_{12}-W_1^T & 0 & -W_{11}C^T & -W_{11} & 0 & -W_{11}E_1^T & 0 \\ * & \Delta_{22} & BX_2 & -W_{12}C^T & \Delta_{25} & \Delta_{26} & -W_{12}E_1^T & \Delta_{28} \\ * & * & -\mu I & I_0^T-W_{13}C^T & X_2^TB^T-W_{13} & X_2^TE_2^T & -W_{13}E_1^T & X_2^TE_2^T \\ * & * & * & \Delta_{44} & -CW_2^T-W_{14} & 0 & -W_{14}E_1^T & 0 \\ * & * & * & * & \Delta_{55} & 0 & -W_2E_1^T & 0 \\ * & * & * & * & * & -\epsilon_1 I & 0 & 0 \\ * & * & * & * & * & * & -\epsilon_1 I & 0 \\ * & * & * & * & * & * & * & -\epsilon_1 I \end{bmatrix} < 0 \tag{5.70}$$

$$\begin{bmatrix} \bar{\Xi}_{11} & \bar{\Xi}_{12}-W_1^T & 0 & -W_{31}C_1^T & -W_{31} & 0 & -W_{31}E_1^T & 0 \\ * & \Delta_{62} & BX_2 & -W_{32}C_1^T & \Delta_{65} & \Delta_{66} & -W_{32}E_1^T & \Delta_{68} \\ * & * & -I & I_1^T-W_{33}C_1^T & X_2^TB^T-W_{33} & X_2^TE_2^T & -W_{33}E_1^T & X_2^TE_2^T \\ * & * & * & \Delta_{74} & -CW_2^T-W_{34} & 0 & -W_{34}E_1^T & 0 \\ * & * & * & * & \Delta_{85} & 0 & -W_4E_1^T & 0 \\ * & * & * & * & * & -\epsilon_2 I & 0 & 0 \\ * & * & * & * & * & * & -\epsilon_2 I & 0 \\ * & * & * & * & * & * & * & -\epsilon_2 I \end{bmatrix} < 0 \tag{5.71}$$

where

$$
\begin{aligned}
\Delta_{22} &= \Xi_{22} + sym\{AW\} + \epsilon_1 H_1 H_1^T, \\
\Delta_{25} &= W_1^T A^T - W_{12}, \\
\Delta_{26} &= \Delta_{28} = W_1^T E_1^T, \\
\Delta_{44} &= -I - sym\{CW_{14}^T\} + \epsilon_1 H_2 H_2^T, \\
\Delta_{55} &= -W_2 - W_2^T + \epsilon_1 H_1 H_1^T \\
\Delta_{62} &= \bar{\Xi}_{22} + sym\{AW\} + \epsilon_2 H_1 H_1^T, \\
\Delta_{65} &= W_1^T A^T - W_{32}, \\
\Delta_{66} &= \Delta_{68} = W_1^T E_1^T, \\
\Delta_{74} &= -I - sym\{CW_{34}^T\} + \epsilon_2 H_2 H_2^T, \\
\Delta_{85} &= -W_4 - W_4^T + \epsilon_2 H_1 H_1^T,
\end{aligned}
$$

and I_0, I_1, C_1 are defined in (5.32), and Ξ_{22}, $\bar{\Xi}_{11}$, $\bar{\Xi}_{12}$, $\bar{\Xi}_{22}$ form Ξ and $\bar{\Xi}$ in Lemma 2.16. If the LMIs (5.70), (5.71) are satisfied, stabilizing control law matrices are given by

$$
[K_{M-1}, ..., \ K_1, \ K_0] = X_2 \tag{5.72}
$$

with use of the linear objective minimization procedure (5.69).

Proof. This follows identical steps to that of Theorem 5.7 and here the details are omitted. □

and

Theorem 5.16. *If for $\gamma \in (0, 1/\sqrt{M})$ the design in Theorem 5.15 is feasible, the tracking error converges to zero as $k \to \infty$ over the finite frequency range defined in Lemma 2.16 even with the presence of model uncertainties ΔA, ΔB and ΔC. Moreover, the convergence is monotonic in the sense that*

$$
\max\{\|e_{k+1}\|, ..., \|e_{k-M+2}\|\} < \gamma \max\{\|e_k\|, ..., \|e_{k-M+1}\|\}
$$

Proof. This follows identical steps to that of Theorem 5.2 and here the details are omitted. □

5.4 Numerical Examples

In this section, examples are to test the new design algorithms developed earlier in this chapter. In this simulation, the value of memory length M is from 1 to 5, and the number of trial is 40, the trial length is 2 sec. The reference trajectory and system model that are used in this section is as the same as that in the previous chapters. Also use same definition of the 2-norm of the error signal. The example is a simple 2th-order systems model with state-space model matrices

$$A = \begin{bmatrix} -0.3 & 0 \\ 0.35 & -0.22 \end{bmatrix},$$
$$B = \begin{bmatrix} 0.15 & 0 \end{bmatrix}^T,$$
$$C = \begin{bmatrix} 0.15 & 0 \end{bmatrix},$$

for continuous-time model, and after sampling by using 100Hz sample frequency, obtain the discrete-time system with state-space model matrices

$$A = \begin{bmatrix} 0.9970 & 0 \\ 0.0035 & 0.9978 \end{bmatrix},$$
$$B = \begin{bmatrix} 0.0015 & 0 \end{bmatrix}^T,$$
$$C = \begin{bmatrix} 0.15 & 0 \end{bmatrix},$$

There are two parts, first part shows the simulation results for design algorithm by using KYP lemma, and the latter part is for design algorithm by using generalized KYP lemma.

The first simulation study investigated the effect of the memory length M on the trial-to-trial error convergence performance. Using Theorem 5.1 for discrete-time systems and Theorem 5.9 for continuous-time systems, and the relation between value of M and γ is given in table 5.1. These confirm that as M increases, i.e., more information from the past is used, the value of γ decreases and the tracking error converges faster, see also figure 5.1. For example, the control law matrices when $M = 2$ are $K_1 = 1.0013$, $K_0 = 1512.0081$ for discrete-time systems and $K_1 = 1.2113$, $K_0 = 59.1081$ for continuous-time systems. As the figure shows, the error convergence is faster with larger M, and error convergence based different value of M is in figure 5.1.

M	γ (discrete-time version)	γ (continuous-time version)
1	0.6774	0.6781
2	0.6312	0.6314
3	0.5211	0.5423
4	0.4672	0.4601
5	0.4214	0.4217

Table 5.1: Relation between value of M and γ for design by using algorithm in Theorem 5.1 and Theorem 5.9.

To examine the effectiveness of the robust design developed in Theorem 5.3 for discrete-time systems and Theorem 5.11 for continuous-time systems, consider the case when the

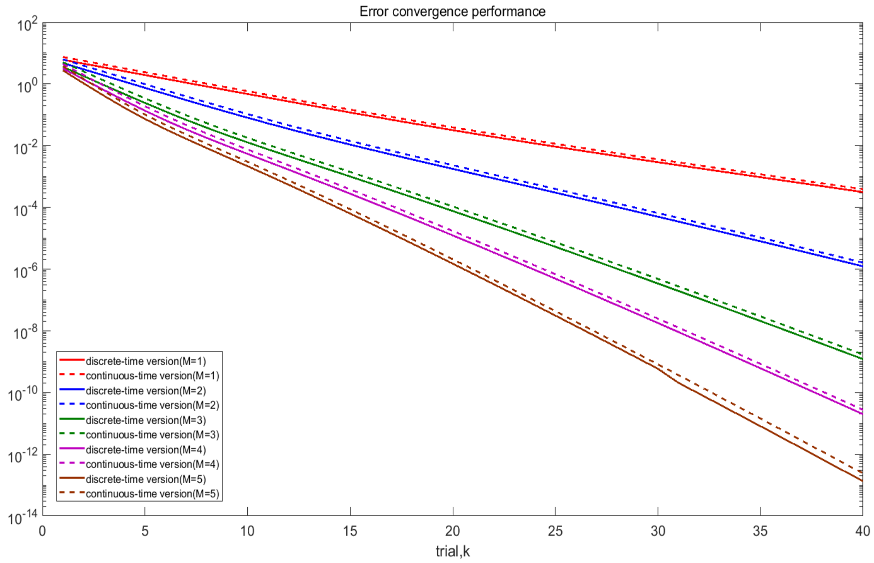

Figure 5.1: Error convergence performance along the trial by using algorithm in Theorem 5.1 and Theorem 5.9.

matrices defining the same uncertainty model as in previous chapters. The results for different M are shown in figure 5.2, and also confirm that: 1) the tracking error decreases monotonically and 2) increasing M improves the convergence speed. Table 5.2 shows the relationship between M and value of γ, and error convergence based different value

M	γ (discrete-time version)	γ (continuous-time version)
1	0.6811	0.6869
2	0.6324	0.6402
3	0.5391	0.5531
4	0.4721	0.4832
5	0.4301	0.4334

Table 5.2: Relation between value of M and γ for robust design result by using algorithm in Theorem 5.3 and Theorem 5.11.

of M is in figure 5.2. In table 5.2, γ satisfies $\gamma \in [0, 1)$ and since the design is applied to an uncertain system, the value of γ with model uncertainty is larger than that without, which is the price paid for robust design.

Then simulation study investigated the effect of the memory length M on the trial-to-trial error convergence performance for generalized KYP lemma based design algorithms in Theorem 5.5 and Theorem 5.13, and the relation between value of M and γ is given in Table 5.3. These also confirm that as M increases, i.e., more information from the past is used, the value of γ decreases and the tracking error converges faster, see also figure 5.3. For example, the control law matrices when $M = 2$ are $K_1 = 1.2023$, $K_0 = 1541.2284$ for discrete-time systems and $K_1 = 1.4111$, $K_0 = 51.2082$ for continuous-time systems. As the figure shows, the error convergence is faster with larger M, and error convergence

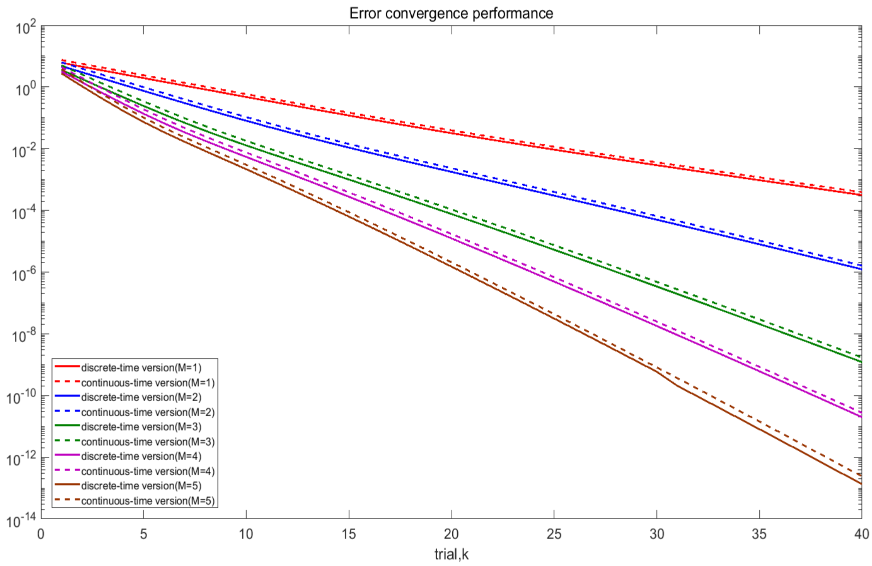

Figure 5.2: Error convergence performance along the trial by using algorithm in Theorem 5.3 and Theorem 5.11.

M	γ (discrete-time version)	γ (continuous-time version)
1	0.6741	0.6764
2	0.6142	0.6172
3	0.5132	0.5311
4	0.4511	0.4571
5	0.4131	0.4201

Table 5.3: Relation between value of M and γ for design by using algorithm in Theorem 5.5 and Theorem 5.13.

based different value of M is in figure 5.3.

To examine the effectiveness of the robust design in Theorem 5.7 and Theorem 5.15, consider the case when the matrices defining the same uncertainty model. The results for different M are shown in figure 5.4, and confirm that: 1) the tracking error decreases monotonically and 2) increasing M improves the convergence speed. Table 5.4 shows the relationship between M and value of γ, and error convergence based different value

M	γ (discrete-time version)	γ (continuous-time version)
1	0.6802	0.6810
2	0.6299	0.6311
3	0.5312	0.5510
4	0.4611	0.4634
5	0.4217	0.4270

Table 5.4: Relation between value of M and γ for robust design result by using algorithm in Theorem 5.7 and Theorem 5.15.

of M is in figure 5.4. In table 5.4, γ satisfies $\gamma \in [0, 1)$ and since the design is applied to an uncertain system, the value of γ with model uncertainty is larger than that without.

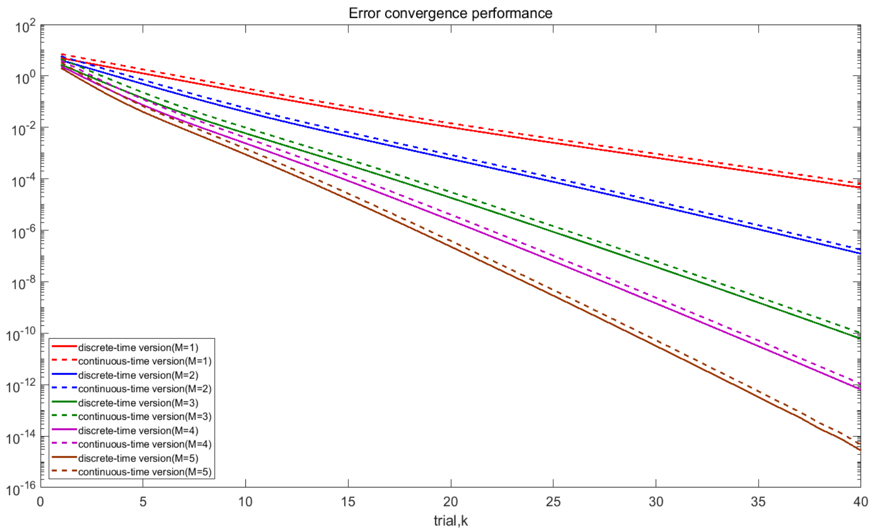

Figure 5.3: Error convergence performance along the trial by using algorithm in Theorem 5.5 and Theorem 5.13.

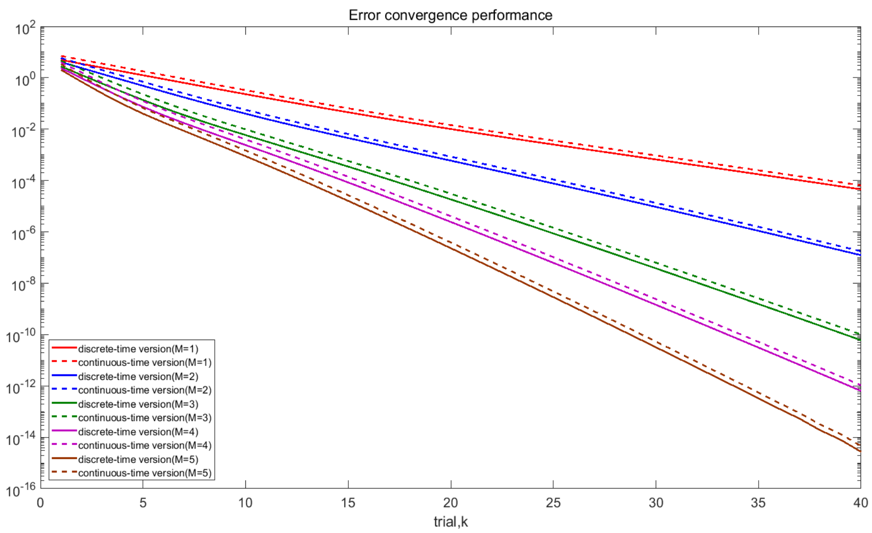

Figure 5.4: Error convergence performance along the trial by using algorithm in Theorem 5.7 and Theorem 5.15.

5.5 Summary

In this chapter, a new design algorithm has been developed for higher-order ILC control law matrices. The higher-order control law uses output-feedback, and design is based on the KYP lemma and its generalized version. This new design requires attenuation of the frequency content of the previous trial error over the complete trial length. In some applications, however, only a finite frequency range need to be considered. In other applications, it may be required to impose different frequency specifications over various frequency ranges. For such applications, the generalized KYP lemma based design algorithm can be used. In the next chapter, the gantry robot model is used to test different design algorithms based state-feedback and output-feedback control, also the comparison and discussion is given.

Chapter 6

Simulation Based Case Studies

6.1 Introduction

In the previous chapters, algorithms for ILC design based on repetitive process stability conditions are developed. In this chapter, a gantry robot is used to test the performance of these ILC design algorithms. The gantry robot replicates a pick and place task which consists of: i) collect the payload from a fixed location, ii) transferring it over a finite duration, iii) place it at a fixed location or under synchronization on a moving conveyor, iv) return to the starting location and v) repeat i)–iv) as many times as required or until a halt for maintenance or for other reasons is required. The design and commissioning of this system is described in [70] and the relevant cited references, including the construction of transfer-function approximate models of the dynamics of each axis from frequency response tests.

This experimental facility has been used to compare many ILC designs, including those designed in the repetitive process setting. The gantry robot is shown in figure 6.1, which consists of three separate axes which are mounted perpendicular to each other. In this chapter, only 7th order X-axis of model is used, it is the highest order axis in the gantry robot, and its frequency response is shown in figure 6.2, and the reference trajectory of X-axis with trial length as 2 sec is in figure 6.3. The continuous-time state-space model

Figure 6.1: The gantry robot with the three axes marked.

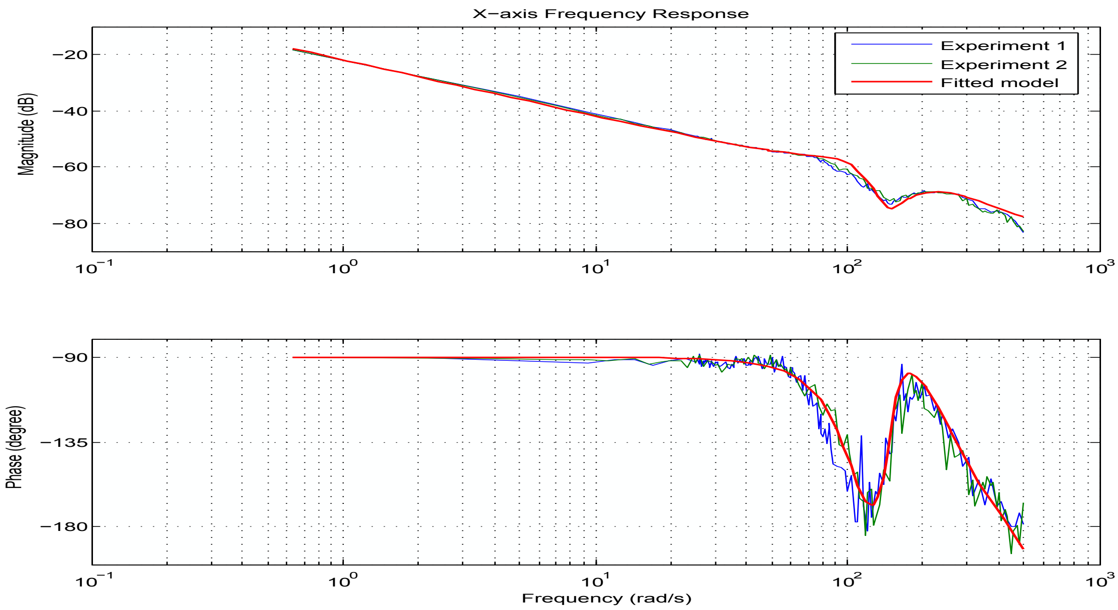

Figure 6.2: Frequency response testing results for the X-axis of the gantry robot.

matrices are

$$A = \begin{bmatrix} -30.7846 & 162.5501 & 16.0032 & 5.9864 & 5.4855 & 6.2566 & 5.8107 \\ -63.3620 & -30.7846 & 35.5443 & -39.2850 & 33.3716 & -40.3732 & -2.8846 \\ 0 & 0 & -113.9526 & 187.1883 & -19.1232 & -131.0272 & -53.4097 \\ 0 & 0 & -232.3381 & -113.9526 & -143.3183 & 391.9655 & 95.1775 \\ 0 & 0 & 0 & 0 & -233.1077 & 662.0887 & 223.8695 \\ 0 & 0 & 0 & 0 & -21.7165 & -233.1077 & -64.1019 \\ 0 & 0 & 0 & 0 & 0 & 0 & 0 \end{bmatrix},$$

$$B = \begin{bmatrix} -0.2643 & 0.4654 & 4.0497 & -8.1245 & -16.5316 & 3.7272 & 9.1000 \end{bmatrix}^T,$$

$$C = \begin{bmatrix} 0.0391 & 0 & 0.0146 & 0 & 0.0071 & 0 & 0.0057 \end{bmatrix}.$$

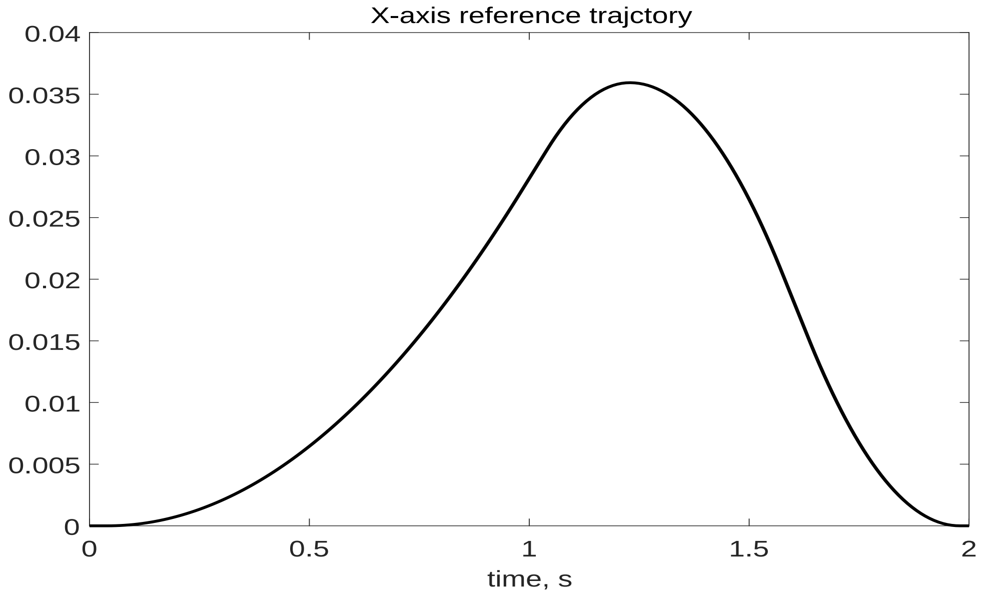

Figure 6.3: The reference trajectory for the X-axis.

Sampling at $T_s = 0.01s$ sec given the discrete-time state-space model matrices

$$A = \begin{bmatrix} 0.3879 & 1.0000 & 0.2138 & 0 & 0.1041 & 0 & 0.0832 \\ -0.3898 & 0.3879 & 0.1744 & 0 & 0.0849 & 0 & 0.0678 \\ 0 & 0 & -0.1575 & 0.2500 & -0.2006 & 0 & -0.1603 \\ 0 & 0 & -0.3103 & -0.1575 & -0.0555 & 0 & -0.0444 \\ 0 & 0 & 0 & 0 & 0.0353 & 0.5000 & 0.2809 \\ 0 & 0 & 0 & 0 & -0.0164 & 0.0353 & -0.2757 \\ 0 & 0 & 0 & 0 & 0 & 0 & 1.0000 \end{bmatrix},$$

$$B = \begin{bmatrix} 0 & 0 & 0 & 0 & 0 & 0 & 0.0910 \end{bmatrix}^T,$$

$$C = \begin{bmatrix} 0.0391 & 0 & 0.0146 & 0 & 0.0071 & 0 & 0.0057 \end{bmatrix}.$$

6.2 Results for the KYP lemma based design

In this section, gantry robot is used to test the design algorithms based on KYP lemma.

6.2.1 Simulation results for the state-feedback control design

In this section, the simulation results are for designers of state-feedback scheme. The value of memory length M is from 1 to 5.

As one example of the application of Theorem 3.1, the results for $M = 2$ are

$$K = [\ -17.8484\ \ -42.8556\ \ -9.4786\ \ -1.4860\ \ -4.2474\ \ -1.8368\ \ -19.5956]$$

and

$$K_1 = 0.3825, \quad K_0 = 181.9765$$

Table 6.1 gives the values of γ for different M, and the error convergence performance

M	γ(discrete-time version)	γ(continuous-time version)
1	0.9996	0.9998
2	0.7008	0.7041
3	0.5021	0.5209
4	0.4572	0.4591
5	0.3913	0.4158

Table 6.1: Relation between value of M and γ for the state feedback design(State-feedback, KYP lemma based design algorithm).

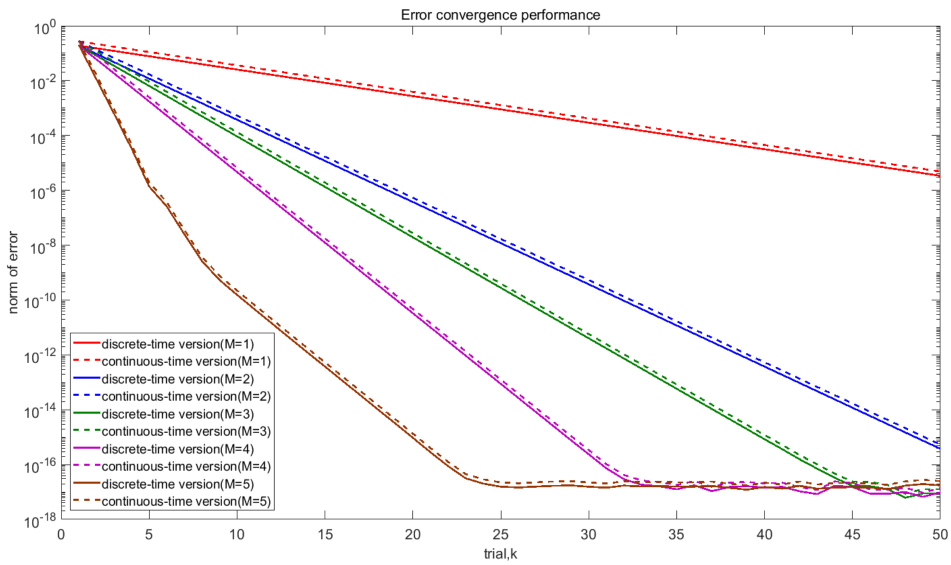

Figure 6.4: Error convergence performance from trial to trial (State-feedback, KYP lemma based design algorithm).

is shown in figure 6.4. The results confirm that as M increases the speed of error convergence also increases.

As a robust design example, consider additive uncertainty in the case when

$$H_1 = \begin{bmatrix} 0.1 & 0 & 0 & 0 & 0 & 0 & 0 \end{bmatrix}^T, H_2 = 0.01, E_2 = 0.01,$$
$$E_1 = \begin{bmatrix} 0.1 & -0.1 & 0.1 & -0.1 & 0.05 & -0.05 & 0.1 \end{bmatrix}.$$

M	γ(discrete-time version)	γ(continuous-time version)
1	0.9996	0.9999
2	0.7015	0.7062
3	0.5988	0.6010
4	0.4591	0.4980
5	0.3985	0.4456

Table 6.2: Relation between value of M and γ for robust design (State-feedback, KYP lemma based design algorithm).

Again M from 1 to 5 is considered over 50 trials. The results are in the next table and figure, and the figure of error convergence with different M is shown in figure 6.5. The

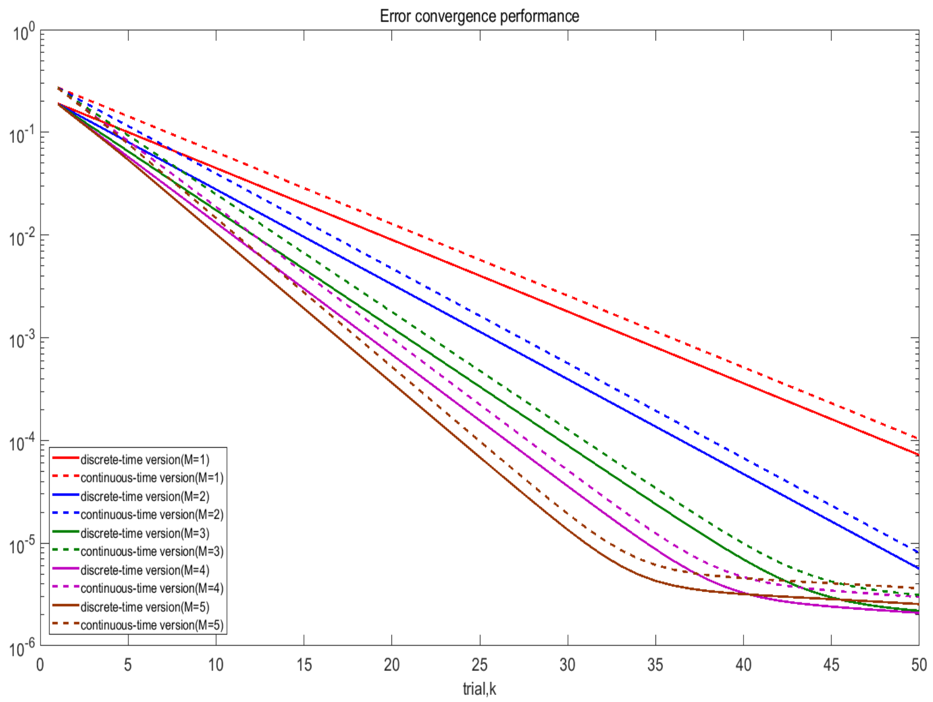

Figure 6.5: Error convergence performance along the trial for the robust design (State-feedback, KYP lemma based design algorithm).

results also show the same relation that when M increases, the speed of error convergence also increases.

6.2.2 Simulation results for the output-feedback control design

Applying the design algorithms in Theorem 5.1 and Theorem 5.7, choose different values of M, table 6.3 shows relation between M and γ, and figure 6.6 shows error convergence performance. In the result, the total number of trials is 50, and it shows that when M increases, the speed of error convergence also increases. Consider the same additive uncertainty part, relation between M and γ is shown in table 6.4, and next figure gives

M	γ(discrete-time version)	γ(continuous-time version)
1	0.9997	0.9998
2	0.7033	0.7051
3	0.5321	0.5321
4	0.4647	0.4651
5	0.4211	0.4215

Table 6.3: Relation between value of M and γ for output-feedback design result(Output-feedback, KYP lemma based design algorithm).

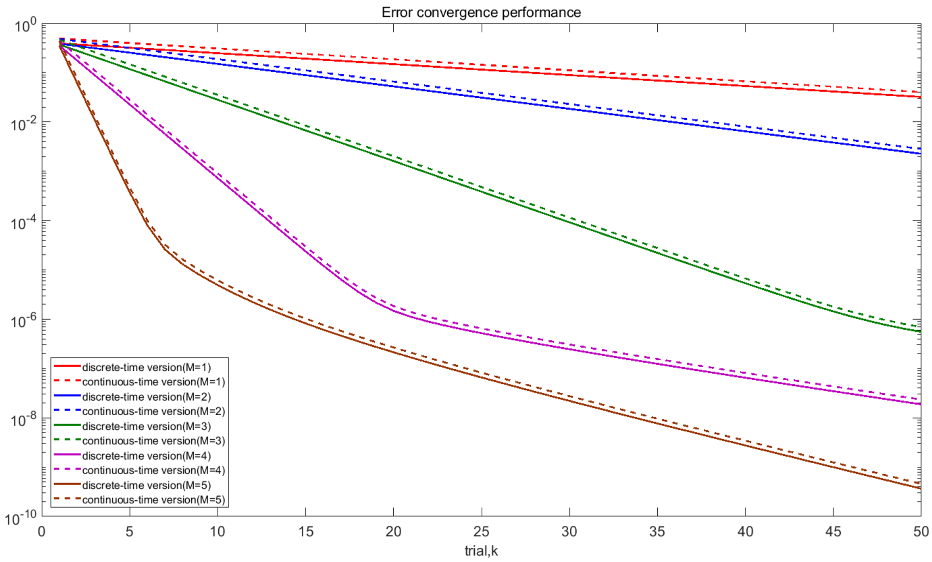

Figure 6.6: Error convergence performance along the trial(Output-feedback, KYP lemma based design algorithm).

M	γ(discrete-time version)	γ(continuous-time version)
1	0.9997	0.9999
2	0.7041	0.7064
3	0.5993	0.6021
4	0.4871	0.4991
5	0.4372	0.4463

Table 6.4: Relation between value of M and γ for robust design result(Output-feedback, KYP lemma based design algorithm).

the performance results.

6.3 Simulation results by using Generalized KYP design

Applying the Fourier transform to the reference trajectory gives the result shown in figure 6.8 and confirms that it has significant frequency content within 0 and 5Hz. Hence the generalized KYP lemma based design algorithms are used. The cut-off frequency is

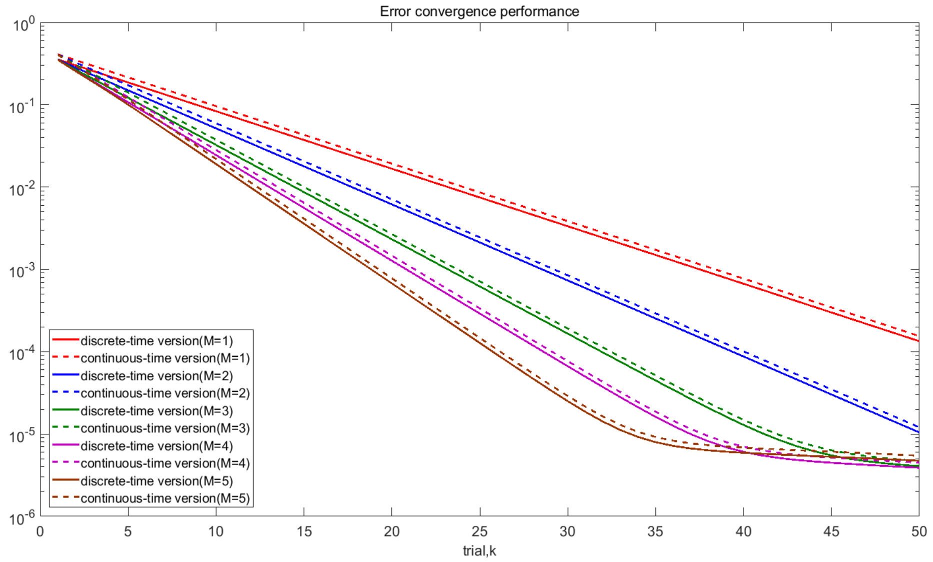

Figure 6.7: Error convergence performance along the trial for the robust design(Output-feedback, KYP lemma based design algorithm).

taken as 5Hz and the designs force the controlled ILC system track the reference signal within this frequency range. The results are divided into two parts.

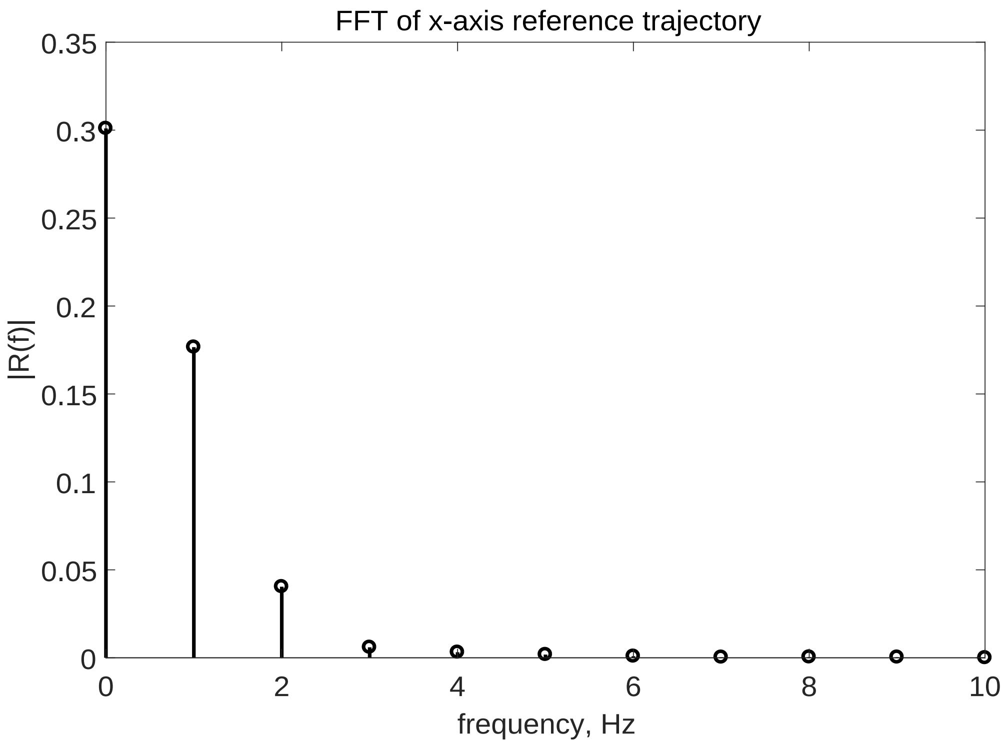

Figure 6.8: The reference trajectory for the x-axis.

6.3.1 Simulation results for the state-feedback control design

In this part, the simulation results include design algorithms for state-feedback scheme using generalized KYP lemma and their robust design algorithms, the design algorithms are shown in Chapter 4. In the simulation, the value of memory length M is from 1 to 5. The state matrix A has one eigenvalue on the unit circle. To highlight the use of Theorem 4.1, consider the case when $M = 2$ with $\rho_1 = 1$ and $\rho_2 = -2$, which can satisfies $\rho_1^2 < \rho_2^2$. Completing the design gives

$$K = [-29.2402 \; -75.3808 \; -11.6832 \; -7.0368 \; -2.6840 \; -6.8440 \; -16.5937]$$

and

$$K_1 = 0.9080, \quad K_0 = 182.7897$$

Here $\gamma = 0.6811$. The plot of the frequency gain for controlled system transfer-function over the range 0 to 5Hz is shown in figure 6.9 and the gain decreases with increasing frequency. Table 6.5 shows the results for M and γ in both cases. The figure 6.10 gives error convergence performance.

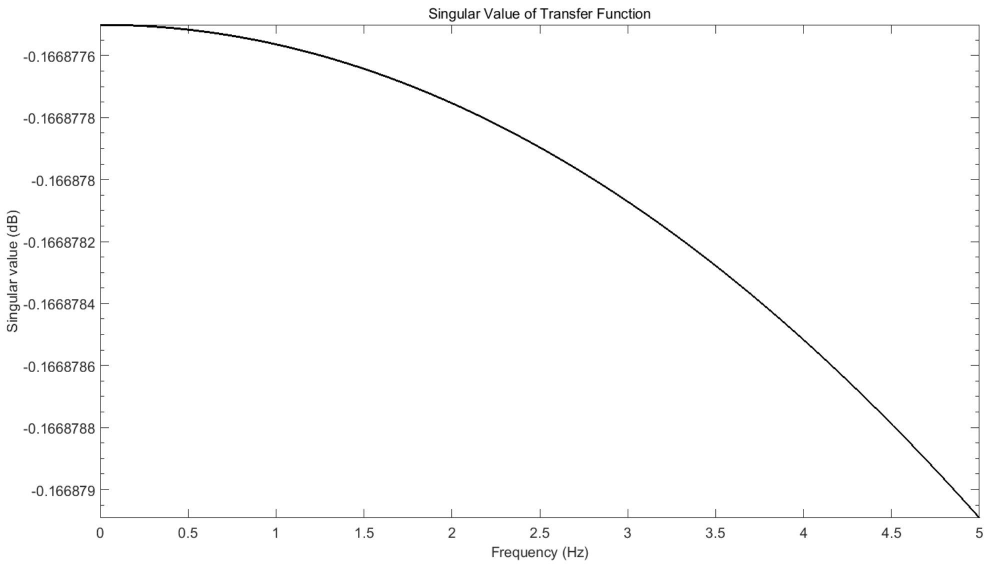

Figure 6.9: Feedback ILC system transfer function(State-feedback, GKYP lemma based design algorithm).

In this figure, the absolute value of the transfer function $\|G(e^{j\omega})\|$ is decrease when frequency increases, and the biggest value is in $0Hz$, which is 0.6810. Both consider the continuous-time version, the relation between M and γ is shown in table 6.6.

Also when M increases the speed of the error convergence also increases.

M	γ(discrete-time version)	γ(continuous-time version)
1	0.9818	0.9987
2	0.6811	0.6911
3	0.5001	0.5202
4	0.4221	0.4585
5	0.3877	0.4157

Table 6.5: Relation between value of M and γ for LMI design (State-feedback, GKYP lemma based design algorithm).

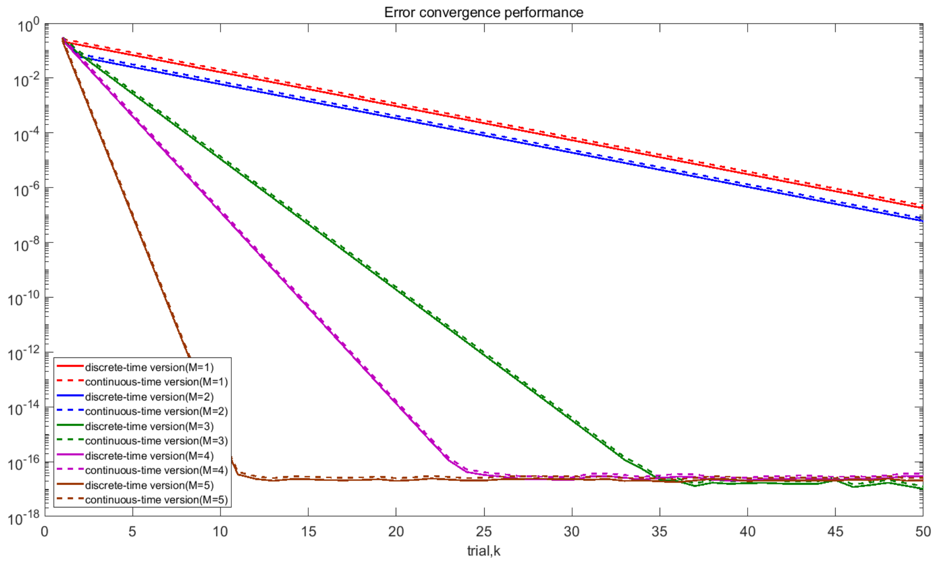

Figure 6.10: Error convergence performance along the trial for LMI design(State-feedback, GKYP lemma based design algorithm).

Next, the robust design algorithm of Chapter 4 is considered. The next table and figure confirm that the same conclusion holds in this case, and the figure of trial-to-trial error

M	γ(discrete-time version)	γ(continuous-time version)
1	0.9877	0.9997
2	0.6866	0.6962
3	0.5554	0.5667
4	0.4426	0.4965
5	0.3974	0.4427

Table 6.6: Relation between value of M and γ for robust design (State-feedback, GKYP lemma based design algorithm).

convergence is in figure 6.11. In the result, it also shows the same relation that when M increase, the speed of error convergence also increase and error convergence becomes faster.

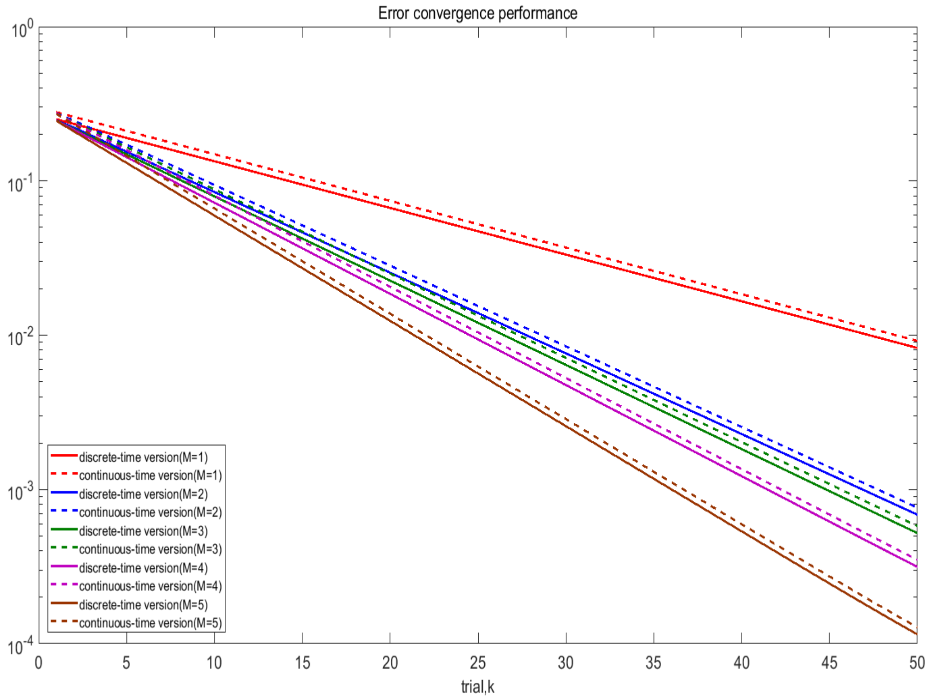

Figure 6.11: Error convergence performance along the trial for robust design (State-feedback, GKYP lemma based design algorithm).

6.3.2 Simulation results for the output-feedback control design

Using the algorithm in Theorem 5.5 and Theorem 5.9 to design the control law matrices. When choose $M = 2$, the value of ρ_1 and ρ_2 are 1 and -2 which can satisfy the condition $\rho_1^2 - \rho_2^2 < 0$. The value of γ is computed as $\gamma = \sqrt{\mu}$ and its value is 0.6911. The plot of the absolute value for controlled system transfer function $\|G(e^{j\omega})\|$ over the frequency range from $0Hz$ to $5Hz$ is shown in figure 6.12. In this figure, the biggest value is in $0Hz$, which is 0.6910, and the value decreases as the frequency increases. Therefore, the curve is below the $\gamma = 0.6365$. Also consider the continuous-time version, the relation between M and γ is shown in next table, and the figure 6.13 shows trial-to-trial error

M	γ(discrete-time version)	γ(continuous-time version)
1	0.9731	0.9799
2	0.6911	0.7021
3	0.5121	0.5146
4	0.4367	0.4423
5	0.3234	0.4021

Table 6.7: Relation between value of M and γ for LMI design (Output-feedback, GKYP lemma based design algorithm).

convergence performance. The figure shows that when M increase, the speed of error convergence also increase and error convergence becomes faster. Test the robust design algorithms for the same uncertainty part, the relation between M and γ is in table 6.8.

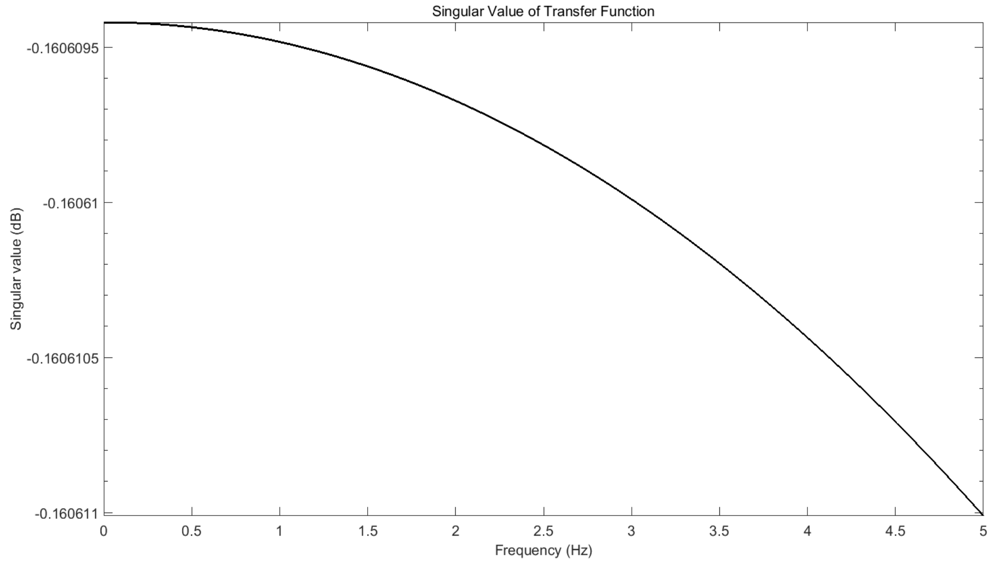

Figure 6.12: Feedback ILC system transfer function(Output-feedback, GKYP lemma based design algorithm).

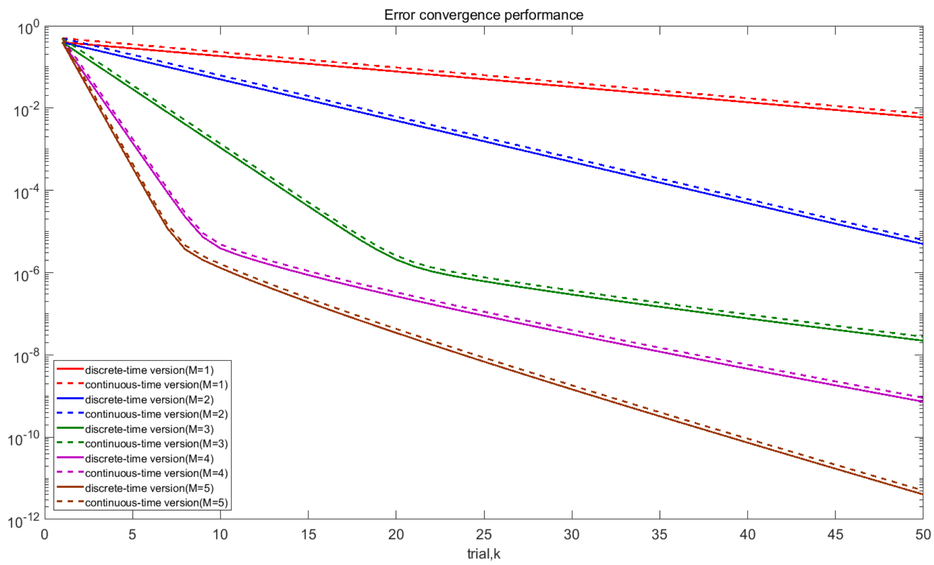

Figure 6.13: Error convergence performance along the trial for LMI design(Output-feedback, GKYP lemma based design algorithm).

The figure of error convergence is in figure 6.14. In this section, the relations between different M and γ is shown in the Tables based different design algorithms. The next section will gives the comparison between different control schemes and KYP/GKYP lemma based design algorithms.

M	γ(discrete-time version)	γ(continuous-time version)
1	0.9822	0.9982
2	0.7018	0.7043
3	0.5351	0.5455
4	0.4601	0.4841
5	0.3857	0.4220

Table 6.8: Relation between value of M and γ for robust design (Output-feedback, GKYP lemma based design algorithm).

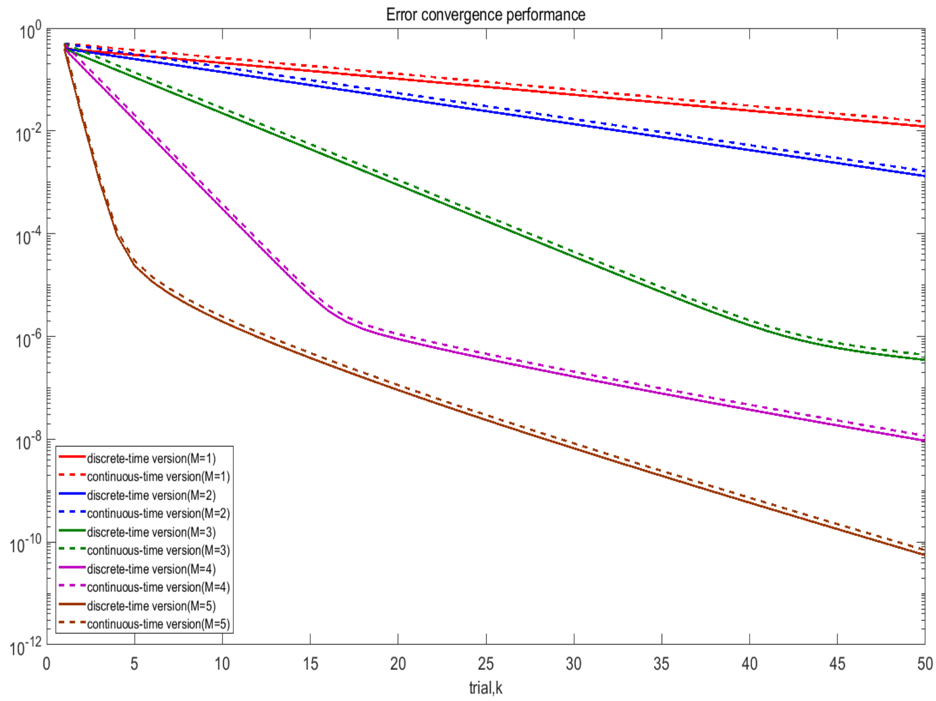

Figure 6.14: Error convergence performance along the trial for the robust design(Output-feedback, GKYP lemma based design algorithm).

6.4 Comparisons

In this section, the comparison between different design algorithms are given. In the previous chapters, the repetitive processing based ILC design algorithm which use KYP lemma and its generalized version are proposed for state feedback and output feedback scheme. In this section, there are four subsections, the first subsection gives comparison between different design algorithm for state feedback scheme, and the second subsection gives comparison between different design algorithm for output feedback scheme. Moreover, the third subsection gives the comparison between different feedback scheme by using repetitive processing based ILC design algorithm which use KYP lemma and the last subsection gives the comparison between different feedback scheme by using repetitive processing based ILC design algorithm which use generalized KYP lemma.

6.4.1 Comparison Between KYP/GKYP Lemma Based Design Algorithm For State Feedback Control Scheme

In this subsection, the simulation results are for state-feedback based ILC laws. Consider the discrete/continuous-time system. The KYP lemma based design algorithm is proposed in chapter 3 and the generalized KYP lemma based design algorithm is proposed in chapter 4, both design algorithms are applied for state feedback control law. In this subsection, the key performance of error convergence speed is focus on. It is clear that

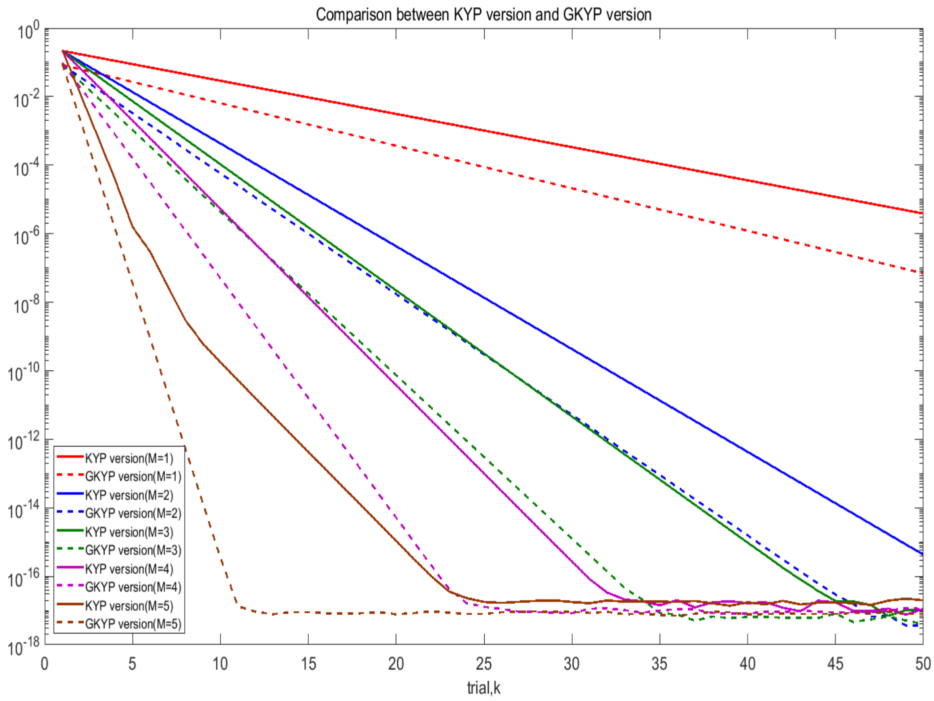

Figure 6.15: Comparison between KYP/GKYP lemma based design algorithms for state feedback control scheme (discrete-time system version).

in all situations, the curve of the trial-to-trial error convergence performance that by using the generalized KYP lemma based design algorithm is lower than the curve of the result by using KYP lemma based design algorithm. This means that the generalized KYP lemma based design algorithms can support better trial-to-trial error convergence performance, and it can get higher speed of error convergence.

6.4.2 Comparison Between KYP/GKYP Lemma Based Design Algorithm For Output Feedback Control Law

In this section, the comparison between different design algorithms is given. Consider the discrete/continuous-time system. The KYP lemma based design algorithm is proposed in section 5.2 and the generalized KYP lemma based design algorithm is proposed in

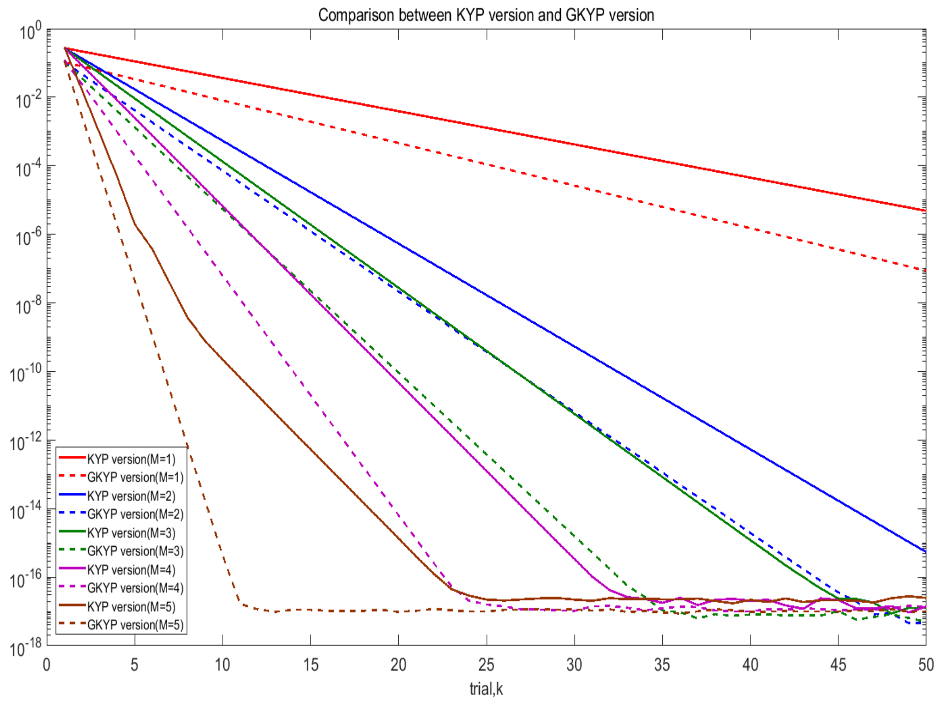

Figure 6.16: Comparison between KYP/GKYP lemma based design algorithms for state feedback control scheme (continuous-time system version).

section 5.3, both design algorithms are applied for state feedback control law. In this subsection, the key performance of error convergence speed is focus on. The figures are given in figure 6.17 and figure 6.18. As the figures shown, even the control scheme here is changed to be output-feedback scheme, the relation is as the same as that by using state-feedback scheme. It is that the generalized KYP lemma based design algorithm can obtain the better performance,

6.4.3 Comparison Between KYP Based Design Algorithms For State/Output Feedback Control Law

In this section, the comparison between different design algorithms is given. Consider the discrete/continuous-time system. The KYP lemma based design algorithm for state feedback control scheme is proposed in Chapter 3 and the KYP lemma based design algorithm for output feedback control scheme is proposed in chapter 5. In this subsection, the key performance of error convergence speed is focus on. The figures are given in figure 6.19 and figure 6.20. As the figures shown, when use the same type of design algorithm(here is KYP lemma based design algorithm), the state-feedback control law can achieve the higher speed of trial-to-trial error convergence. In this simulations, the state-feedback control scheme can focus on the transient performance along the trial, thus it can obtain better performance.

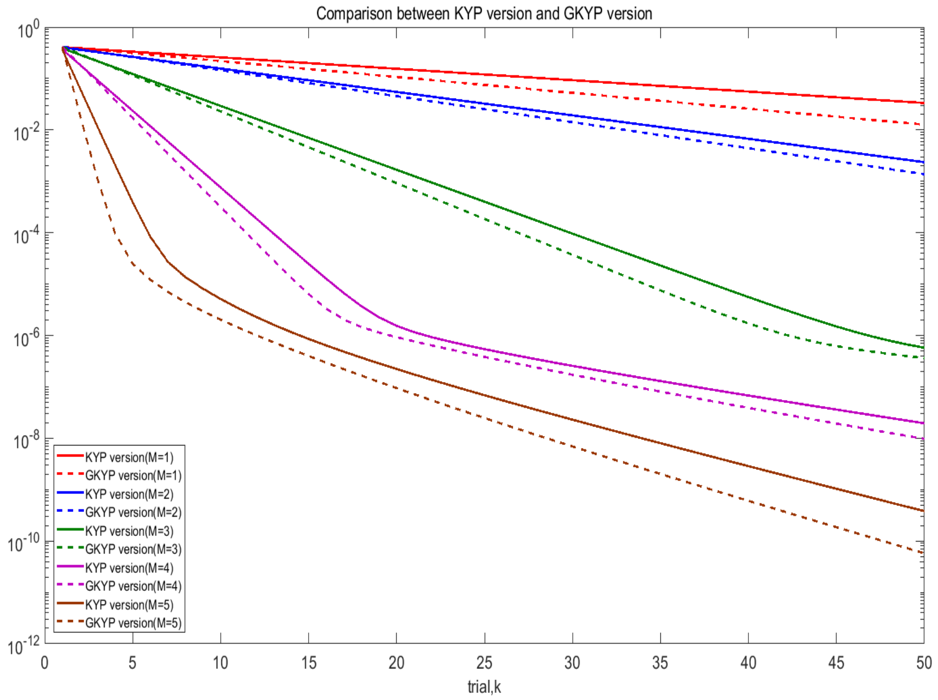

Figure 6.17: Comparison between KYP/GKYP lemma based design algorithms for output feedback control scheme (discrete-time system).

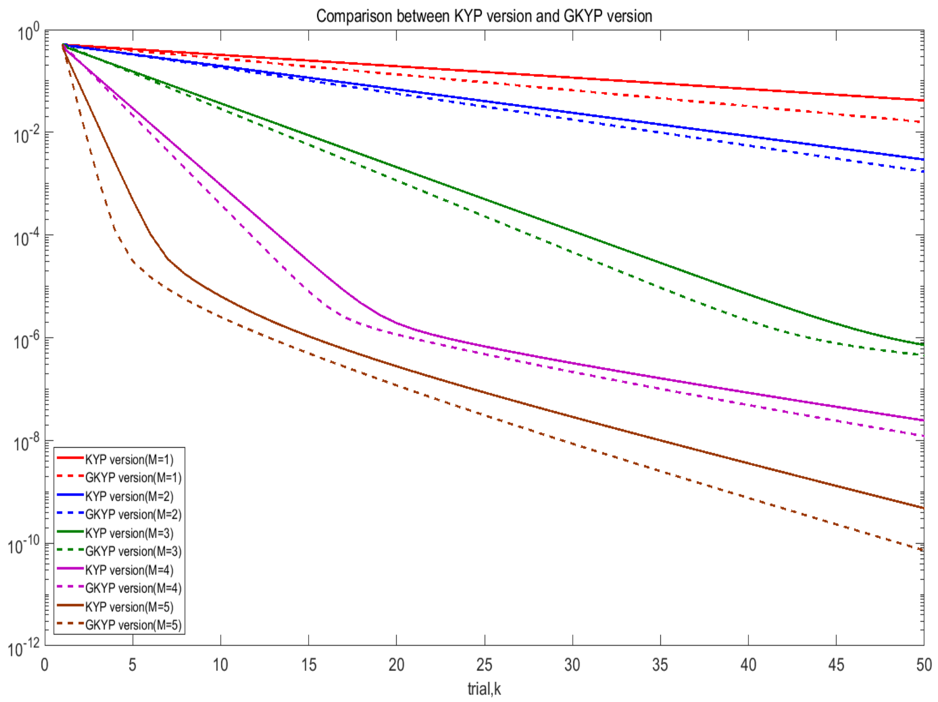

Figure 6.18: Comparison between KYP/GKYP lemma based design algorithms for output feedback control scheme (continuous-time system).

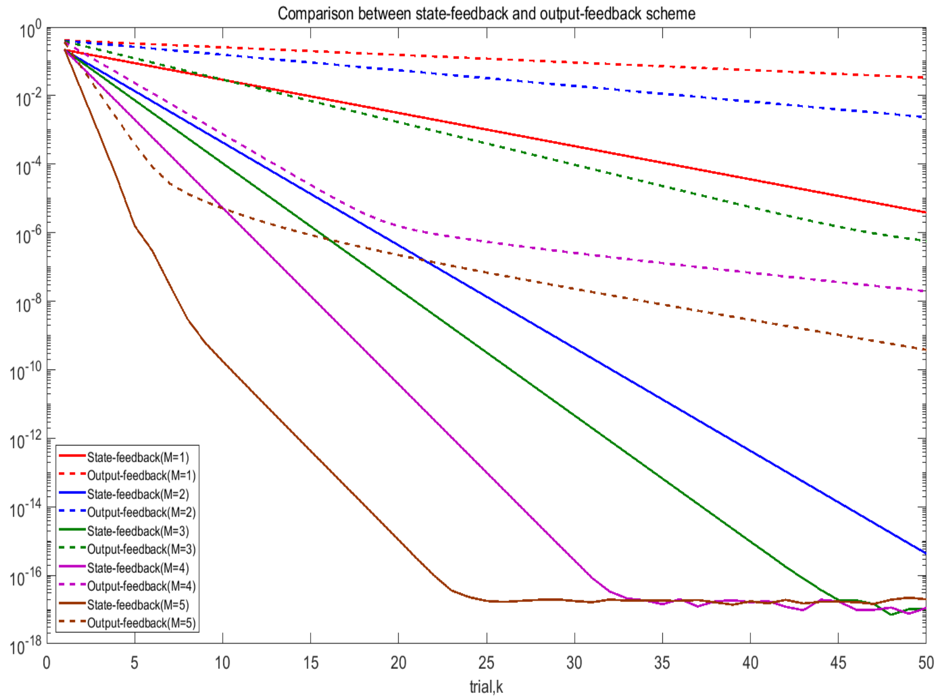

Figure 6.19: Comparison between KYP based design algorithms for different feedback control scheme (discrete-time system).

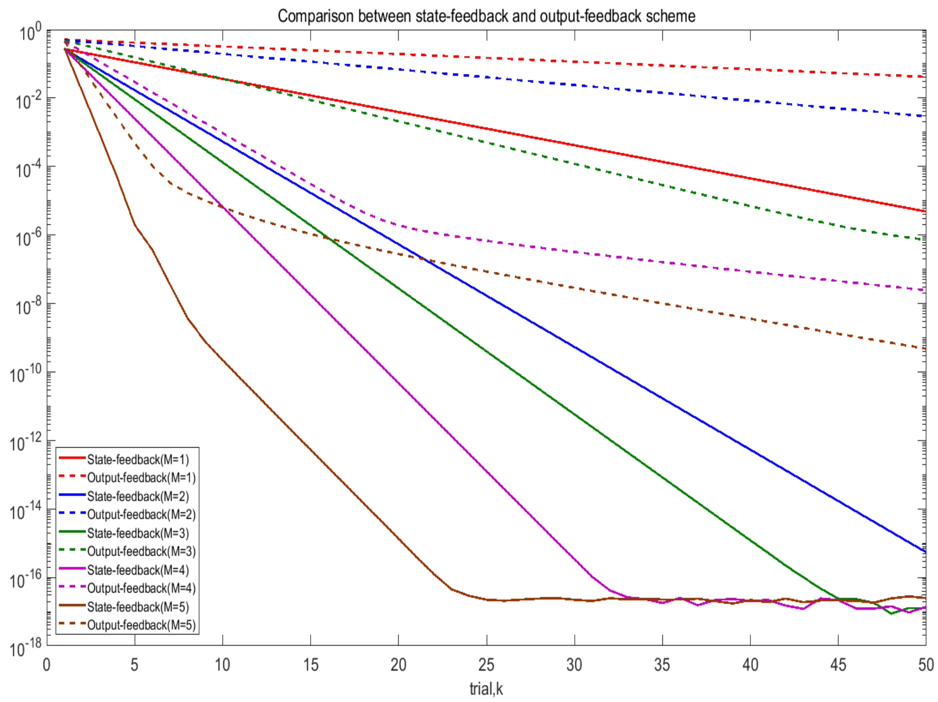

Figure 6.20: Comparison between KYP lemma based design algorithms for different feedback control scheme (continuous-time system).

6.4.4 Comparison Between GKYP Based Design Algorithms For State /Output Feedback Control Law

In this subsection, the comparison between different design algorithms is given. Consider the discrete/continuous-time system. The KYP lemma based design algorithm for state feedback control scheme is proposed in Chapter 4 and the KYP lemma based design algorithm for output feedback control scheme is proposed in chapter 5. In this subsection, the key performance of error convergence speed is focus on. The figures are given in figure 6.21 and figure 6.22. The result is as similar as that using the KYP lemma based

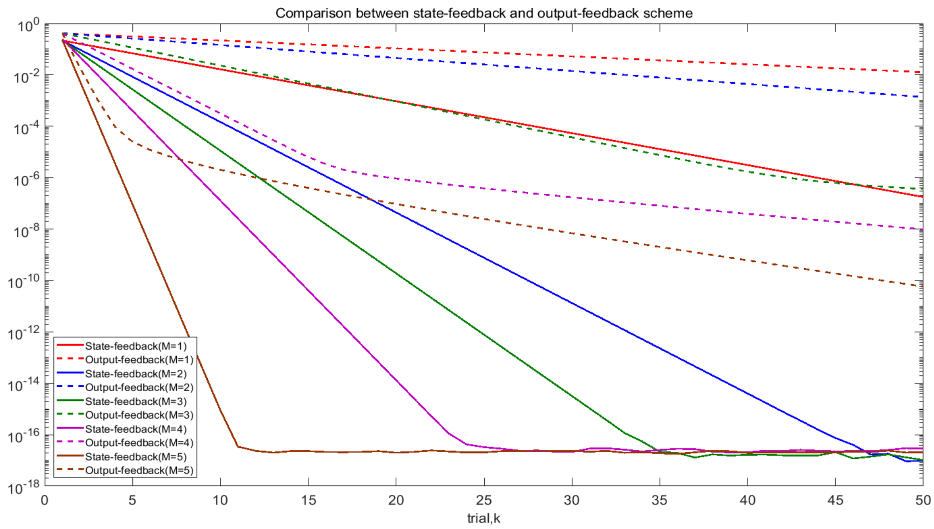

Figure 6.21: Comparison between GKYP based design algorithms for different feedback control scheme (discrete-time system).

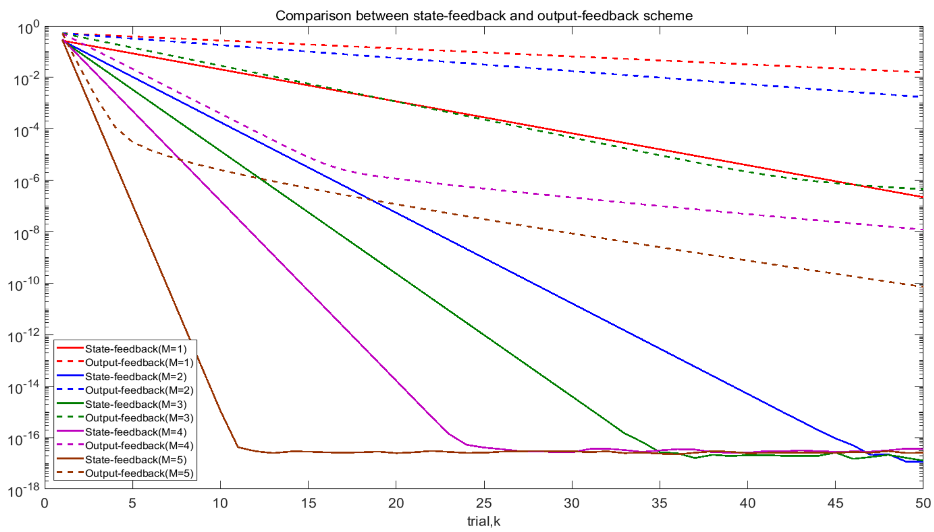

Figure 6.22: Comparison between GKYP lemma based design algorithms for different feedback control scheme (continuous-time system).

design algorithm.

6.5 Summary

In this chapter, the model of gantry robot is used to test the design algorithms in previous chapters. In this chapter, the repetitive process based ILC design algorithms by using KYP lemma and its generalized version are used for state feedback and output feedback higher-order control laws. from the simulation results, the design algorithms are applied well for the gantry robot. Moreover, this chapter also gives the comparison between different kind of design algorithms for different feedback control schemes. Among them, the design algorithm by using generalized KYP lemma and the state feedback control law is proofed to obtain the best performance, which support the highest speed of error convergence.

Chapter 7

Conclusions and Further Work

7.1 Conclusion

This thesis has developed significant new results on the design of ILC laws in the repetitive process setting. The vast majority of the analysis and design of ILC laws only explicitly use information from the previous trials. On any trial, however, all information generated on any previous trial can be used, at the cost having to store the information required. Higher-order ILC is a design where a finite number, greater than unity, of previous trials are explicitly used in the construction of the next trial input. Higher-order ILC has been considered in the literature but missing are results/designs that quantify the benefits possible.

Repetitive process stability theory allows design to simultaneously enforce trial-to-trial error convergence and acceptable transients along the trials. Moreover, this setting extends to differential dynamics unlike alternatives. This allows design by emulation. Also the extension robust control, where the uncertainty is assumed to belong to a particular model class. The first new set of results in this thesis to develop an LMI based design for a higher-order ILC law for both differential and discrete linear time-invariant dynamics. Also the convergence properties of these designs is established.

The repetitive process setting for ILC design imposes frequency attenuation over the complete spectrum of the previous trial error dynamics. This could be very constraining in at least some applications. Moreover, some applications may require different frequency domain specifications over different frequency ranges. The second set of new results in this thesis uses the generalized KYP lemma to allow design with these features. Again the convergence properties of the designs is established.

In the last set of new results in this thesis, the analysis is extended to output feedback higher-order ILC laws. Again the convergence properties of the designs are established. As a necessary step towards to experimental verification, all designs are compared in simulation on the model of one axis of a gantry robot. This robot has been used to test many ILC laws and the model used in this thesis has been determined by frequency response tests.

7.2 Further Work

In this thesis, design algorithms based KYP lemma and generalized KYP lemma have been developed for higher-order ILC control laws matrices. Moreover, a model of gantry robot has been used to test the performance of these algorithms. Areas for further research include the following.

- The design algorithms have been evaluated on a model of the gantry robot. An obvious next step is to test these designs experimentally.
- As the simulations in this thesis demonstrate, as the value of M increases, the speed of error convergence also increases. However, an exact relationship between M and speed of error convergence has yet to be established.
- This thesis has developed some results on robust control and these require further development and experimental verification. There is also a need to deal with disturbances.
- The design algorithms developed in this thesis place no constraints on process variables, e.g., input and/or output constraints. This are should be the subject of research effort.

References

[1] Ahn, H.-S., Chen, Y. Q., Moore, K. L.: Iterative learning control: brief survey and characterization. IEEE Transactions on Systems Man and Cybernetics Part C, *37(6)*, 1099–1121 (2007).

[2] Al-Towlain, T.: Practical implementation of norm-optimal and predictive iterative learning control on a chain conveyor system. PhD thesis, University of Southampton, UK (2004).

[3] Amann, N., Owens, D. H.: Non-minimum phase plants in iterative learning control. Intelligent Systems Engineering, 107–112 (1994).

[4] Amann, N., Owens, D. H., Rogers, E.: Iterative learning control using optimal feedback and feedforward actions. International Journal of Control, *65*, 277–293 (1996).

[5] Amann, N., Owens, D. H., Rogers, E.: Iterative learning control for discrete-time systems with exponential rate of convergence. IEE Proc.-Control Theory and Applications, *143(2)*, 217–224 (1996).

[6] Arimoto, S., Kawamura, S., Miyazaki, F.: Bettering operation of robots by learning. Journal of Robotic Systems, *2(1)*, 123–140 (1984).

[7] Arimoto, S., Kawamura, S., Miyazaki, F., Tamaki, S.: Learning control theory for dynamical systems. 24*th* IEEE Conference on Decision and Control, *24*, 1375–1380 (1985).

[8] Avrachenkov, K. E.: Iterative learning control based on quasi-newton methods. 37*th* IEEE Conference on Decision and Control, *1*, 170–174 (1998).

[9] Benzaouia, A., Hmamed, A., Tadeo, F.: Two-Dimensional Systems From Introduction to State of the Art. Springer, (2016).

[10] Bien, Z., Huh, K. M.: Higher-order iterative learning control algorithm. IEE Proc.-Control Theory and Applications, *136(3)*, 105–112 (1989).

[11] Boyd, S., Chaoui, L. E., Feron, E., Balakrishnan, V.: Linear matrix inequalities in system and control theory. SIAM, (1994).

[12] Bristow, D. A., Tharayil, M., Alleyne, A. G.: A survey of iterative learning control: a learning based method for high performance tracking control. IEEE Control Systems Magazine, *26(3)*, 96–114 (2006).

[13] Chen, Y., Wen, C., Gong, Z., Sun, M.: An iterative learning controller with initial state learning. IEEE Transaction on Automatic Control, *44(2)*, 371–376 (1999).

[14] Chandra, R. S., D'Andrea, R.: A scaled small gain theorem with applications to spatially interconnected systems. IEEE Transactions on Automatic Control, *51(3)*, 465–469, (2006).

[15] Cichy, B., Galkowski, K., Rogers, E., Kummet, A.: Control law design for discrete linear repetitive processes with non-local updating structures. Multidim Syst Sign Process, *24*, 707–726 (2013).

[16] Cichy, B., Galkowski, K., Rogers, E.: 2D systems based robust iterative learning control using noncausal finite-time interval data. System and Control Letters, *64*, 36–42 (2014).

[17] Dabkowski, P., Galkowski, K., Rogers, E., Kummert, A.: Strong practical stability and stabilization of discrete linear repetitive processes. Multidim Syst Sign Process, *20*, 311–331 (2009).

[18] Dabkowski, P., Galkowski, K., Rogers, E., Bachelier, O.: Strong practical stability and stabilization of differential linear repetitive processes.Systems and Control Letters, *59*, 639–644 (2010).

[19] Dabkowski, P., Galkowski, K., Bachelier, O., Rogers, E., Kummert, A., Lam J.: Strong practical stability based robust stabilization of uncertain discrete linear repetitive processes. Numerical Linear Algebra with Applications, *00*, 1–13 (2011).

[20] Dabkowski, P., Galkowski, K., Bachelier, O., Rogers, E.: Control of discrete linear repetitive processes using strong practical stability and H_∞ disturbance attenuation. Systems and Control Letters, *61*, 1138–1144 (2012).

[21] Dabkowski, P., Galkowski, K., Rogers, E., Cai, Z., Freeman, C. T., Lewin, P. L.: Iterative learning control based on relaxed 2-D systems stability criteria. IEEE Transactions on Control Systems Technology, *21(3)*, 1016–1023 (2013).

[22] De Souza, C.E., Lihua, X.: On the discrete-time bounded real lemma. Systems and Control Letters, *18*, 61–71 (1992).

[23] Dullerud, G. E., Paganini, F. G.:A course in robust control theory a convex approach. Springer. (2005).

[24] Fang, Y., Tommy. W: 2-D analysis for iterative learning controller for discrete-time systems with variable initial condition. IEEE Transactions on Circuits and Systems-I:Fundamental Theory and Applications, *50(5)*, 722–727 (2003).

[25] Fornasini, E., Marchesini, G.: State-space realization theory of two-dimensional filters. IEEE Transactions on Automatic Control, *21(4)*, 484–492 (1976).

[26] Freeman, C. T.: Constrained point-to-point iterative learning control with experimental verification. Control Engineering Practice, *20*, 489–498 (2012).

[27] Freeman, C. T., Tan, Y.: Iterative learning control with mixed constraints for point-to-point tracking. IEEE Transactions on Control Systems Technology, *21(3)*, 604–616 (2013).

[28] Gahinet, P., Apkarian, P.: A linear matrix inequality approach to H_∞ control. International Journal of Robust and Nonlinear Control, *4*, 421–448 (1994).

[29] Galkowski, K.: State-space Realisations of Linear 2-D Systems with Extensions to the General nD(n¿2) Case. Springer, (2001).

[30] Galkowski, K., Rogers, E., Xu, S., Lam, J., Owens, D. H.: LMIs - a fundamental tool in analysis and controller design for discrete linear repetitive processes. IEEE Transactions on Circuit and Systems-I: Fundamental Theory and Applications, *49(6)*, 768–778 (2002).

[31] Galkowski, K., Lam, J., Rogers, E., Xu, S., Sulikowski, B., Paszke, W., Owens, D. H.: LMI based stability analysis and robust controller design for discrete linear repetitive processes. International Journal of Robust and Nonlinear Control, *13*, 1195–1211 (2003).

[32] Geng, Z.: Learning control system analysis and design based on 2-D system theory. Journal of Intelligent and Robotic Systems, *3*, 17–26 (1990).

[33] Geng, Z., Carroll, R., Xies, J.: Two-dimensional model and algorithm analysis for a class of iterative learning control system. International Journal of Control, *52*, 833–862 (1990).

[34] Gu, Y.-L., Loh, N. K.: Learning control in robotic systems. Journal of Intelligent and Robotic Systems, *2*, 297–305 (1989).

[35] Green, M., Limebeer, D.: Linear Robust Control. Prentice-Hall, (2012).

[36] Harte, T. J., H*ä*t*ö*nen, J., Owens, D. H.: Discrete-time inverse model-based iterative learning control: stability, monotonicity and robustness. International Journal of Control, *78(8)*, 577–586 (2005).

[37] Heinzinger, G., Fenwick, D., Paden, B., Miyazaki, F.: Stability of learning control with disturbances and uncertain initial conditions. IEEE Transactions on Automatic Control, *37(1)*, 110–114 (1992).

[38] Hladowski, L., Galkowski, K., Cai, Z., Rogers, E., Freeman, C. T., Lewin, P. L.,: Experimentally supported 2D systems based iterative learning control law design for error convergence and performance. Control Engineering Practice, *18(4)*, 339–348 (2010).

[39] Hladowski, L., Rogers, E., Galkowski, K., Sule, V.: On control laws for discrete linear repetitive processes with dynamic boundary conditions.Multidim Syst Sign Process, *19*, 477–488 (2008).

[40] Hladowski, L., Galkowski, K., Cai, Z., Rogers, E., Freeman, C. T., Lewin, P. L.: Output information based iterative learning control design with experimental verification. ASME Journal of Dynamic Systems, Measurement and Control, *134*, 021012-1–021012-10 (2012).

[41] Iwasaki, T., Hara, S.: Generalized KYP lemma: unified frequency domain inequalities with design applications. IEEE Transactions on Automatic Control, *50(1)*, 41–59 (2005).

[42] Hara, S., Iwasaki, T., Shiokata, D.: Robust PID control using generalized KYP synthesis. IEEE Control Systems Magazine, 80–91 (2006).

[43] Iwasaki, T., Hara, S.: Feedback control synthesis of multiple frequency domain specifications via generalized KYP lemma. International Journal of Robust and Nonlinear Control, *17*, 415–434 (2007).

[44] Kaczorek, T.: Two Dimensional Linear Systems. Lecture Notes in Control and Information Sciences, Springer-Verlag, Vol.*68*, (1985).

[45] Khargonekar, P. P., Petersen, I. R., Zhou, K.: Robust stabilization of uncertain linear systems: quadratic stabilizability and H_∞ control theory. IEEE Transactions on Automatic Control, *35(3)*, 356–361 (1990).

[46] Kim, D., Kim, S.: An iterative learning control method with application for CNC machine tools. IEEE Conference on Industry Applications Society Annual Meeting, *3(2)*, 2106–2111 (1990).

[47] Kung, S.Y., Levy, B.C., Morf, M., Kailath, T.: New results in 2-D systems theory, part II: 2-D state-space models—realization and the notions of controllability,observability, and minimality. Proceedings of IEEE, *65(6)*, 945–961 (1977).

[48] Kurek, J. E., Zaremba, M. B.: Iterative learning control synthesis based on 2-D system theory. IEEE Transactions on Automatic Control, *38(1)*, 121–125 (1993).

[49] Lin, T., Owens, D. H., H*ä*t*ö*nen, J.: Newton-method based iterative learning control for sampled nonlinear systems. 4th International Workshop on Multidimensional Systems, 142–147 (2005).

[50] Lin, T., Owens, D. H., H*ä*t*ö*nen, J.: Newton method based iterative learning control for discrete non-linear systems. International Journal of Control, *79*, 1263–1276 (2006).

[51] Lu, W., Antoniou, A.: Two-Dimensional Digital Filters. CRC Press, (1992).

[52] Moore, K.L, Chen, Y. Q., On monotonic convergence of higher order iterative learning update laws. 15th IFAC conference, 19–24 (2002).

[53] Madady, A.: PID type iterative learning control with optimal gains. International Journal of Control, Automation and Systems, *6*, 194–203 (2008).

[54] Owens, D. H., Feng, K.: Parameter optimization in iterative learning control. International Journal of Control, *76*, 1059–1069 (2003).

[55] Owens, D. H., H*ä*t*ö*nen, J.: Iterative learning control - an optimization paradigm. Annual Reviews in Control, *29(1)*, 57–70 (2005).

[56] Owens, D. H., H*ä*t*ö*nen, J., Daley, S.: Robust monotone gradient-based discrete-time iterative learning control. International Journal of Robust and Nonlinear Control, *19*, 634–661 (2009).

[57] Owens, D. H.: Iterative Learning Control: An Optimization Paradigm. Springer (2016).

[58] Paszke, W.: Analysis and synthesis of multidimensional system classes using linear matrix inequality methods. Lecture Notes in Control and Computer Science, Vol.*8*, (2005).

[59] Paszke, W., Galkowski, K., Rogers, E., Owens, D. H.: H_∞ and guaranteed cost control of discrete linear repetitive processes. Linear Algebra and its Applications, *412*, 93–131 (2006).

[60] Paszke, W., Galkowski, K., Rogers, E., Owens, D. H.: H_∞ control of differential linear repetitive processes. IEEE Transactions on Circuits and Systems-II: Express Briefs, *53(1)*, 39–44 (2006).

[61] Paszke, W., Galkowski, K., Rogers, E., Lam J: H_2 and mixed H_2/H_∞ stabilization and diturbance attenuation for differential linear repetitive processes. IEEE Transactions on Circuits and Systems-I: Regular Papers, *55(9)*, 2813–2826 (2008).

[62] Paszke, W., Rogers, E., Galkowski, K.: H_2/H_∞ output information-based disturbance attenuation for differential linear repetitive processes. Interational Journal of Robust and Nonlinear Control, *21*, 1981–1993 (2011).

[63] Paszke, W., Rogers, E., Galkowski, K., Cai, Z.: Robust finite frequency range iterative learning control design and exprimental verification. Control Engineering Practice *21*, 1310–1320 (2013).

[64] Paszke, W., Bachelier O.: Robust control with finite frequency specification for uncertain discrete linear repetitive processes. Multidim Syst Sign Process *24*, 727–745 (2013).

[65] Paszke, W., Rogers, E., Galkowski, K.: KYP lemma based stability and control law design for differential linear repetitive processes with applications. Systems and Control Letters *62*, 560–566 (2013).

[66] Paszke, W., Dabkowski, P, Rogers, E., Galkowski, K.: New results on strong practical stability and stabilization of discrete linear repetitive processes. Systems and Control Letters *77*, 22–29 (2015).

[67] Paszke, W., Rogers, E., Galkowski, K.: Experimentally verified generalized KYP lemma based iterative learning control design. Control Engineering Practice *53*, 57–67 (2016).

[68] Rantzer, A.: On the Kalman-Yakubovich-Popov lemma. Systems Control Letters, *28(1)*, 7—10 (1995).

[69] Ratcliffe, J. D., Lewin, P. L., Rogers, E., H*ä*t*ö*nen, J., Owens, D. H.: Norm-optimal iterative learning control applied to gantry robots for automation applications. IEEE Transactions on robotics *22(6)*, 1303–1307 (2006).

[70] Ratcliffe, J. D., H*ä*t*ö*nen, J., Lewin, P. L., Rogers, E., Owens, D. H.: Robustness analysis of an adjoint optimal iterative learning controller with experimental verification. International Journal of Robust and Nonlinear Control, *18*, 1089-1113 (2007).

[71] Roesser, R. P.: A discrete state-space model for linear image processing. IEEE Transactions on Automatic Control, *20(1)*, 1–10 (1975).

[72] Rogers, E., Owens, D. H.: Stability Analysis for Linear Repetitive Processes. Lecture Notes in Control and Information Sciences Series, Vol.*175*, (1992).

[73] Rogers, E., Galkowski, K., Gramacki, A., Gramacki, J., Owens, D.H.: Stability and Controllability of s class of 2-D linear systems with dynamic boundary conditions. IEEE Transactions on circuits and systems-I: Fundamental Theory and Applications, *49(2)*, 181–195 (2002).

[74] Rogers, E., Galkowski, K., Owens, D. H.: Control systems theory and applications for linear repetitive processes. Lecture Notes in Control and Information Sciences. Springer Verlag, Vol.*349*, (2007).

[75] Rogers, E., Owens, D. H., Wemer, H., Freeman, C. T., Lewin, P. L., Kichhoff, S., Schmidt, C., Lichtenberg, G.: Norm-optimal iterative learning control with application to problems in accelerator-based free electron lasers and rehabilitation robotics. European Journal of Control, *16(5)*, 497–522 (2010).

[76] Rogers, E., Galkowski, K., Owens, D. H.: Two decades of research on linear repetitive processes part I: Theory. 8th Int. Workshop on Multidimensional Systems(nDS'13), 27–32 (2013).

[77] Rogers, E., Galkowski, K., Paszke, W., Owens, D. H.: Two decades of research on linear repetitive processes part II: Applications. 8th Int. Workshop on Multidimensional Systems(nDS'13), 121–126 (2013).

[78] Rogers, E., Galkowski, K., Paszke, W., Moore, K.L., Bauer, P.H., Hladowski, L., Dabkowski, P.: Multidimensional control systems: case studies in design and evaluation. Multidim Syst Sign Process *26*, 895–939 (2015).

[79] Sutanto, E., Alleyne, A. G.: Norm optimal iterative learning control for a roll to roll nano/micromanufacturing system. ACC Conference, 5935–5941 (2013).

[80] Tommy, W. S., Fang, Y.: An iterative learning control method for continuous-time systems based on 2-D system theory. IEEE Transactions on Circuits and Systems-I: Fundamental Theory and Applications, *45(4)*, 683–689 (1998).

[81] Towaim, T., Barton, A.D., Lewin, P.L., Rogers, E., Owens, D.H.: Iterative learning control — 2D control systems from theory to application. International Journal of Control, *77(9)*, 877-893 (2004).

[82] Wang, D.: On D-type and P-type ILC design and anticipatory approach. International Journal of Control, *73(10)*, 890–901 (2000).

[83] Wang, D., Ye, Y.: Design and Experiments of anticipatory learning control: frequency-domain approach. IEEE/ASME Transactions on Mechatronics, *10(3)*, 305–313 (2005).

[84] Wang, D., Ye, Y., Zhang, B.: Practical Iterative Learning Control with Frequency Domain Design and Sampled Data Implementation. Springer (2014).

[85] Wang, Y., Gao, F., D, F. J.: Survey on iterative learning control, repetitive control, and run-to-run control. Journal of Process Control, *19*, 1589–1600 (2009).

[86] Wu, L., Lam, J., Paszke, W, Galkowski, K., Rogers, E., Kummert, A.: Control and filtering for discrete linear repetitive processes with H_∞ and l_2-l_∞ performance. Multidim Syst Sign Process *20*, 235–364 (2009).

[87] Wu, L., Su, X., Shi, P.: Mixed H_2/H_∞ approach to fault detection of discrete linear repetitive processes. Journal of the Franklin Institute, *348*, 393–414 (2011).

[88] Wu, L., Zheng, W., Su, X.: Generalized H_2 model approximation for differential linear repetitive processes. Optimal Control Applications and Methods, *32*, 65–82 (2011).

[89] Xu, J.X., Tan, Y.: Linear and nonlinear iterative learning control. Springer. (2003).

[90] Zhang, B., Wang, D., Ye, Y.: On learning transient, auto-tunings of learnable bandwidth and lead step in iterative learning control. International Journal of Control, *41(4)*, 353–363 (2010).

[91] Zhou, K., Doyle, J.C., and Glover, K.: Robust and optimal control. Prentice Hall. (1996).